UNIVERSITY OF NOTTINGHAM



SCHOOL OF MATHEMATICAL SCIENCES

Periodic Behaviours Emergent in Discrete Systems with Random Dynamics

John-Nathan Edward Pickton, MMath

A thesis submitted to the University of Nottingham for the degree of

DOCTOR OF PHILOSOPHY

JANUARY 2017

ABSTRACT

Periodic behaviours in continuous media can be described with great power and economy using conceptual machinery such as the notion of a field. However periodic effects can also be 'observed' in collections of discrete objects, be they individuals sending emails, fire-flies signalling to attract mates, synapses firing in the brain or photons emerging from a cavity. The origin of periodic behaviours becomes more difficult to identify and interpret in these instances; particularly for systems whose individual components are fundamentally stochastic and memoryless. This thesis describes how periodic behaviour can emerge from intrinsic fluctuations in a fully discrete system that is completely isolated from any external coherent forcing.

This thesis identifies the essential elements required to produce naturally emerging periodic behaviours in a collection of interacting 'particles' which are constrained to a finite set of 'states', represented by the nodes of a network. The network can be identified with a type of a spatial structure throughout which particles can move by spontaneously jumping between nodes. The particles interact by affecting the rate at which other particles jump. In such systems it is the collective ensemble of particles, rather than the individual particles themselves, that exhibit periodic behaviours. The existence or non-existence of such collective periodic behaviours is attributed to the structure of the network and the form of interaction between particles that together describe the microscopic dynamics of the system. This thesis develops a methodology for deriving the macroscopic description of the ensemble of particles from the microscopic dynamics that govern the behaviour of individual particles and uses this to find key ingredients for collective periodic behaviour.

In order for periodic behaviours to emerge and persist it is necessary that the microscopic dynamics be irreversible and hence violate the principle of detailed balance. However such a condition is not sufficient and irreversibility must also manifest on the macroscopic level. Simple systems that admit collective periodic behaviours are presented, analysed and used to hypothesise on the essential elements needed for such behaviour. Important general results are then proven. It is necessary that the network have more than two nodes and directed edges such that particles jump between states at different rates in both directions. Perhaps most significantly, it is demonstrated that collective periodic behaviours are possible without invoking 'action at a distance' - there need not be a field providing a mechanism for the interactions between particles.

ACKNOWLEDGEMENTS

I would like to thank my supervisors **Dr. Keith Hopcraft** and **Prof. Eric Jakeman** for their enthusiasm and invaluable input to this work. I am particularly grateful to Keith, who has spent countless hours discussing my results and possibly read this thesis more times than I have.

I wish to acknowledge the School of Mathematical Sciences, University of Nottingham for funding this work.

I extend my gratitude to my parents **Jacqui Pickton** and **John Pickton** for their support and sacrifice over the years.

Finally, I would like to thank **Paulina Powałowska** who has provided me with both love and friendship over the last three years, and most kindly supported me through writing my thesis.

Contents

1 Introduction **1**

1.1 Interacting Particle Systems 2

1.2 Statistical Mechanics 4

1.3 Stochastic Dynamics 5

1.4 Overview of the Thesis 7

2 Interacting Particle Systems **9**

2.1 Interacting Particle Systems 9

2.2 Mechanism for Interactions 11

2.3 Markov Property 12

2.4 Master Equation 14

2.5 Macroscopic Equations 15

2.6 Steady-State Solutions 16

2.7 Backwards Master Equation 17

2.8 Reversibility and Detailed Balance 18

2.9 Particles on a Network with Two Nodes 18

2.10 Discussion 19

3 Systems of Non-Interacting Particles **21**

3.1 Non-Interacting Particles 22

3.2 Macroscopic equations 23

3.3 Single Particle Systems 25

3.4 Time-Invariant Distribution 27

3.5 Detailed Balance 29

3.6 Two-State Systems 30
3.7 Irreversible Systems 31
3.8 Three-State Loop System 33
3.9 N-State Loop System 38
3.10 Discussion 39

4 Birth-Death-Migration Process **41**
4.1 Migration Process 42
4.2 Birth Process 43
4.3 Death Process 46
4.4 Dynamics at the Boundaries 49
4.5 Monte-Carlo Simulations 53
4.6 Qualitative Behaviour of the System 55
4.7 Frequency of the Limit Cycle 57
4.8 Amplitude of the Limit Cycle 62
4.9 Discussion 65

5 Conditions of Collective Periodic Behaviours **67**
5.1 Deriving the Macroscopic Equations 68
5.2 BDM-process in the context of interacting particle systems 72
5.3 Undirected Systems 76
5.4 Local Interactions 78
5.5 Local Speed-Altering Interactions 78
5.6 Periodic Behaviour from Local Interactions 82
5.7 Discussion 89

6 Conclusions and Further Work **91**
6.1 Overview of the Thesis 91
6.2 Further Work 94

Chapter 1

Introduction

Manifestations of collective periodic behaviours are so ubiquitous and familiar that the underlying conditions enabling oscillatory behaviour to emerge and persist may be taken for granted. These considerations are particularly relevant for systems of a fundamentally discrete nature where the consequences that obtain from a continuum description cannot be assumed [1–8]. This prompts enquiring what essential ingredients are required for collective periodic behaviours to emerge in a system whose components transition incoherently between only a finite number of states. Such systems are the topic of this thesis.

Collective periodic behaviour has long attracted the attention of the scientific community with commonly cited documentations including Huygens' record of the synchronisation of pendulum clocks [9], Asian tree canopies filled with fireflies flashing in unison [10, 11], circadian clocks [12, 13], oscillations in ecological systems [14], chemical oscillations [15, 16], synchronous neuronal spiking times [17–19] and pedestrians causing the wave-like wobbling of London's millennium bridge [20]. See [21, 22] for a review of such phenomena. At least three related areas of research warrant immediate discussion: *weakly coupled oscillators*, *integrate-and-fire models* and *stochastic resonance*.

1.0.1 Weakly Coupled Oscillators and Integrate-and-Fire

Synchronisation is currently a highly researched topic, with various models describing the phenomena in particular situations. Of particular note are systems of weakly-coupled oscillators [23,24], including the Kuramoto model [25,26] and various integrate-and-fire models, which find a particular use in biology and neuroscience [27–29]. Both of these models consist of a network of interconnected components. For weakly-coupled oscillators, the connections may be viewed as springs, although there is a

wide application in an electrical engineering setting [30, 31]. In the integrate-and-fire models connections are made to signify how one individual firing can influence others to fire themselves. Much research then focuses on describing how synchronisation conditions depend on these connections [32–37]. However, these models are based on the idea that each component has a built-in oscillatory mechanism and therefore shed no light on the origin of the periodic effects that transpire. This is especially true for systems described by dynamics that are, at the most fundamental level, entirely incoherent, stochastic and memoryless.

1.0.2 Stochastic Resonance

The constructive role that complete randomness, or noise, could play in establishing periodic behaviours was illuminated in 1981 by the discovery of *stochastic resonance* [38–40]. Originally posed as an explanation for the periodic occurrence of ice ages [41, 42], stochastic resonance is a nonlinear phenomenon whereby the effects of a weak periodic forcing to a deterministic system are amplified in the presence of noise. This resonance may occur even without a periodic driving force, which has been investigated more recently under the name *coherent resonance* [43, 44]. Reviews of stochastic resonance are provided by [45–47]. A common feature of these phenomena is that noise 'resonates' periodic behaviour that is latent in any underlying deterministic dynamics. But how can stochastic dynamics result in periodic behaviour?

Prior to the discovery of stochastic resonance, noise had been mostly thought of as a nuisance, or something that could only destroy order. In decades since, many other phenomena linked with the positive effect of noise have been found: *noise-induced transport* [48–52], *stochastic focusing* [53], *noise suppressing noise* [54] and *stochastic synchronisation* [55–59].

1.1 Interacting Particle Systems

In this thesis we consider a system containing a large number of *identical components* that individually assume one of a finite number of *states*. At each instant of time, a component may spontaneously *transition* into another state. Coupling between the components is then induced by allowing each component to influence the transition rates of every other. The coupling is assumed to be 'all-to-all' in the sense that the components are *indistinguishable*: it is possible to switch any two components without affecting the system. For this discrete system it is then the ensemble of components rather than the individuals themselves that can exhibit the characteristics of collective

periodic phenomena that may emerge despite the individual components behaving incoherently.

This general framework may be used to model a wide variety of different systems. The states may represent; energy levels, quantum states [60], cities, people [61–63], chemical species [64–67], lattice points [68], game strategies [2, 69–71], stages of an illness [72–75], gene states [76, 77], and the list goes on. Correspondingly, the components themselves may represent; atoms, photons, cars [78–80], e-mails, chemical compounds, electrons, players, people, proteins, and so on. Nevertheless, as an aid to provide a way to visualise the system and to allow for use of less abstract language, the components of the system are interpreted throughout the thesis as *particles* and the *states* as a discrete medium in which particles are able to *jump*, *hop* or *migrate* around.

1.1.1 Spatial Structure and Action at a Distance

One fundamental representation of a discrete medium is a network [81–86], being an arrangement of sites or nodes that are connected by edges, via which particles may move from one node to another. The topology of the nodes and edges defines the spatial structure. The qualities exhibited by the collection of particles on the *'macroscopic level'* is thus fully determined by the *'microscopic'* dynamics that govern the number of particles at each node, how they move from one node to another, and how they interact with other particles both *locally* and *globally*.

The spatial interpretation of the network allows one to identify the interaction between particles that are in different states as a type of *global interaction*, or *action at a distance* [87–89]. The concept of a *field* is especially effective in providing a mechanism to facilitate action or influence to occur at a distance: fields can combine both the medium and particles within the same theoretical construct. The idea of long-range interactions is often taken for granted in particle systems with a spatial continuum as particles are rarely at the same place at the same time. By contrast, in a system where space is discrete, particles can often be in the same place at the same time, hence a coupling that only allows particles to influence each other at the same node is certainly not trivial [90, 91].

1.1.2 Three Important Questions

With the spatial implications of the network in mind, three main questions are central to this thesis;

1. "What is the minimum number of nodes needed for periodic behaviour?"

2. “Can periodic behaviour emerge when single particles jump at an equal rate in both directions along an edge joining nodes?”

3. “Does collective periodic behaviour rely on interactions between particles that are at different nodes?”

Each of these questions is addressed at various stages throughout the thesis with the most conclusive answers being given in chapter 5.

1.2 Statistical Mechanics

Roughly speaking, *statistical mechanics* is a branch of physics that aims to derive the *macroscopic* properties of a system from the dynamics of its *microscopic* components. Here the terms ‘microscopic’ and ‘macroscopic’ should be understood in a relative sense [92]. The behaviour of the individual components and thus the dynamics describing them; classical mechanics, quantum mechanics or perhaps something more exotic, will depend on the particular system of interest. The theory introduces the concept of *probability* in order to explain the statistical properties of the system. However this is not to say that it necessarily assumes the true dynamics is stochastic, but rather that much of the detail of the microscopic dynamics is inaccessible or even irrelevant.

1.2.1 Thermodynamic Equilibrium

Equilibrium statistical mechanics is primarily concerned with describing the properties of a system that is in, or close to, *thermodynamic equilibrium*. Thermodynamic equilibrium is characterised by an absence of macroscopic flows of matter or of energy, despite the system remaining dynamical on the microscopic level. In equilibrium, the system appears to be motionless. Consequently it does not take much to convince oneself that a system that behaves periodically must necessarily be ‘away from’ thermodynamic equilibrium.

The study of systems that are not at thermodynamic equilibrium comes under the field of *non-equilibrium statistical mechanics* [93]. There are two types of non-equilibrium phenomena to consider: (i) *time-dependent* systems on their way to equilibrium, and (ii) *time-invariant (steady state)* systems, somehow kept away from equilibrium. A system categorised by the former cannot exhibit sustained oscillations but it may, however, behave periodically for a ‘very long’ time. On the other hand the second type of system may have persistent periodic behaviour, and then the task is to identify how the system is being “kept away from equilibrium”.

1.2.2 Micro-reversibility and Detailed Balance

In his development of the kinetic theory of gases in 1872 [94], Boltzmann introduced the statistical representation of a macroscopic process as an ensemble of elementary events that obeyed the laws of classical mechanics. The *time-reversibility* of Newton's equations then led him to the *principle of detailed balance*: at the equilibrium ensemble each collision is equilibrated by its reverse collision [95]. The idea allowed Boltzmann to demonstrate how microscopic reversibility could give rise to macroscopic irreversibility and proved that a thermodynamically closed system would converge to thermodynamic equilibrium.

The principle of detailed balance for chemical kinetics was introduced by Wegscheider in 1901, who subsequently found explicit relations between kinetic constants [96]. In addition, it was demonstrated that irreversible reaction cycles such as $A_1 \rightarrow A_2 \rightarrow A_3 \rightarrow A_1$ are not permitted. In 1931 Onsager proposed a general theory relating the principle of detailed balance with the symmetry of kinetic coefficients [97, 98]. The so-called *Onsager reciprocal relations* imply that damped oscillations in *homogeneous closed* systems near thermodynamic equilibrium are impossible, due to the necessarily real spectrum of eigenvalues associated with symmetric operators. Similar results for the systems of interacting particles are demonstrated in chapter 2.

1.3 Stochastic Dynamics

Over recent decades, some approaches to non-equilibrium statistical mechanics have developed a common unified mathematical framework. The main characteristic feature of these approaches is the assumption that the microscopic evolution of a system is stochastic, as opposed to being described by deterministic Hamiltonian dynamics. One benefit of this approach is that it can be extended to include systems where the microscopic components are far too complex to describe with classical or quantum mechanics. Examples of such systems are biological, ecological and even social systems [61].

The motivations for adopting a stochastic type of dynamics come from different backgrounds, and one can find authors with at least three different views. *(i) Coarse graining* [99, 100] - microscopic dynamics are deterministic but the macroscopic dynamics are only known to the level of discrete cells. *(ii) Interventionism/tracing/open systems* [101–103] - microscopic dynamics are deterministic but must be coupled with the environment. Observing only the system in isolation leads to non-deterministic dynamics. *(iii)* Remain agnostic about, or deny, the existence of an underlying deterministic

dynamics and regard the evolution as a stochastic process that forms the dynamics in its own right [104, 105].

1.3.1 Markov Processes

Regardless of differing interpretations, many authors adopt a similar mathematical formalism, in making the technical assumption, that the stochastic process describing the microscopic dynamics is in fact a *homogeneous (time independent) Markov process* [106, 107], or equivalently, the evolution of the system is governed by a first order ordinary differential equation, known as the *master equation* [108, 109].

Markov processes have the property of being *memoryless*, meaning that their stochastic evolution at each time is independent of their state at values at other times: the process does not 'remember' the past. If the evolution does not explicitly depend on time, the process is further called *time-independent* or *homogenous*. In the sequel this property is implied unless otherwise stated.

Whether or not the Markov assumption can justifiably describe physical processes is outside the scope of this thesis. However, time-independent Markov processes are prime candidates for exploring the fundamental requirements for periodic behaviour for two main reasons:

1. There are no intrinsic time correlations that could result in latent oscillations emerging, whose origin is completely artificial.

The Markov property imposes that the particles, and the entire system, are unable to retain any information of past times. In particular this forbids any kind of dead-time or delay period that would introduce artificial timescales into the system. In fact, the Markov property implies the distribution of the *sojourn times* of the particle at each node are *exponentially distributed random variables*, characteristic of the 'no memory' property.

2. Spontaneity completely contrasts, in some sense, with periodic order.

The period of a sustained oscillation can be defined as the stochastic recurrence time of some 'event' - such as the instant the number of particles at a node reaches a local maximum. The distribution of recurrence times in the case of a *perfectly periodic process* would be degenerate, spiked at some value corresponding to the period. The information entropy of such deterministic recurrence times is then identically zero, as there is no uncertainty. In contrast the exponential distributions of the particle sojourn times have maximum entropy, given the existence of a mean sojourn time.

In addition to the two theoretical reasons for imposing the Markov property, Markov processes are easy to simulate directly [110–112], and perhaps more importantly, they are relatively tractable mathematically.

1.4 Overview of the Thesis

In this chapter we have posed the question as to what are the essential ingredients for collective periodic behaviour in discrete systems with stochastic dynamics. *Weakly coupled oscillator* and *integrate-and-fire* models were briefly discussed for their prevalence in describing synchronisation in complex systems. The phenomena of *stochastic resonance* and *coherent resonance* were identified as an example of how incoherent noise could amplify latent oscillations in deterministic dynamics. The systems of interacting 'particles' that are studied throughout this thesis were introduced in section 1.1 and three important questions about particular requirements for periodic behaviour were posed. Section 1.2 gave a brief overview of statistical mechanics and in particular the principle of *detailed balance* and its relation to a systems approach to thermal equilibrium. Possible motivations for using *stochastic dynamics* were discussed in section 1.3. The reasons for assuming the *Markov property* and its use in exploring the fundamental requirements for periodic behaviour were provided.

The remainder of this thesis is organised as follows:

Chapter 2

We introduce the mathematical framework for interacting particle systems and discuss some immediate conditions for collective periodic behaviours. In particular we explore whether periodic behaviours can emerge in two-state systems.

Chapter 3

We discuss systems of non-interacting particles. We introduce some important aspects in the theory of Markov processes. We explore the link between detailed balance and the appearance of oscillations. We gain insights into which kinds of interactions may result in collective period behaviour.

Chapter 4

We introduce a model whereby the dynamics describing non-interacting particles is augmented by simple birth and death processes. Simulations of this model is show emergent periodic behaviour among other types of phenomena. Key ingredients for collective periodic behaviour are hypothesised.

Chapter 5

We consider general systems of interacting particles. We discuss how to derive the macroscopic description of the system from the microscopic dynamics. Conclusive answers to the second and third questions posed in section 1.1.2 are then provided and discussed.

Chapter 6

Discussion of the main results of the thesis, how the results generalise to other systems and their limitations. Additionally we discuss some possible routes for further research.

Chapter 2

Interacting Particle Systems

In this chapter the general properties of interacting particle systems are described. These are systems whereby particles interchange spontaneously between a finite number of states. In section 2.1 the mathematical framework is introduced. Two different interpretations of how interactions between the particles may arise are discussed in section 2.2.

In section 2.3 we discuss the *Markov property* that characterises 'memoryless' nature of the system. It implies that the probabilities that describe the particular configurations of the particles in the system are described by a *master equation* which is given in section 2.4. In section 2.5 we discuss the *macroscopic equations* that provide a deterministic continuum approximation to the evolution of the system. These equations can then be used to define the occurrence of collective periodic phenomena.

In section 2.6 we study probability distributions that are invariant under the dynamics and their connection to periodic behaviours. Periodic behaviours remain periodic when the direction of time is reversed, and so the equations that describe the evolution of probabilities when time runs backwards are outlined in section 2.7. In section 2.8 we describe the property of *detailed balance* and its implications to the *time reversibility* of the system, in particular we discuss the possibility of collective periodic behaviours when particles can only occupy two states in section 2.9.

2.1 Interacting Particle Systems

Consider a system of n indistinguishable particles that are each constrained to a finite set of states, $\{s_1, s_2, \ldots, s_N\} \stackrel{\text{def}}{=} \mathcal{S}$. Each state s_i is associated with the i^{th} node of a network that defines a type of spatial structure, whereby a particle can jump from a state s_i to another state s_j via a directed edge connecting i^{th} and j^{th} nodes. The system is

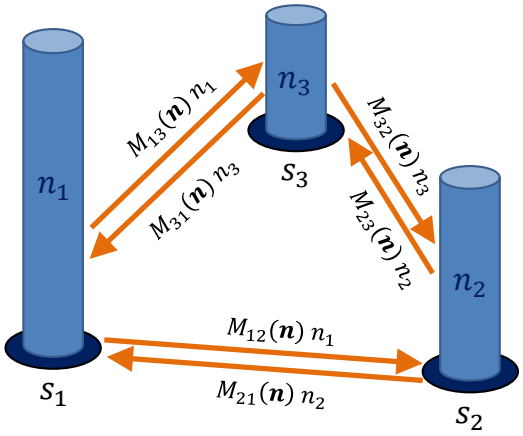


Figure 2.1: *Illustration of the populations of particles at each node of a three node network. Arrows show the total rate at which particles jump between different nodes.*

assumed to hold no memory of the past and so these jumps occur spontaneously at some rate M_{ij} that is generally dependent on the number of particles at each node. Thus the particles are coupled through an ability to influence the transition rate of other particles.

As the particles are *indistinguishable*, the configuration of the system at time t is completely specified by $\boldsymbol{n}(t) = (n_1(t), n_2(t), \ldots, n_N(t))$, where $n_i(t)$ is the number of particles that are located at the i^{th} node, see figure 2.1. The time evolution of $\boldsymbol{n}(t)$ follows a stochastic process on the configuration-space Ω, defined to be the set of all possible configurations of the system,

$$\Omega \overset{\text{def}}{=} \left\{ (n_1, n_2, \ldots, n_N) \ : \ n_i \in \mathbb{N}, \ \sum_i n_i = n \right\}. \tag{2.1.1}$$

An illustration of a configuration space is given in figure 2.2. If the total number of components n is not necessarily fixed, the condition $\sum_i n_i = n$ can be excluded from equation (2.1.1). The spontaneous nature of the particles implies that the stochastic process $\boldsymbol{n}(t)$ satisfies the *Markov property*, described in section 2.3. The evolution of the probabilities $P_\omega(t)$ that the configuration of the system is ω at time $t \geq 0$, conditioned on some initial probability distribution for the configuration of the system at time 0, is given by the *master equation* [108, 109], discussed further in section 2.4.

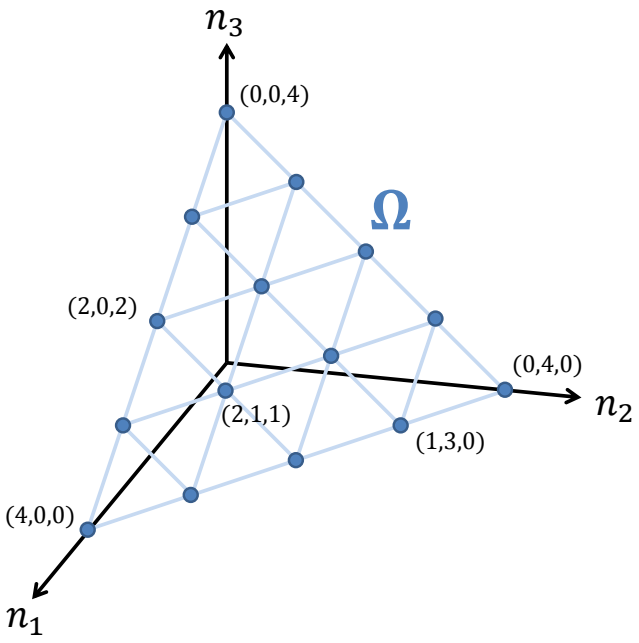


Figure 2.2: *Illustration of the configuration space Ω for a system with four particles and three states; $n = 4$ and $N = 3$. Blue circles represent different configurations.*

2.2 Mechanism for Interactions

Specifying the dynamics via the particle jump rates determines the behaviour of the system. However, it does not determine the mechanism for the interactions. While the mechanism for the interactions does not directly affect how the system behaves, it does change how one would interpret the results and so it is worth discussing some different ways of viewing how the interactions arise.

Particles interacting directly

Firstly one can view the particles as interacting directly, by some 'force'. This force then supplements the rates given by the network. The rate that a particle jumps is then dependent on both the spatial structure of the network and the position of other particles. From this viewpoint, the spatial structure is unaffected by the particles. A schematic of the interactions between the network and the particles is given by figure 2.3(a). Of course this says nothing about the cause of the force experienced between particles.

Interactions between particles that are located at different nodes can be viewed as a type of 'action at a distance', i.e. a non-local interaction of objects separated in space. It is therefore possible to define types of interaction that do not allow for such a non-local interaction, by only allowing particles to influence the behaviour of other particles that

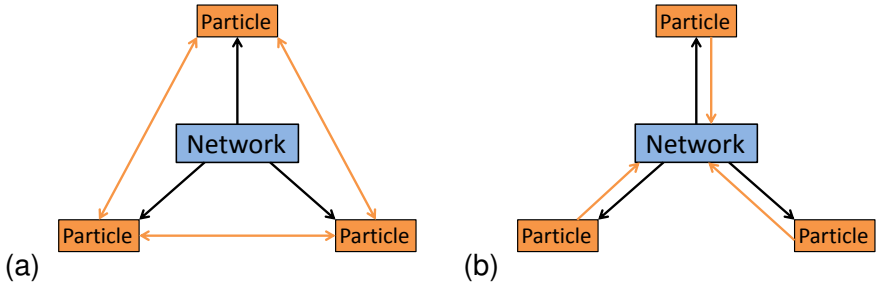


Figure 2.3: *Schematic of the mechanism for interactions between particles and the network. Arrows show the interactions between the components. (a) Particles interacting directly. (b) Particles interacting indirectly through the network.*

are at the same node. Such interactions are often called zero-range processes [90, 91] and are discussed further in chapter 5.

Particles interacting indirectly

An alternative view is to assume that the particles interact indirectly, via an interaction with the spatial structure itself. Thus the particles change the spatial structure of the network, implicitly affecting other particles. A schematic of this is given in figure 2.3(b). This is similar to the way massive particles interact in the theory of General Relativity [113].

To allow for action at a distance, a particle must have a non-local effect on the spatial structure, i.e. it must change the edges directed from nodes other than its current node. The analogue of the zero-range interactions is the specification that particles can only affect the local spatial structure, and thus only particles located at the same node can interact.

2.3 Markov Property

The spontaneity of the particles implies that the configuration vector $\boldsymbol{n}(t)$ follows a *Markov process* with state-space Ω [106, 107]. Markov processes have the property of being *memoryless*, meaning that their stochastic evolution at each time is independent of their state at other times, i.e. the process does not 'remember' the past. If the evolution does not explicitly depend on time, the process is further called *time-independent* or *time-homogeneous*. The memoryless property can be stated as

$$\Pr\{\boldsymbol{n}(t_3) = \omega_i | \boldsymbol{n}(t_2) = \omega_j,\ \boldsymbol{n}(t_1) = \omega_k\} \quad = \quad \Pr\{\boldsymbol{n}(t_3) = \omega_i | \boldsymbol{n}(t_2) = \omega_j\}, \qquad (2.3.1)$$

for all $t_3 > t_2 > t_1$. This is often called the *Markov property*. An equivalent way to state the Markov property is to say that the past and future are conditionally independent given the present,

$$\begin{aligned}&\mathsf{Pr}\left\{\boldsymbol{n}(t_3) = \omega_i,\ \boldsymbol{n}(t_1) = \omega_k | \boldsymbol{n}(t_2) = \omega_j\right\} \\ &\quad = \mathsf{Pr}\left\{\boldsymbol{n}(t_3) = \omega_i | \boldsymbol{n}(t_2) = \omega_j\right\}\ \mathsf{Pr}\left\{\boldsymbol{n}(t_1) = \omega_i | \boldsymbol{n}(t_2) = \omega_j\right\}. \qquad (2.3.2)\end{aligned}$$

The memoryless nature of the particle, together with time-homogeneity has implications on the distribution of the time taken for the particle to *jump* away from a state. Let T be the random variable representing the jump time and define the non-increasing function $s(t) \stackrel{\text{def}}{=} \mathsf{Pr}\{T > t\}$. The Markov property (2.3.1) gives

$$s(\tau) \;=\; \mathsf{Pr}\{T > t + \tau | T > t\} \;=\; \frac{\mathsf{Pr}\{T > t + \tau\}}{\mathsf{Pr}\{T > t\}} \;=\; \frac{s(t+\tau)}{s(t)}\,. \qquad (2.3.3)$$

Thus $\log s(t)$ is a linear and non-increasing function of t, and therefore $s(t) = e^{-\alpha t}$ for some $\alpha > 0$. This implies that T follows an *exponential distribution* with rate parameter α.

2.3.1 Properties of the Exponential Distribution

The exponential distribution has a number of useful properties. Assume that $T_1, T_2, \ldots$ are all independent and exponentially distributed with rates $\alpha_1, \alpha_2, \ldots$ respectively, then $\min_i T_i$ is also exponentially distributed with rate $\sum_i \alpha_i$. In other words, the first of many spontaneous events is itself spontaneous. To prove this result, simply use

$$\mathsf{Pr}\{\min_i T_i > t\} \;=\; \prod_i \mathsf{Pr}\{T_i > t\} \;=\; \prod_i e^{-\alpha_i t} \;=\; e^{-\sum_i \alpha_i t}\,. \qquad (2.3.4)$$

To determine the probability $\mathsf{Pr}\{T_1 = \min_i T_i\}$ use the fact that the minimum of all other times T_i is exponentially distributed with rate $\beta \equiv \sum_{i>1} \alpha_i$. The probability is then determined by

$$\begin{aligned}\mathsf{Pr}\{T_1 < \min_{i>1} T_i\} \;&=\; \int_0^\infty \alpha_1 e^{-\alpha_1 t}\ \mathsf{Pr}\{\min_{i>1} T_i > t\}\ dt \\ &=\; \alpha_1 \int_0^\infty e^{-\alpha_1 t}\, e^{-\beta t}\ dt \;=\; \frac{\alpha_1}{\alpha_1 + \beta} \;=\; \frac{\alpha_1}{\sum_i \alpha_i}\,. \qquad (2.3.5)\end{aligned}$$

Therefore the probability that the shortest time is T_i is proportional to the corresponding rate α_i. This property is useful when finding the equations which describe the evolution of the system.

2.4 Master Equation

The dynamics of the system is completely specified by the set of all rates at which the system transitions between each pair of configurations. Here the transition rate from configuration ω to $\hat{\omega}$ is defined as

$$\Gamma\{\omega \to \hat{\omega}\} \stackrel{\text{def}}{=} \lim_{\tau \to 0^+} \left\{ \frac{\mathsf{Pr}\{\, \boldsymbol{n}(\tau) = \hat{\omega} \mid \boldsymbol{n}(0) = \omega \,\}}{\tau} \right\}, \tag{2.4.1}$$

for $\omega \neq \hat{\omega}$. These transition rates are zero for each pair of configurations that differ by the position of more than one particle.

The evolution of the probabilities $P_\omega(t) \stackrel{\text{def}}{=} \mathsf{Pr}\{\, \boldsymbol{n}(t) = \omega \mid \boldsymbol{n}(0) \,\}$ that the configuration of the system is ω at time $t \geq 0$, conditioned on some initial probability distribution for the configuration $\boldsymbol{n}(0)$ of the system at time 0, is given by the *master equation* [108, 109],

$$\frac{d}{dt} P_\omega(t) \;=\; \sum_{\hat{\omega} \neq \omega} P_{\hat{\omega}}(t) \Gamma\{\hat{\omega} \to \omega\} - P_\omega(t) \Gamma\{\omega \to \hat{\omega}\} \,, \tag{2.4.2}$$

where the summation is taken over the entire configuration space Ω, except for ω. The master equation is a type of gain-loss equation for the probabilities P_ω. The first term in the summation represents the total gain of probability of the configuration ω from all other configurations. The second term represents the total loss of probability from the configuration ω to all other configurations.

2.4.1 Derivation of the Master Equation

To derive the master equation (2.4.2), calculate the evolution of the probabilities by rewriting,

$$\begin{aligned} P_\omega(t+\tau) &= \mathsf{Pr}\{\, \boldsymbol{n}(t+\tau) = \omega \mid \boldsymbol{n}(0) \,\} \\ &= \sum_{\hat{\omega}} \mathsf{Pr}\{\, \boldsymbol{n}(t+\tau) = \omega \mid \boldsymbol{n}(t) = \hat{\omega},\, \boldsymbol{n}(0) \,\} \mathsf{Pr}\{\, \boldsymbol{n}(t) = \hat{\omega} \mid \boldsymbol{n}(0) \,\} \\ &= \sum_{\hat{\omega}} \mathsf{Pr}\{\, \boldsymbol{n}(t+\tau) = \omega \mid \boldsymbol{n}(t) = \hat{\omega} \,\} P_{\hat{\omega}}(t) \\ &= \sum_{\hat{\omega}} \mathsf{Pr}\{\, \boldsymbol{n}(\tau) = \omega \mid \boldsymbol{n}(0) = \hat{\omega} \,\} P_{\hat{\omega}}(t) \,. \end{aligned} \tag{2.4.3}$$

These are known as the Chapman-Kolmogorov equations [107, 114]. The first step follows from the law of total probability, the second from the Markov property, and the third from time-homogeneity. One can then substitute the following into equation (2.4.3),

$$\mathsf{Pr}\{\boldsymbol{n}(\tau) = \omega | \boldsymbol{n}(0) = \omega\} \;=\; 1 - \sum_{\hat{\omega} \neq \omega} \mathsf{Pr}\{\boldsymbol{n}(\tau) = \hat{\omega} | \boldsymbol{n}(0) = \omega\} \tag{2.4.4}$$

to arrive at,

$$P_\omega(t+\tau) - P_\omega(t) = \sum_{\hat{\omega}\neq\omega} [\, \mathsf{Pr}\{\, \boldsymbol{n}(\tau) = \omega \mid \boldsymbol{n}(0) = \hat{\omega} \,\} P_{\hat{\omega}}(t) - \mathsf{Pr}\{\, \boldsymbol{n}(\tau) = \hat{\omega} \mid \boldsymbol{n}(0) = \omega \,\} P_\omega(t) \,] \,. \tag{2.4.5}$$

The master equation (2.4.2) follows from dividing by τ, taking the limit $\tau \to 0^+$ and using (2.4.1).

2.5 Macroscopic Equations

In general finding a solution to the master equation (2.4.2) is difficult due to the large number of configurations and the nonlinear dependence of the transition rates on the occupation numbers n_i at each state. Moreover, the master equation often contains 'too much information' as it describes the system fully on the microscopic level. In searching for the emergence of collective periodic behaviour in systems with a large number of particles, one is primarily concerned with the macroscopic description of the system, through variables such as $x_i(t) \stackrel{\text{def}}{=} n_i(t)/n$, where n is the total number of particles in the system. These macroscopic variables are stochastic and discrete. However under the assumption that the distributions $P_\omega(t)$ remain sharply peaked for the period of time under consideration, one can make the approximation $x_i(t) \approx \frac{1}{n}\sum_\omega n_i P_\omega(t)$ and treat $x_i(t)$ as if it is continuous and evolves deterministically. The deterministic equations that describe the evolution of the system are called the *macroscopic equations* and they are a set of first order differential equations,

$$\frac{d\boldsymbol{x}(t)}{dt} = \boldsymbol{f}(\boldsymbol{x}(t)) \,, \tag{2.5.1}$$

where $\boldsymbol{f}(\boldsymbol{x})$ is some vector valued function that can be determined as the leading order term in a system-size expansion of the master equation (2.4.2) [108, 115]. This approximation would be exact in the limiting case of systems with an infinite number of particles.

The emergence of collective periodic behaviour in the system is characterised by a *stable limit cycle* in the macroscopic equations (2.5.1), see figure 2.4. It may be possible for a system to oscillate even when no such limit cycle exists. This occurs due to fluctuation effects that are present in the next order of the size expansion, i.e. the *linear noise approximation*. This phenomenon is often called *amplification* [116–122]. However, oscillations that arise in this way are more erratic, do not form stable oscillations and are therefore not considered further in this thesis.

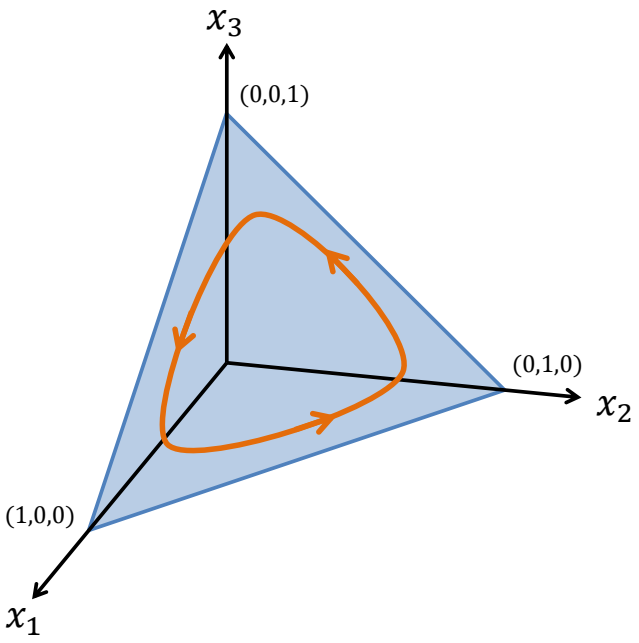


Figure 2.4: *Illustration of the phase space of the macroscopic equations (blue triangle) for a system with three states;* $N = 3$*. The orange trajectory represents a limit cycle corresponding to collective periodic behaviour.*

2.6 Steady-State Solutions

Of particular importance are solutions of the master equation that do not change with time. We call such a solution a *steady-state solution*. A probability distribution P^s_ω over the configurations Ω is called a steady-state solution of the master equation (2.4.2) if it is independent of time,

$$\sum_{\hat{\omega}\neq\omega} P^s_{\hat{\omega}}\,\Gamma\{\hat{\omega}\to\omega\} - P^s_\omega\,\Gamma\{\omega\to\hat{\omega}\} \;=\; 0\,. \tag{2.6.1}$$

As the configuration space Ω is finite, a steady-state solution is guaranteed to exist. Furthermore, it is unique if the system under consideration is *ergodic*. The system is called ergodic if, for every pair of configurations $\omega_i, \omega_j \in \Omega$, it can get from a configuration ω_i to ω_j in a finite number of steps. Ergodicity is assumed to hold for all systems considered in this thesis. Proof of the existence and uniqueness of the steady-state solution is given in section 3.4.

The probabilities $\Pr\{\boldsymbol{n}(t) = \omega\}$ are independent of time, and are therefore equal to the steady-state solution; $\Pr\{\boldsymbol{n}(t) = \omega\} \equiv P^s_\omega$. It follows that every configuration is visited an infinite number of times, with probability one and moreover P^s_ω is the average proportion of time spent by the system in the configuration ω. In the next chapter

it is proven that solutions to the master equation (2.4.2) approach the steady-state exponentially fast as time goes to infinity, for any initial distribution $P_\omega(0)$.

The terms in the summation in equation (2.6.1) are called the steady-state *probability currents* from $\hat{\omega}$ into ω, defined as

$$J\{\hat{\omega} \to \omega\} \quad \stackrel{\text{def}}{=} \quad P^s_{\hat{\omega}}\, \Gamma\{\hat{\omega} \to \omega\} - P^s_{\omega}\, \Gamma\{\omega \to \hat{\omega}\}. \tag{2.6.2}$$

The steady-state solutions are such that the total probability current into each configuration is zero. For systems with a large number of particles the collective behaviour can be explained, to leading order, using the macroscopic equations (2.5.1), where collective periodic behaviours are identified with stable limit-cycles. The limiting behaviour of the macroscopic equations is intimately linked with the steady-state solution to the master equation, and the associated probability currents (2.6.2). This link is explored further in chapter 5.

2.7 Backwards Master Equation

Periodic behaviour that is observed in the system must also be periodic if the direction of time is reversed. In order to describe evolution backwards in time, one uses a master equation that is generally different to (2.4.2). The evolution of probabilities for times, $t < 0$, prior to the initial condition obeys a master equation with transition rates given by,

$$\Gamma^b\{\omega \to \hat{\omega}\} \quad \stackrel{\text{def}}{=} \quad \lim_{\tau \to 0^+} \left\{ \frac{\mathsf{Pr}\{\, \boldsymbol{n}(-\tau) = \hat{\omega} \mid \boldsymbol{n}(0) = \omega \,\}}{\tau} \right\}, \tag{2.7.1}$$

for $\omega \neq \hat{\omega}$. The *backwards master equation* is then given by,

$$\frac{d}{dt} P_\omega(t) \quad = \quad \sum_{\hat{\omega} \neq \omega} P_{\hat{\omega}}(t) \Gamma^b\{\hat{\omega} \to \omega\} - P_\omega(t) \Gamma^b\{\omega \to \hat{\omega}\}\ . \tag{2.7.2}$$

Each backwards rate $\Gamma^b\{\omega \to \hat{\omega}\}$ can be related to the (forwards) rate $\Gamma\{\hat{\omega} \to \omega\}$ given in equation (2.4.1) by a simple application of Bayes' theorem,

$$P^s_\omega\, \Gamma^b\{\omega \to \hat{\omega}\} \quad = \quad P^s_{\hat{\omega}}\, \Gamma\{\hat{\omega} \to \omega\}\ , \tag{2.7.3}$$

for all pairs of configurations ω and $\hat{\omega}$. This relation is intuitive as the left-hand side is the rate of the transition $\omega \to \hat{\omega}$ occurring when time is run backwards, the right-hand side is the rate of the transition $\hat{\omega} \to \omega$ occurring when time runs forwards. These are equal because they both correspond to the same events.

Given a steady-state solution P^s_ω for the original master equation (2.4.2) is equivalent to $\mathsf{Pr}\{\boldsymbol{n}(t) = \omega\}$, it is apparent that this is also a steady-state solution of the backwards

master equation (2.7.2). From the relation (2.7.3) the backwards probability currents $J^b\{\omega \to \hat{\omega}\}$ are respectively equal to the $J\{\hat{\omega} \to \omega\}$, as one would expect from reversing the direction of time. Similarly if a periodic limit cycle is present in the macroscopic equations (2.5.1), then reversing time reverses the direction of the limit cycle.

2.8 Reversibility and Detailed Balance

A sufficient, but not necessary, condition for a probability distribution P^s_ω to be a steady-state solution, i.e. satisfying (2.6.1), is for the distribution to satisfy,

$$P^s_\omega \, \Gamma\{\omega \to \hat{\omega}\} \quad = \quad P^s_{\hat{\omega}} \, \Gamma\{\hat{\omega} \to \omega\} \, . \tag{2.8.1}$$

This is called the *detailed-balance* property [123–127]. The property of detailed balance asserts that in the steady-state, every transition $\omega \to \hat{\omega}$ occurs as often as its reverse transition $\hat{\omega} \to \omega$. Alternatively it can be interpreted as saying that the steady state probability currents $J\{\omega \to \hat{\omega}\}$ are identically zero. For this reason, a steady-state that satisfies detailed balance is said to be in *thermodynamic equilibrium*, or called an *equilibrium steady-state*, see section 1.2.1.

The detailed balance condition (2.8.1) can be used with equation (2.7.3) for the rates of the backwards master equation (2.7.2) to establish that an equilibrium steady-state requires the forwards and backwards rates to be equal,

$$\Gamma^b\{\omega \to \hat{\omega}\} \quad = \quad \Gamma\{\omega \to \hat{\omega}\} \, . \tag{2.8.2}$$

This means that the backwards master equation (2.7.2) and the forwards master equation (2.4.2) are the same, and therefore the past and the future are statistically the equivalent, conditioned on the present. Processes that satisfy (2.8.2) are called *reversible*.

The Markov property (2.3.2) states that the past and the future are independent, given the present, and so this suggests that a system satisfying detailed balance cannot behave periodically - a periodic orbit in the macroscopic equations is in violation of the reversibility of time. For collective periodic behaviour to emerge in systems of interacting particles, the principle of detailed balance must not hold.

2.9 Particles on a Network with Two Nodes

The fact that collective periodic phenomena cannot occur in a system that satisfies detailed balance can be simply applied to systems of n interacting particles that are

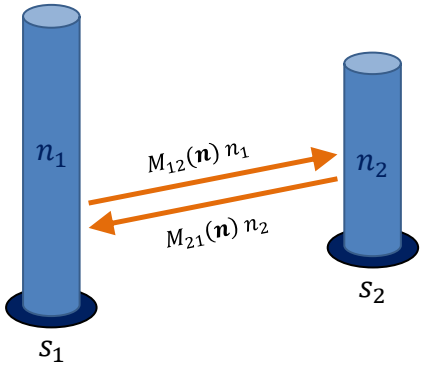


Figure 2.5: *Illustration of the populations of particles at each node of a two node network. Arrows show the total rate at which particles jump between different nodes.*

constrained to a network with only two nodes. For such systems the configuration space is given by $\Omega = \{(k, n-k) \ : \ k \in \{0, 1, \ldots, n\}\}$ and the equation (2.6.1) for the steady-state solutions of the master equation (2.4.2) can be written as

$$\sum_{j=0}^{n} J\{(j, n-j) \to (k, n-k)\} \quad = \quad 0 \, , \tag{2.9.1}$$

for $k \in \{0, 1, \ldots, n\}$. Here the J's are the probability currents defined in (2.6.2). When $k = 0$, equation (2.9.1) gives $J\{(1, n-1) \to (0, n)\} = 0$, and so the probability current between the configurations $(0, n)$ and $(1, n-1)$ is necessarily zero. This can be used when $k = 1$ in equation (2.9.1) to give $J\{(2, n-2) \to (1, n-1)\} = 0$, implying that the probability current between the configurations $(1, n-1)$ and $(2, n-2)$ is also zero. Continuing inductively implies that all of the probability currents are identically zero. This shows that a system of interacting particles constrained to two states must satisfy detailed balance and consequently the process is reversible and collective periodic behaviour cannot arise.

2.10 Discussion

In this chapter systems of interacting particles that are constrained to spontaneously jumping between the discrete nodes of a network were introduced. It was discussed in section 2.1 that the configuration of the system at particular time is given by the number of particles that occupy each of the nodes. Different interpretations of how interactions between the particles may arise were outlined in section 2.2.

Particles jump spontaneously between nodes and so the evolution of the system satisfies the *Markov property*, introduced in section 2.3. The Markov property states that

the past and the future are conditionally independent. The dynamics of the system is completely specified by the transition rates between different configurations of the system. In section 2.4 it was shown that the evolution of the probabilities that determine the likely configuration of the system at a particular time obey a first order differential equation, the *master equation*. In general this equation is difficult to solve and so deterministic *macroscopic equations*, as seen in section 2.5, are used as an approximation. Collective periodic phenomena can then be identified with limit cycles in the macroscopic equations.

Steady-state solutions of the master equation were defined in section 2.6 to be the time invariant probability distributions on the set of all configurations. Together with the assumption of *ergodicity*, steady state solutions and their associated *probability currents* describe the long term behaviour of the system and are strongly linked with any periodic behaviours that may emerge and persist.

In section 2.7, the *backwards master equations* describing the evolution of the system when the direction of time is reversed were discussed and a relation between the backwards and forwards transition rates was stated. The property of *detailed balance* and its link with *time reversibility* was discussed in section 2.8. Reversibility excludes the possibility for collective periodic behaviours. This was used in section 2.9 to prove that collective periodic behaviours could not emerge when particles are constrained to only two possible states.

In the next chapter 3 we explore the simplest type of system where the particles behave independently. In this context we prove some of the assertions that were made in this chapter if ergodicity is assumed, namely that the steady-state solutions are unique and represent the limiting distribution of all solutions to the master equation.

Chapter 3

Systems of Non-Interacting Particles

In this chapter we explore the extent to which oscillatory behaviour can exist in systems of non-interacting particles, jumping spontaneously around the nodes of a network. It is demonstrated that some form of interaction is critical for collective phenomena, but nevertheless systems of non-interacting particles provide a useful insight into what ingredients are necessary for periodic behaviours to be able to emerge and persist. Through exploring some known results, with emphasis on oscillatory behaviour, this chapter develops some of the ideas and systems that form the foundation for the main results presented in later chapters.

In the previous chapter we introduced systems of interacting particles and discussed two main equations that are useful for describing the time evolution - the *master equation* (2.4.2) and the *macroscopic equations* (2.5.1). In section 3.1 the master equation is introduced in the context of non-interacting particle systems. Section 3.2 then describes how the macroscopic equations can be derived from the master equation.

In the absence of interactions, each particle behaves independently and so the behaviour of a single particle is discussed in section 3.3. It is then demonstrated in section 3.4 that the solutions to the macroscopic equations evolve towards a distribution of particles that is independent of time. This distribution is subsequently linked with the *steady-state solutions* of the master equation.

The consequences of *detailed balance* for non-interacting particles systems is discussed in section 3.5. It is shown that systems where particles jump between states equally in both directions do not display oscillatory behaviour. Furthermore, in section 3.6 we see that particles constrained to only two-states are also unable to oscillate.

In section 3.7 we discuss how the solutions to the macroscopic equations for irreversible

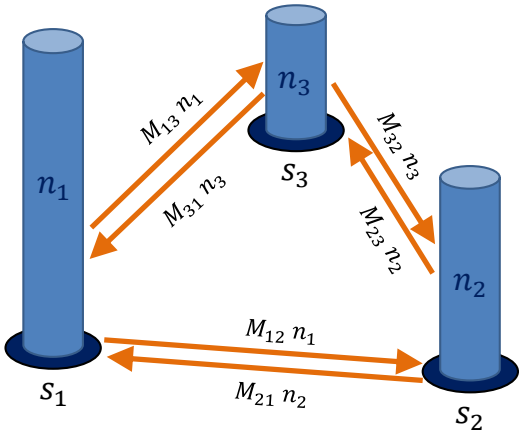


Figure 3.1: *Illustration of the populations of non-interacting particles at each node of a three node network. Arrows show the total rate at which particles jump between different nodes. As the particles do not interact, the rates M_{ij} do not depend on the configuration $\boldsymbol{n}(t)$.*

systems can be expanded in terms of *wave-packets* that may have both an oscillatory and decaying component.

In section 3.8 we analyse a simple three-state system that displays heavily damped oscillatory behaviour. This forms the basis for models used in later chapters 4 and 5. An extension to larger sized systems is given in section 3.9, where it is demonstrated that oscillations may be more prominent when there are more states available to the particles.

3.1 Non-Interacting Particles

For a system consisting of n non-interacting particles constrained to the state-space $\{s_1, s_2, \ldots, s_N\}$, each particle jumps around the network independently of the positions of all other particles. A particle located at the i^{th} node jumps to the j^{th} node at a rate M_{ij}, with $M_{ij} = 0$ if the particle cannot jump directly between the two nodes. These jump rates can be be expressed in a *rate matrix* $\boldsymbol{M}$ with an $(i,j)^{th}$ component M_{ij}. The diagonal components M_{ii} are defined to be the negative of the rate at which a particle jumps from the i^{th} node, so that $\sum_j M_{ij} = 0$.

3.1.1 Master Equation

The configuration of the system at a time t is specified by the vector $\boldsymbol{n}(t)$, whose component $n_i(t)$ is the number of particles located at the i^{th} node. The rate at which the system interchanges from a configuration $\boldsymbol{j}$ into another configuration $\boldsymbol{k}$ is given by $\Gamma\{\boldsymbol{j} \to \boldsymbol{k}\}$. Given an initial configuration $\boldsymbol{n}(0)$ at time zero, the evolution of probabilities $P_{\boldsymbol{k}}(t)$ of the system having the configuration $\boldsymbol{k}$ at times $t \geq 0$ is given by the master equation,

$$\frac{d}{dt}P_{\boldsymbol{k}}(t) \;=\; \sum_{\boldsymbol{j}\neq\boldsymbol{k}} P_{\boldsymbol{j}}(t)\Gamma\{\boldsymbol{j} \to \boldsymbol{k}\} - P_{\boldsymbol{k}}(t)\Gamma\{\boldsymbol{k} \to \boldsymbol{j}\}\;, \tag{3.1.1}$$

where the summation is over the set of all possible configurations Ω, except for the configuration $\boldsymbol{k}$. The transition rates $\Gamma\{\boldsymbol{j} \to \boldsymbol{k}\}$ are zero for each pair of configurations that differ by the position of more than one particle. Thus the non-zero rates are those of the form $\Gamma\{\boldsymbol{k} \to \boldsymbol{k} - \boldsymbol{e}_i + \boldsymbol{e}_j\}$, with $\boldsymbol{e}_i$ being a vector taking the value of unity for the i^{th} component and zero elsewhere. These represent the total rate that one of the particles at the i^{th} node jumps to the j^{th} node. As there are k_i such particles the transition rates are given by,

$$\Gamma\{\boldsymbol{k} \to \boldsymbol{k} - \boldsymbol{e}_i + \boldsymbol{e}_j\} \;=\; M_{ij}\, k_i\;, \tag{3.1.2}$$

for $i \neq j$. These transition rates are demonstrated in figure 3.1. It is convenient to define the total transition rate out of the configuration $\boldsymbol{k}$ to be

$$-\Gamma\{\boldsymbol{k} \to \boldsymbol{k}\} \;\stackrel{\text{def}}{=}\; \sum_{\boldsymbol{j}\neq\boldsymbol{k}} \Gamma\{\boldsymbol{k} \to \boldsymbol{j}\}\;, \tag{3.1.3}$$

so that the master equation (3.1.1) can then be rewritten as,

$$\frac{d}{dt}P_{\boldsymbol{k}}(t) \;=\; \sum_{\boldsymbol{j}\in\Omega} P_{\boldsymbol{j}}(t)\Gamma\{\boldsymbol{j} \to \boldsymbol{k}\}\;, \tag{3.1.4}$$

where now the summation is over all configurations.

3.2 Macroscopic equations

The macroscopic equations are deterministic equations concerning the macroscopic variables $\boldsymbol{x}(t) = \boldsymbol{n}(t)/n$ that approximate the evolution of the system by making the assumption $\boldsymbol{n}(t) \approx \langle \boldsymbol{n}(t) \rangle$ that the configuration is sufficiently approximated by the mean configuration,

$$\langle \boldsymbol{n}(t) \rangle \;\stackrel{\text{def}}{=}\; \sum_{\boldsymbol{k}\in\Omega} \boldsymbol{k}\; P_{\boldsymbol{k}}(t)\;. \tag{3.2.1}$$

The macroscopic equations are then derived by considering the evolution of the mean configuration. Using the master equation (3.1.4),

$$\begin{aligned}\frac{d}{dt}\langle \boldsymbol{n}(t)\rangle &= \sum_{\boldsymbol{k}\in\Omega} \boldsymbol{k} \sum_{\boldsymbol{j}\in\Omega} \Gamma\left\{\boldsymbol{j}\to\boldsymbol{k}\right\} P_{\boldsymbol{j}}(t) \\ &= \sum_{\boldsymbol{j}\in\Omega} P_{\boldsymbol{j}}(t) \sum_{\boldsymbol{k}\in\Omega} \boldsymbol{k}\, \Gamma\left\{\boldsymbol{j}\to\boldsymbol{k}\right\} \ . \end{aligned} \tag{3.2.2}$$

The summation over $\boldsymbol{k}$ can be expanded, by using equation (3.1.2), as

$$\begin{aligned}\sum_{\boldsymbol{k}\in\Omega} \boldsymbol{k}\, \Gamma\left\{\boldsymbol{j}\to\boldsymbol{k}\right\} &= \sum_{a,b=1}^{N} \left(\boldsymbol{j}-\boldsymbol{e}_a+\boldsymbol{e}_b\right)\ j_a\ M_{ab} \\ &= \sum_{b=1}^{N} \boldsymbol{e}_b \sum_{a=1}^{N} j_a\ M_{ab}\ , \end{aligned} \tag{3.2.3}$$

where the last equality follows from $\sum_b M_{ab} = 0$. Substituting back into the equation (3.2.2) for $d\langle \boldsymbol{n}(t)\rangle/dt$ then gives

$$\frac{d}{dt}\langle \boldsymbol{n}(t)\rangle = \sum_{b=1}^{N} \boldsymbol{e}_b \sum_{\boldsymbol{j}\in\Omega} P_{\boldsymbol{j}}(t) \sum_{a=1}^{N} M_{ab}\ j_a\ , \tag{3.2.4}$$

or equivalently

$$\frac{d}{dt}\langle \boldsymbol{n}(t)\rangle = \langle \boldsymbol{n}(t)\ \boldsymbol{M}\rangle\ . \tag{3.2.5}$$

In this derivation of this equation nothing has been assumed about the dependence of the rate matrix $\boldsymbol{M}$ on the configuration $\boldsymbol{n}(t)$. Therefore equation (3.2.5) holds for general interacting particle systems, and is revisited again in section 5.1. For non-interacting particles equation (3.2.5) can be divided by the total number of particles n, and the independence of $\boldsymbol{M}$ on $\boldsymbol{n}(t)$ can be used to take the rate matrix out of the expectation. The result is the macroscopic equations,

$$\frac{d\boldsymbol{x}}{dt} = \boldsymbol{x}(t)\ \boldsymbol{M}\ . \tag{3.2.6}$$

It is shown in the next section that the macroscopic variables $\boldsymbol{x}(t)$ follow the same equations as the probability distribution for the position of a single particle. It follows from the properties of the rate matrix that the macroscopic equations (3.2.6) decay towards a fixed point and do not have any periodic orbits.

3.2.1 Properties of the Rate Matrix

Because the macroscopic equations (3.2.6) are linear, the behaviour of the system can be determined by the properties of the rate matrix $\boldsymbol{M}$. There are two important properties to consider.

1. The rate matrix $\boldsymbol{M}$ has a zero eigenvalue.

This follows from the fact that the columns of $\boldsymbol{M}$ are linearly dependent, $\sum_j M_{ij} = 0$. A corresponding right-eigenvector to the zero eigenvalue is $\mathbf{1}^T$, the unit column vector. The zero eigenvalue is unique (has multiplicity one) if the system is assumed to be *ergodic*, i.e. every configuration can be reached from any initial configuration, as discussed further in section 3.3.2.

2. All non-zero eigenvalues of $\boldsymbol{M}$ have a negative real part.

The *Gershgorin Circle Theorem* [128, 129] states that the eigenvalues of the matrix $\boldsymbol{M}$ must lie on the union of N discs with centres M_{ii} and radii $\sum_{j \neq i} M_{ij} = -M_{ii}$ in the complex plane. All of such discs are fully within the negative (left) half of the complex plane except for a single point at the origin.

3.3 Single Particle Systems

As the particles do not interact it makes sense to consider the behaviour of a system with just one single particle. The configuration of a single particle system at each time t is specified by position $X(t)$ of the particle, and the stochastic process $X(t)$ is a Markov process on the state-space $\mathcal{S} = \{s_1, s_2, \ldots, s_N\}$. Let the probability distribution of the particle at time zero be an arbitrary distribution $\boldsymbol{p}(0)$ over the state-space $\mathcal{S}$, then the *distribution of the particle* at time t, $\boldsymbol{p}(t)$, is defined component-wise as,

$$p_i(t) \stackrel{\text{def}}{=} \Pr\{X(t) = s_i | \boldsymbol{p}(0)\} \ . \tag{3.3.1}$$

The rates at which the particle jumps between different states are simply given by the rate matrix $\boldsymbol{M}$, and so the probabilities satisfy the following master equation for all i,

$$\frac{dp_i}{dt} = \sum_{j \neq i} M_{ji}\, p_j(t) - M_{ij}\, p_i(t) = \sum_j M_{ji}\, p_j(t) \ . \tag{3.3.2}$$

Written as a matrix equation, the master equation is

$$\frac{d\boldsymbol{p}}{dt} = \boldsymbol{p}(t)\, \boldsymbol{M} \ . \tag{3.3.3}$$

This equation has the same form as the macroscopic equations (3.2.6), and thus the macroscopic behaviour of a system with a large number of non-interacting particles is determined by the probability distribution of an individual particle. The solution to the linear differential equation (3.3.3), with initial condition $\boldsymbol{p}(0)$ is

$$\boldsymbol{p}(t) = \boldsymbol{p}(0)\, \exp(t\boldsymbol{M}) \ , \tag{3.3.4}$$

where $\exp(t\boldsymbol{M})$ is a matrix exponential defined by

$$\exp(t\boldsymbol{M}) \quad \stackrel{\text{def}}{=} \quad \sum_{k=0}^{\infty} \frac{t^k}{k!} \boldsymbol{M}^k \ . \tag{3.3.5}$$

3.3.1 Transition Matrix

The probabilities $\boldsymbol{p}(t)$ can also be expressed in terms of the probabilities $\boldsymbol{p}(0)$ via a *transition matrix* [107]. Define the transition matrix $\boldsymbol{\Phi}(t)$ by the components

$$\Phi(t)_{ij} \quad \stackrel{\text{def}}{=} \quad \text{Pr}\left\{X(t) = s_j | X(0) = s_i\right\} \ . \tag{3.3.6}$$

Thus the $(i,j)^{th}$ component is the probability that a particle at the i^{th} node at time zero, is at the j^{th} node at time t. One has the equation $\boldsymbol{p}(t) = \boldsymbol{p}(0)\ \boldsymbol{\Phi}(t)$, and by comparing to equation (3.3.4) it is apparent that the transition matrix is related to the rate matrix via

$$\boldsymbol{\Phi}(t) \quad = \quad \exp(t\boldsymbol{M}) \ . \tag{3.3.7}$$

From this relationship it can be seen that if λ is an eigenvalue of the rate matrix $\boldsymbol{M}$, then $e^{\lambda t}$ is an eigenvalue of the transition matrix $\boldsymbol{\Phi}(t)$. In particular, as the rate matrix has a zero eigenvalue, the transition matrix necessarily has a unit eigenvalue. Indeed it can be confirmed that the unit column vector $\boldsymbol{1}^T$ is a right-eigenvector corresponding to this eigenvalue, simply by the sum of probabilities $\sum_j \Phi_{ij}(t) = 1$.

3.3.2 Ergodicity

In section 2.6 a system of interacting particles was said to be *ergodic* [106] if it was possible for the system to change between every pair of configurations in a finite number of steps, i.e. a sequence of particle jumps. For a system of non-interacting particles, ergodicity can be determined from the form of the rate matrix $\boldsymbol{M}$ for a single particle. If the rate $M_{ij} > 0$, the particle is able to jump directly from a state s_i to state s_j, represented by a directed edge in the network from i^{th} node to the j^{th} node. The system is ergodic if for each pair of states s_i, s_j there exists a sequence of states $(s_{i_k})_{k=1}^{L}$ with $s_{i_1} = s_i$, $s_{i_L} = s_j$ such that $\prod_{k=1}^{k=L-1} M_{i_k i_{k+1}} > 0$. The particle can find a *path* between every pair of states.

Figure 3.2 provides an illustration of two ways in which ergodicity may not hold. If the system is ergodic each component of the transition matrix $\Phi_{ij}(t)$ is non-zero for all $t > 0$ and a particle will visit each node infinitely often, with probability one.

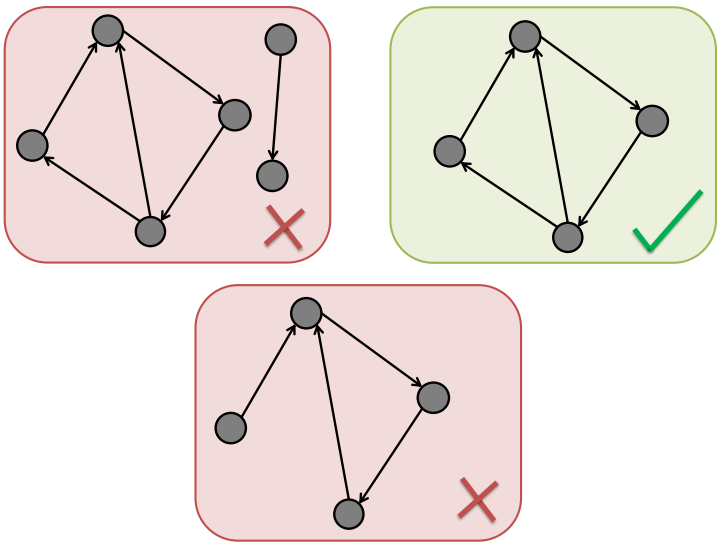


Figure 3.2: *Networks corresponding to three different systems. Nodes of the network correspond to states. Edges show which direction particles are able to jump between states. The leftmost system is not ergodic because it comprises two components that are not connected. The bottom system is not ergodic because one of the states cannot be reached by a particle at any of the other states. The system on the right is ergodic because a particle can find a path between every pair of states.*

3.4 Time-Invariant Distribution

Given that the probability distribution of a single particle evolves according to the master equation (3.3.3), it is natural to ask about probability distributions that are *time-invariant*. Such a distribution $\boldsymbol{\pi}$ is a left-eigenvector of the rate matrix $\boldsymbol{M}$ corresponding to the zero eigenvalue, and hence also an eigenvector of the transition matrix $\boldsymbol{\Phi}(t)$ for all times $t > 0$, with a unit eigenvalue such that

$$\sum_i \pi_i \, M_{ij} \;\; = \;\; 0 \, , \tag{3.4.1}$$

$$\sum_i \pi_i \, \Phi_{ij} \;\; = \;\; \pi_j \, . \tag{3.4.2}$$

It must be confirmed that all $\pi_i \geq 0$ so that $\boldsymbol{\pi}$ is indeed a probability distribution [107]. If the system is ergodic then $\Phi_{ij} > 0$ and the proof is as follows. Assume that some of the $\pi_i < 0$. Then by taking absolute values of equation (3.4.2) one gets, $\sum_i |\pi_i| \, \Phi_{ij} < |\pi_j|$ as some cancellation occurs. By taking a summation over the index j and using the sum of probabilities $\sum_j \Phi_{ij} = 1$, one arrives at the contradiction $\sum_i |\pi_i| < \sum_j |\pi_j|$. Thus the assumption is false and from (3.4.2) all $\pi_i > 0$.

Ergodicity also guarantees the uniqueness of the time-invariant distribution $\boldsymbol{\pi}$. If this

were not the case, it would be possible to find another distribution $\hat{\boldsymbol{\pi}}$ such that $\boldsymbol{\pi} \cdot \hat{\boldsymbol{\pi}} = 0$. However, this is impossible because all π_i and $\hat{\pi}_i$ are strictly positive. Given the time-invariant distribution $\boldsymbol{\pi}$ is unique, it can be interpreted as the probability distribution of a particle at time t given no information about the particle at any other time, thus

$$\pi_i = \mathsf{Pr}\{X(t) = s_i\} \tag{3.4.3}$$

for all times t. It is simple to confirm that equation (3.4.2) does indeed hold for these probabilities.

3.4.1 Limiting Behaviour of the Particle

In section 3.2.1 it was proven that the non-zero eigenvalues of the rate matrix $\boldsymbol{M}$ must have a negative real part. Consequently, any time dependent probability distribution $\boldsymbol{p}(t)$ of particle necessarily converges to the time-invariant distribution,

$$\lim_{t\to\infty} \boldsymbol{p}(t) \;\; = \;\; \boldsymbol{\pi} \; , \tag{3.4.4}$$

for any initial condition $\boldsymbol{p}(0)$. When a particle with known location at an initial time zero is left unobserved, information about its position is lost over time, eventually resulting in knowledge of the distribution at the initial time becoming practically irrelevant. To prove the limit (3.4.4) consider the time evolution of the energy-like function [130]

$$\phi(\boldsymbol{p}(t)) \;\; \stackrel{\mathsf{def}}{=} \;\; \sum_i \frac{1}{\pi_i} \, p_i(t)^2 \; . \tag{3.4.5}$$

The time derivative of this function is

$$\frac{d\phi}{dt} \;\; = \;\; \sum_{j=1}^{N} \frac{dp_j}{dt} \, \frac{\partial \phi}{\partial p_j} \;\; = \;\; \sum_{i,j=1}^{N} 2M_{ij} \, \pi_i \, \frac{p_i(t)}{\pi_i} \, \frac{p_j(t)}{\pi_j} \; . \tag{3.4.6}$$

This is a quadratic form associated with a matrix with the $(i,j)^{th}$ components given by $\pi_i \, M_{ij}$. The quadratic form in equation (3.4.6) can be written in terms of a symmetric matrix,

$$\frac{d\phi}{dt} \;\; = \;\; \sum_{i,j=1}^{N} (M_{ij} \, \pi_i + M_{ji} \, \pi_j) \, \frac{p_i(t)}{\pi_i} \, \frac{p_j(t)}{\pi_j} \; . \tag{3.4.7}$$

As the matrix with $(i,j)^{th}$ components given by $\pi_i \, M_{ij} + M_{ji} \, \pi_j$ is symmetric, it necessarily has real eigenvalues [131]. Moreover it is a rate matrix for a Markov process in its own right - the off-diagonal terms are non-negative and the rows sum to zero. It follows that the non-zero eigenvalues of this matrix are negative and so the quadratic form in equation (3.4.7) is non-positive definite, giving

$$\frac{d\phi}{dt} \;\; \leq \;\; 0 \; . \tag{3.4.8}$$

Ergodicity of the system with rate matrix M implies ergodicity of a system with rates $\pi_i\ M_{ij} + M_{ji}\ \pi_j$, and hence equality in equation (3.4.8) holds if and only if $\boldsymbol{p}(t) = \boldsymbol{\pi}$. For time dependent probability distributions, the value of ϕ is strictly decreasing in time and the limit (3.4.4) is proven.

3.4.2 Steady-State Solution

For a system with n particles, possibly interacting, the *steady-state* solution is simply the time-invariant distribution for the Markov process $\boldsymbol{n}(t)$ on the configuration space Ω. Thus the existence, uniqueness and limiting distribution of the steady state simply follow from the results for the time-invariant distribution $\boldsymbol{\pi}$ in this equation.

When the particles do not interact, the *steady-state* solution of the n particle system is given by the multinomial probability distribution,

$$P^s_{\boldsymbol{k}} \quad = \quad \frac{n!}{k_1!k_2!\ldots k_N!}\ \pi_1^{k_1}\pi_2^{k_2}\ldots\pi_N^{k_N}\ . \tag{3.4.9}$$

The steady-state solution has the associated *probability currents* given by

$$\begin{aligned} J\{\boldsymbol{k} \to \boldsymbol{k} - \boldsymbol{e}_i + \boldsymbol{e}_j\} \quad &= \quad P^s_{\boldsymbol{k}}\ k_i\ M_{ij} - P^s_{\boldsymbol{k}-\boldsymbol{e}_i+\boldsymbol{e}_j}\ (k_j+1)\ M_{ji} \\ &= \quad P^s_{\boldsymbol{k}}\ k_i\ \pi_i^{-1}\ (\pi_i\ M_{ij} - \pi_j\ M_{ji})\ . \end{aligned} \tag{3.4.10}$$

The probability currents for a system with non-interacting particles are therefore multiples of the probability currents for the single particle system, $\pi_i\ M_{ij} - \pi_j\ M_{ji}$.

3.5 Detailed Balance

The property of *detailed balance* holds for an interacting particle system if and only if all of the probability currents are identically zero. From equation (3.4.10) it is apparent that the property of detailed balance holds for a system of n non-interacting particles if and only if it holds for the single particle system,

$$\pi_i\ M_{ij} \quad = \quad \pi_j\ M_{ji}\ . \tag{3.5.1}$$

In section 2.8 it was shown that an interacting particle system satisfying detailed balance is time-reversible, meaning that the evolution of the system is statistically equivalent if the direction of time is reversed. If a system of non-interacting particles satisfies detailed balance, the eigenvalues of the rate matrix M must be real and so the system cannot display oscillatory behaviour on its approach to the steady-state. To prove this rewrite the detailed balance condition given by equation (3.5.1) as,

$$\sqrt{\frac{\pi_i}{\pi_j}}\ M_{ij} \quad = \quad \sqrt{\frac{\pi_j}{\pi_i}}\ M_{ji}\ , \tag{3.5.2}$$

which is valid when the system is ergodic because all $\pi_i > 0$. Equation (3.5.2) states that the matrix with the $(i,j)^{th}$ components given by $\sqrt{\frac{\pi_i}{\pi_j}}\, M_{ij}$ is symmetric, and therefore has real eigenvalues. However such a matrix is a similar transformation $\boldsymbol{A}\, \boldsymbol{M}\, \boldsymbol{A}^{-1}$ of the rate matrix $\boldsymbol{M}$, where $\boldsymbol{A}$ is a diagonal matrix with $A_{ii} = \sqrt{\pi_i}$. Because any two similar matrices have the same eigenvalues [131], the rate matrix $\boldsymbol{M}$ also has real eigenvalues.

3.5.1 Undirected Systems

A type of system that automatically satisfies detailed balance is one where the rate at which a particle jumps between every pair of nodes is equal to the rate in which a particle jumps in the opposite direction. Such systems are characterised by a symmetric rate matrix and are named *undirected systems*, because the edges of the corresponding network structure are undirected.

By the symmetry of the rate matrix $\boldsymbol{M}$, time-independent distribution is necessarily uniform, $\boldsymbol{\pi} = \mathbf{1}/N$. Furthermore it is possible to find a set of orthonormal left-eigenvectors $\boldsymbol{\psi}_j$ corresponding to each eigenvalue λ_j,

$$\boldsymbol{\psi}_j\, \boldsymbol{M} = \lambda_j\, \boldsymbol{\psi}_j, \qquad \boldsymbol{\psi}_j \cdot \boldsymbol{\psi}_k = \delta_{jk}\ , \tag{3.5.3}$$

where δ_{jk} is equal to unity when $j = k$, and zero otherwise [83]. The solutions to the macroscopic equations (3.2.6) can then be written in the form

$$\boldsymbol{x}(t) \;\; = \;\; \sum_{j=1}^{N} c_j\, e^{\lambda_j t}\, \boldsymbol{\psi}_j\ , \tag{3.5.4}$$

with the values c_j being determined by the initial condition $\boldsymbol{x}(0)$. It is not difficult to extend this result to more general system that satisfies detailed balance. As the eigenvalues λ_i are real, equation (3.5.4) explicitly demonstrates that solutions to the macroscopic equations (3.2.6) decay towards the time-invariant distribution $\boldsymbol{\pi}$ exponentially fast, without oscillating. In order for oscillatory behaviour to ensue, the system must violate detailed balance, having non-zero probability currents. Without interactions between particles, any oscillations in the macroscopic equations are necessarily damped.

3.6 Two-State Systems

As an example of a system that satisfies detailed balance, consider a system of non-interacting particles that can each be in one of two possible states s_1 and s_2, as illustrated in figure 3.3. In section 2.9 it was shown that a two-state system satisfies detailed

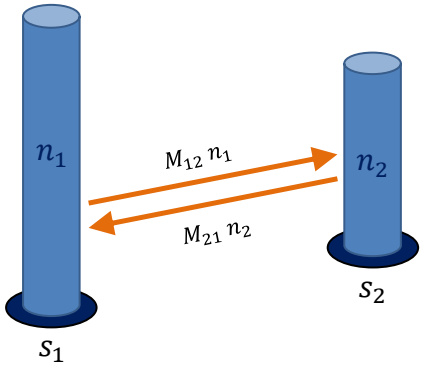


Figure 3.3: *Illustration of the populations of non-interacting particles at each node of a two node network. Arrows show the total rate at which particles jump between the two nodes.*

balance regardless of particle interactions. Let r_i be the rate that a particle in the state s_i jumps to the other state, so the rate matrix is simply,

$$\boldsymbol{M} \;=\; \begin{pmatrix} -r_1 & r_1 \\ r_2 & -r_2 \end{pmatrix} . \tag{3.6.1}$$

The time-invariant distribution $\boldsymbol{\pi}$ is easily found from the detailed balance condition $\pi_1\, r_1 = \pi_2\, r_2$,

$$\boldsymbol{\pi} \;=\; \left(\frac{r_2}{r_1 + r_2} \,,\, \frac{r_1}{r_1 + r_2} \right) . \tag{3.6.2}$$

By using $x_1 + x_2 = 1$, the macroscopic equations (3.2.6) reduce to

$$\frac{dx_1}{dt} \;=\; r_2 - (r_1 + r_2)\, x_1(t) \,. \tag{3.6.3}$$

The solution to this equation is

$$x_1(t) \;=\; \frac{r_2}{r_1 + r_2} + \left(x_1(0) - \frac{r_2}{r_1 + r_2} \right) e^{-(r_1 + r_2)\, t} \,. \tag{3.6.4}$$

This shows that the system does indeed decay exponentially towards the time-invariant distribution $\boldsymbol{\pi}$, as demonstrated in figure 3.4 for a system with $r_1 = 3$ and $r_2 = 1$.

3.7 Irreversible Systems

When a system does not satisfy detailed balance, the dynamics are *irreversible*, the particles jump along some edges at a different rate to the opposite direction, and the rate matrix $\boldsymbol{M}$ may have non-real eigenvalues,

$$\lambda_j \;=\; \delta_j + \mathrm{i}\, \omega_j \,, \tag{3.7.1}$$

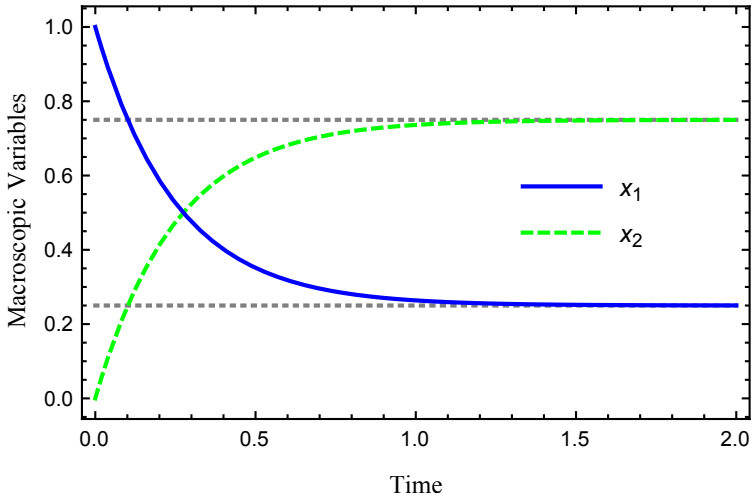


Figure 3.4: *Macroscopic variables $\boldsymbol{x}(t)$ for a two-state system. All particles are initially in the first state s_1, i.e. $\boldsymbol{x}(0) = (1, 0)$. The rate parameters are $r_1 = 3$ and $r_2 = 1$. The variables $x_1(t)$ and $x_2(t)$ are given by the solid (blue) line, and dashed (green) line respectively. The system evolves exponentially towards the time-invariant distribution $\boldsymbol{\pi} = (1/4, 3/4)$, indicated by horizonal, dotted (grey) lines.*

with $\delta_j,\ \omega_j \in \mathbb{R}$, and $\mathrm{i} \stackrel{\text{def}}{=} \sqrt{-1}$. Assuming the eigenvalues are distinct, it is possible to find associated left-eigenvectors $\boldsymbol{\psi}_j$. However such eigenvectors are not necessarily orthogonal as is the case for undirected systems (3.5.3). The solutions to the macroscopic equations (3.2.6) can still be expressed as in equation (3.5.4), from which taking the real part and using the identity $\Re[z_1\ z_2] \equiv \Re[z_1]\Re[z_2] - \Im[z_1]\Im[z_2]$ for complex numbers $z_1, z_2 \in \mathbb{C}$, where $\Re[.]$ and $\Im[.]$ are the real and imaginary parts respectively, results in the equation

$$\boldsymbol{x}(t) \quad = \quad \sum_{j=1}^{N} \Re\left[c_j\ e^{\lambda_j t}\right] \Re\left[\boldsymbol{\psi}_j\right] - \Im\left[c_j\ e^{\lambda_j t}\right] \Im\left[\boldsymbol{\psi}_j\right] \ . \tag{3.7.2}$$

By writing $c_j = a_j\ e^{\mathrm{i}\theta_j}$ with $a_i,\ \theta_i \in \mathbb{R}$, the solution to the macroscopic equations can be rewritten as

$$\boldsymbol{x}(t) \quad = \quad \sum_{j=1}^{N} a_j\ e^{\delta_j t} \left[\ \cos\left(\omega_j t + \theta_j\right) \Re[\boldsymbol{\psi}_j] - \sin\left(\omega_j t + \theta_j\right) \Im[\boldsymbol{\psi}_j]\ \right] \ . \tag{3.7.3}$$

The terms in the summation can be interpreted as *wave-packets* associated with each eigenvalue. The *decay* of the wave packet is given by the real part of the eigenvalues, δ_j, and the *angular frequency* is given by the imaginary part, ω_j. The other two variables, a_j and θ_j, represent the *amplitude* and *phase* of the wave-packet at time zero respectively. For real eigenvalues the angular frequency $\omega_j = 0$, and so the wave-packet has no oscillatory term, representing one real component $\boldsymbol{\psi}_j$ decaying expo-

nentially. When all of the eigenvalues are real, equation (3.7.3) simply reduces back to equation (3.5.4).

If some of the eigenvalues (3.7.1) are equal it may not be possible to find N linearly independent eigenvectors, however as such a system could be approximated by a system with unique eigenvalues to an arbitrary degree of accuracy, there is no issue with finding an expression such as (3.7.3) by taking a limit.

3.8 Three-State Loop System

It has previously been shown that a two-state system always satisfies detailed balance, and so the eigenvalues of the corresponding rate matrix must be real. The simplest type of system that possesses complex eigenvalues has three states, and in this section we consider a particular three-state system that will be used again later chapters 4 and 5 as a simple basis on which to build more complex systems.

Consider a system of n non-interacting particles constrained to three states s_1, s_2 and s_3 whose corresponding network forms a closed loop. Each particle jumps around the loop in the direction $s_1 \to s_2 \to s_3 \to s_1$ at a rate $r\ (1+\rho)/2$ and in the opposite direction at a rate $r\ (1-\rho)/2$, as illustrated in figure 3.5. The parameter $-1 \leq \rho \leq 1$ quantifies the directional preference of the particle jumps, with a value of $\rho = 0$ corresponding no preference of either direction. The rate matrix for a single particle system is

$$\boldsymbol{M} \;=\; \frac{r}{2}\begin{pmatrix} -2 & 1+\rho & 1-\rho \\ 1-\rho & -2 & 1+\rho \\ 1+\rho & 1-\rho & -2 \end{pmatrix}. \tag{3.8.1}$$

Due to the rotational symmetry of the system, the time-invariant distribution is uniform, $\boldsymbol{\pi} = (\frac{1}{3}, \frac{1}{3}, \frac{1}{3})$. The associated probability currents between the states are $J\{s_i \to s_{i+1}\} = \frac{1}{3}r\rho$, where addition in the indices is performed cyclicly (modulo three). When the particles have no preference to the direction in which they jump around the network, $\rho = 0$, the rate matrix $\boldsymbol{M}$ is symmetric, the probability currents are zero and the system satisfies detailed balance. In order for oscillations to appear in the macroscopic equations (3.2.6) the particles must have a preferred direction of jumping, i.e. $\rho \neq 0$, causing the system to be irreversible.

To find the solution to the macroscopic equations (3.2.6) it is useful to find the eigenvalues of the rate matrix $\boldsymbol{M}$. As the rate matrix $\boldsymbol{M}$ is *circulant* [132] it can be expressed

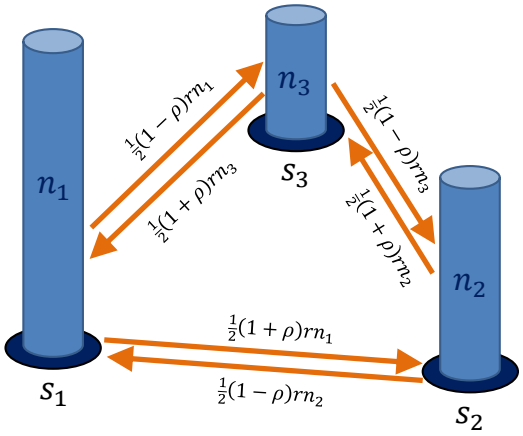


Figure 3.5: *Illustration of the populations of non-interacting particles in a three-state loop system. Arrows show the total rate at which particles jump between different nodes.*

in the form

$$\frac{1}{r}\,\boldsymbol{M} \;=\; -\boldsymbol{I} + \frac{1+\rho}{2}\,\boldsymbol{A} + \frac{1-\rho}{2}\,\boldsymbol{A}^2\,, \qquad \boldsymbol{A} \stackrel{\text{def}}{=} \begin{pmatrix} 0 & 1 & 0 \\ 0 & 0 & 1 \\ 1 & 0 & 0 \end{pmatrix}. \tag{3.8.2}$$

Therefore the rate matrix $\boldsymbol{M}$ is a polynomial of the cyclic permutation matrix $\boldsymbol{A}$. The eigenvalues of the matrix $\boldsymbol{A}$ are 1, γ_3 and γ_3^2, where γ_3 is the primitive third root of unity

$$\gamma_3 \;\stackrel{\text{def}}{=}\; e^{\mathrm{i}\frac{2\pi}{3}} \;\equiv\; -\frac{1}{2} + \mathrm{i}\,\frac{\sqrt{3}}{2}\,. \tag{3.8.3}$$

The left-eigenvectors corresponding to the three eigenvalues are

$$\boldsymbol{\psi}_1 \;=\; \frac{1}{\sqrt{3}}(1,1,1)\,, \quad \boldsymbol{\psi}_2 = \frac{1}{\sqrt{3}}(1,\gamma_3^2,\gamma_3)\,, \quad \boldsymbol{\psi}_3 = \frac{1}{\sqrt{3}}(1,\gamma_3,\gamma_3^2)\,, \tag{3.8.4}$$

respectively. Alternatively, the eigenvectors can be expressed component-wise, as part of a matrix $\boldsymbol{\Psi}$, whose $(j,k)^{th}$ component is defined as

$$\Psi_{jk} \;=\; [\boldsymbol{\psi}_j]_k \;=\; \frac{1}{\sqrt{3}}\,\gamma_3^{-(j-1)(k-1)}\,. \tag{3.8.5}$$

The matrix $\boldsymbol{\Psi}$ is *unitary* - its inverse is equal to its complex conjugate transpose, $\boldsymbol{\Psi}^{-1} = \boldsymbol{\Psi}^\dagger$.

From equation (3.8.2), the rate matrix $\boldsymbol{M}$ has the same eigenvectors as the matrix $\boldsymbol{A}$, and can therefore be written in the form $\boldsymbol{M} = \boldsymbol{\Psi}^\dagger \boldsymbol{\Lambda} \boldsymbol{\Psi}$, where $\boldsymbol{\Lambda}$ is a diagonal matrix

such that $\Lambda_{ii} = \lambda_i$ are the eigenvalues of the rate matrix. The eigenvalues of $\boldsymbol{M}$ are found from the eigenvalues of $\boldsymbol{A}$ by the polynomial equation (3.8.2) to be,

$$\lambda_1 \;=\; 0\,, \quad \lambda_2 = -\frac{3}{2}\,r + \mathrm{i}\,\frac{\sqrt{3}}{2}\,r\,\rho\,, \quad \lambda_3 = -\frac{3}{2}\,r - \mathrm{i}\,\frac{\sqrt{3}}{2}\,r\,\rho\,. \tag{3.8.6}$$

The eigenvalues are real when the particles have no preference to the direction in which they jump around the network, $\rho = 0$, as is expected from the fact that the system is time-reversible in this case, see section 3.5.1.

With expressions for the eigenvalues and eigenvectors of the rate matrix $\boldsymbol{M}$, the transition matrix can be written as $\boldsymbol{\Phi}(t) = \boldsymbol{\Psi}^\dagger \exp(t\boldsymbol{\Lambda})\boldsymbol{\Psi}$, or in terms of its components,

$$\begin{aligned}
\Phi_{ij}(t) \;&=\; \sum_{a=1}^{3} (\Psi_{ai})^\dagger\; e^{\lambda_a t}\; \Psi_{aj} \\
&=\; \frac{1}{3}\,\sum_{a=1}^{3} \gamma_3^{(a-1)(i-1)}\; e^{\lambda_a t}\; \gamma_3^{-(a-1)(j-1)} \\
&=\; \frac{1}{3}\,\sum_{a=1}^{3} \gamma_3^{(a-1)(i-j)}\; e^{\lambda_a t}\,.
\end{aligned} \tag{3.8.7}$$

Taking the real parts of the terms in the summation (3.8.7),

$$\Phi_{ij}(t) \;=\; \frac{1}{3}\,\sum_{a=1}^{3} e^{\delta_a t}\; \cos\left(\omega_a\; t \;+\; \frac{2\pi}{3}(a-1)(i-j)\right), \tag{3.8.8}$$

where δ_a and ω_a are the real and imaginary parts of the eigenvalues λ_a, as in equation (3.9.4), respectively. By using the expressions (3.8.6) for the eigenvalues, equation (3.8.8) can be rewritten as

$$\Phi_{ij}(t) \;=\; \frac{1}{3} \;+\; \frac{2}{3}\; e^{-\frac{3}{2}rt}\; \cos\left(\frac{\sqrt{3}}{2}\; r\rho\; t \;+\; \frac{2\pi}{3}(i-j)\right). \tag{3.8.9}$$

The macroscopic variables x_1, x_2 and x_3 are demonstrated in figure 3.6 for the case $r = 1$ and $\rho = 1$. Oscillations decay very quickly and are almost too small to see. To quantify this one can calculate the proportion of the initial amplitude of the oscillation that remains after one period of oscillation, $4\pi/(r\rho\sqrt{3})$, to be $\exp\left(-2\pi\sqrt{3}/\rho\right)$. When $\rho = 1$, this proportion is of the order 10^{-5}.

Solutions to the macroscopic equation (3.8.9), $\boldsymbol{x}(t) = \boldsymbol{x}(0)\boldsymbol{\Phi}(t)$, follow exponential spirals in the phase-space towards the uniform, time-invariant distribution $(1/3, 1/3, 1/3)$, as shown in figure 3.7. The real part and the imaginary part of the non-zero eigenvalues give the radial decay rate and the angular frequency of the trajectory respectively. When $\rho = 0$, the angular velocity of the trajectory is zero and the solutions $\boldsymbol{x}(t)$ decay without any form of oscillation.

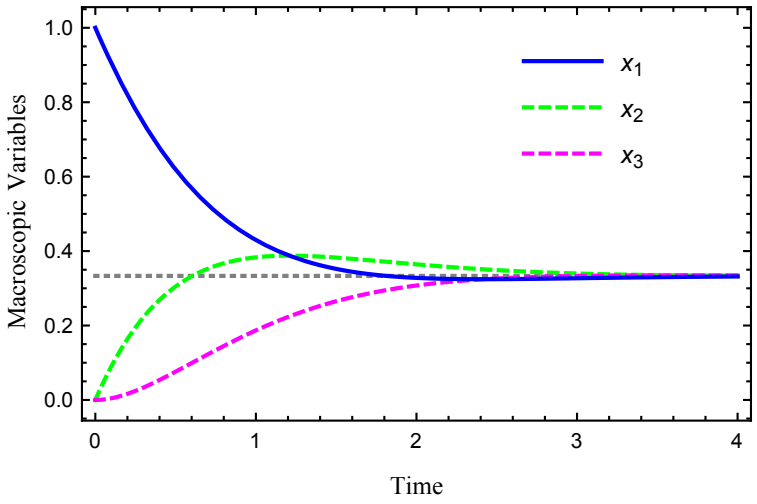


Figure 3.6: *Macroscopic variables $\boldsymbol{x}(t)$ for a three-state loop system. All particles are initially in the first state s_1, $\boldsymbol{x}(0) = (1, 0, 0)$. The rate parameter is $r = 1$ and the preference parameter is $\rho = 1$. The variables $x_1(t)$, $x_2(t)$ and $x_3(t)$ are given by the solid (blue) line, dashed (green) line, and dashed (magenta) line respectively. The system evolves towards the time-invariant distribution $\boldsymbol{\pi} = (1/3, 1/3, 1/3)$ with heavily damped oscillations, indicated by the horizonal, dotted (grey) line.*

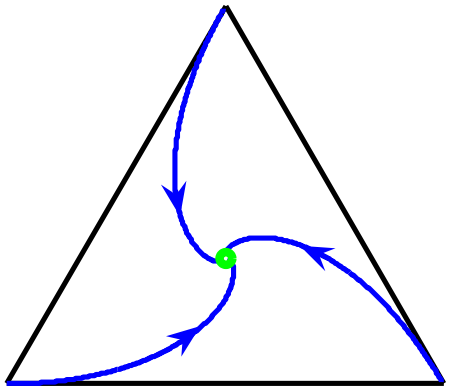


Figure 3.7: *Phase-space solutions $\boldsymbol{x}(t)$ of the macroscopic equations* (3.2.6) *for a three-state loop system. The rate parameter is $r = 1$ and the preference parameter is $\rho = 1$. Trajectories (blue) are initiated at the corners of the phase space $(1, 0, 0)$, $(0, 1, 0)$, and $(0, 0, 1)$, where all of the particles are located at a single node. The solutions follow exponential spirals towards the uniform time-invariant distribution (green circle) at the center of the phase space.*

Regardless of the value of ρ the long-term behaviour of the system is the same - particles are spread uniformly around the network. However the difference in whether there is a directional preference or not will be important in the next chapter, where the dynamics are supplemented with birth and death processes, resulting in several types of emergent phenomena including collective periodic behaviour.

3.8.1 Exponential Spirals

The section justifies the assertion that trajectories in the phase-space of $\boldsymbol{x}(t)$ follow exponential spirals. Define $R(t)$ to be the Euclidean distance from the centre $\boldsymbol{\pi}$ of the phase-space,

$$R(t)^2 \stackrel{\text{def}}{=} (\boldsymbol{x}(t) - \boldsymbol{\pi})(\boldsymbol{x}(t) - \boldsymbol{\pi})^\dagger \,. \tag{3.8.10}$$

Because $\boldsymbol{\pi}\boldsymbol{M} = \boldsymbol{\pi}\boldsymbol{M}^\dagger = \mathbf{0}$, the time derivative of $R(t)^2$ is

$$\begin{aligned} \frac{d}{dt}R^2 &= \boldsymbol{x}\left(\boldsymbol{M} + \boldsymbol{M}^\dagger\right)\boldsymbol{x}^\dagger \\ &= \boldsymbol{x}\boldsymbol{\Psi}^\dagger\left(\boldsymbol{\Lambda} + \boldsymbol{\Lambda}^\dagger\right)\boldsymbol{\Psi}\boldsymbol{x}^\dagger \\ &= 2\delta\, \boldsymbol{x}\boldsymbol{\Psi}^\dagger\, \hat{I}\, \boldsymbol{\Psi}\boldsymbol{x}^\dagger \,, \end{aligned} \tag{3.8.11}$$

where $\delta = -3r/2$ is the real part of the non-zero eigenvalues and

$$\hat{I} \stackrel{\text{def}}{=} \begin{pmatrix} 0 & 0 & 0 \\ 0 & 1 & 0 \\ 0 & 0 & 1 \end{pmatrix}. \tag{3.8.12}$$

One can use the identity

$$(\boldsymbol{x} - \boldsymbol{\pi})\boldsymbol{\Psi}^\dagger = \boldsymbol{x}\boldsymbol{\Psi}^\dagger\, \hat{I}, \tag{3.8.13}$$

to rewrite the definition for $R(t)$,

$$R(t)^2 = \boldsymbol{x}\boldsymbol{\Psi}^\dagger\, \hat{I}\, \boldsymbol{\Psi}\boldsymbol{x}^\dagger \,. \tag{3.8.14}$$

Therefore equation (3.8.11) can be rewritten,

$$\frac{d}{dt}R^2 = 2\,\delta\, R(t)^2 \,, \qquad \Longrightarrow \qquad \frac{dR}{dt} = \delta\, R(t) \,. \tag{3.8.15}$$

To prove that $\omega = \sqrt{3}\rho r/2$ is the angular velocity of the trajectory in the phase space about $\boldsymbol{\pi}$ calculate the magnitude of the velocity

$$\begin{aligned} \left|\frac{d\boldsymbol{x}}{dt}\right|^2 &= \boldsymbol{x}\, \boldsymbol{M}\, \boldsymbol{M}^\dagger\, \boldsymbol{x}^\dagger \\ &= \boldsymbol{x}\boldsymbol{\Psi}^\dagger\, \boldsymbol{\Lambda}\, \boldsymbol{\Lambda}^\dagger\, \boldsymbol{\Psi}\boldsymbol{x}^\dagger \\ &= (\delta^2 + \omega^2)\, \boldsymbol{x}\boldsymbol{\Psi}^\dagger\, \hat{I}\, \boldsymbol{\Psi}\boldsymbol{x}^\dagger \\ &= (\delta^2 + \omega^2)\, R(t)^2 \,. \end{aligned} \tag{3.8.16}$$

The radial component to the velocity is $\delta R(t)$, so the angular component must be $\pm\,\omega R(t)$.

3.9 N-State Loop System

The three-state loop system in the previous section 3.8 can easily be extended to a more general system whereby n non-interacting particles jump around a network of N nodes forming a closed loop. A particle jumps in the direction $s_i \to s_{i+1}$ at a rate $r\ (1+\rho)/2$ and in the opposite direction at a rate $r\ (1-\rho)/2$, with addition of indices performed cyclicly (modulo N). The rate matrix $\boldsymbol{M}$ is given by

$$M_{ij} \;=\; \begin{cases} -r & \text{if } i = j, \\ r\,\frac{1+\rho}{2} & \text{if } j \equiv i+1 \ (\text{mod } N), \\ r\,\frac{1-\rho}{2} & \text{if } j \equiv i-1 \ (\text{mod } N), \\ 0 & \text{otherwise.} \end{cases} \tag{3.9.1}$$

Similar to before, the rate matrix $\boldsymbol{M}$ can be written as the polynomial in equation (3.8.2), with the cyclic permutation matrix $\boldsymbol{A}$ such that $A_{i(i+1)} = 1$ and all other components equalling zero. The eigenvalues of $\boldsymbol{A}$ are the N^{th} roots of unity γ_N^{j-1}, with $j = 1, 2, \ldots, N$ and where γ_N is the primitive root,

$$\gamma_N \;\stackrel{\text{def}}{=}\; e^{\mathrm{i}\frac{2\pi}{N}} \;\equiv\; \cos\left(\frac{2\pi}{N}\right) + \mathrm{i}\,\sin\left(\frac{2\pi}{N}\right). \tag{3.9.2}$$

The corresponding left-eigenvectors $\boldsymbol{\psi}_i$ are the discrete Fourier eigenfunctions [132, 133],

$$[\boldsymbol{\psi}_j]_k \;\stackrel{\text{def}}{=}\; \frac{1}{\sqrt{N}}\,\gamma_N^{-(j-1)(k-1)}. \tag{3.9.3}$$

These are also the left-eigenvectors of the rate matrix $\boldsymbol{M}$. The eigenvalues of the rate matrix are related to the eigenvalues of $\boldsymbol{A}$ through the polynomial equation (3.8.2) and are given by

$$\lambda_j \;=\; -\,r \;+\; r\,\cos\left(\frac{2\pi\,(j-1)}{N}\right) + \mathrm{i}\,r\rho\,\sin\left(\frac{2\pi\,(j-1)}{N}\right), \tag{3.9.4}$$

for $j = 1, 2, \ldots, N$. Similar to the three-state case, the eigenvalues are real when the particles have no preferred direction of jumping, $\rho = 0$, as is expected from the detailed balance property.

The solutions to the macroscopic equations can be found by expanding the transition matrix $\boldsymbol{\Phi}(t)$ by using the eigenvalues and eigenvectors of the rate matrix $\boldsymbol{M}$, and making a calculation similar to (3.8.7). The result is the expansion

$$\Phi_{ij}(t) \;=\; \frac{1}{N}\sum_{a=1}^{N} e^{\delta_a t}\,\cos\left(\omega_a\,t \;+\; \frac{2\pi}{N}(a-1)(i-j)\right), \tag{3.9.5}$$

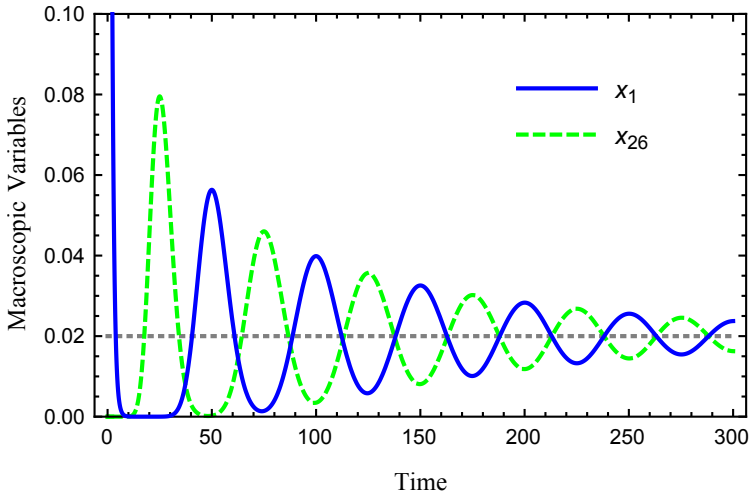


Figure 3.8: *Macroscopic variables $\boldsymbol{x}(t)$ for a 50-state loop system. Note that the range of the vertical axis is between 0 and 0.1. All particles are initially in the first state s_1, $x_1(0) = 1$. The rate parameter is $r = 1$ and the preference parameter is $\rho = 1$. The variables $x_1(t)$ and $x_{26}(t)$ are given by the solid (blue) line, and dashed (green) line respectively. The corresponding oscillations are fully out of phase as the states s_1 and s_{26} are at opposite sides of the network. The system evolves towards the time-invariant distribution $\pi_j = 1/50$ with damped oscillations, indicated by the horizonal, dotted (grey) line.*

where δ_a and ω_a are the real and imaginary parts of the eigenvalues λ_a respectively. The transition probabilities $\Phi_{ij}(t)$ are made up of wave-packets that oscillate with frequency ω_a and decay at a rate δ_a. The most dominant wave-packets in equation (3.9.5) are those with the slowest decay rate, $a = 2$ and $a = N$. These terms correspond to the non-zero eigenvalues with least negative real parts. In one period of oscillation, $2\pi/\omega_a$, the amplitude of the wave-packet decays by a fraction $1 - \exp(2\pi/\omega_a\delta_a)$. When $a/(\rho N)$ is small, this fraction is approximately given by $2\pi^2\ (a-1)/(\rho N)$, and so for the most dominant wave-packets this fraction is inversely proportional to the size of the network N, when the number of nodes is large. Oscillations are more apparent in larger sized networks, as demonstrated in figure 3.8 for a network with 50 nodes.

3.10 Discussion

In this chapter systems of non-interacting particles were considered. It was seen in section 3.2 that the macroscopic equations (3.2.6) can be simply derived from the master equation (3.1.1). The resulting equations were a set of linear first order differential equations. The subsequent evolution is then dependent on the eigenvalues of the rate

matrix. The presence of oscillations is dependent on these eigenvalues being non-real. Indeed in section 3.7 it was demonstrated that the solutions to the macroscopic equations could be expanded in terms of *wave-packets*, with angular frequency determined by the imaginary parts of the eigenvalues of the rate matrix.

The implications of the *detailed balance* property on non-interacting particle systems were discussed in section 3.5. The rate matrix of a system that does satisfy detailed balance necessarily has real eigenvalues, and so such a system cannot display oscillatory behaviour. In particular, it was shown in section 3.5.1 that *undirected systems*, where particles jump between states at an equal rate in both directions, do not allow for oscillations. This result begs the question as to how important *directional preference* is to the emergence of collective periodic behaviour. An answer to this question is provided in chapter 5.

A simple example of a system that does display oscillatory behaviour was given in section 3.8. This *three-state loop system* provides a foundation for other systems used in the remainder of the thesis. Oscillations in this system are heavily damped, to the point where they hardly oscillate visibly. However, by increasing the number of nodes in the network, oscillations become more prominent, as was demonstrated in section 3.9.

Regardless of whether oscillations are present in the dynamics, any disturbances from the steady-state solutions (3.4.9) necessarily diffuse away due to the negative real parts of the eigenvalues of the rate matrix. Therefore, if a mechanism was to be added to the dynamics that somehow shifted eigenvalues into the positive half of the complex plane, we may expect that disturbances may grow. Such an augmentation to the system is discussed in the next chapter.

Chapter 4

Birth-Death-Migration Process

In this chapter we build upon the three-state loop system from section 3.8. We do so by supplementing the dynamics of the non-interacting particles migrating between the three states with stochastic birth and death processes that act at each of the nodes of the network [134–136]. Introduction of these processes implicitly introduces correlations between particles, despite a lack of an explicit interaction being defined between them. The result is that collective periodic behaviour may not only persist in the system, but it can also emerge from the time-independent distribution of particles spread uniformly around the network. In addition, there exist two further types of collective behaviour: particles may condense onto a single state; or they may display intermittent behaviour. The three components to the dynamics: migrations, births and deaths, can be used to hypothesise possible key ingredients for how collective periodic behaviour emerges from randomness in discrete systems.

In the previous chapter we found that the occurrence of oscillatory behaviour in systems of non-interacting particles is determined by the structure of the network throughout which the particles are constrained to move. It was demonstrated that one requirement for oscillations is that the network have directed edges so that particles have a preference to which way they move between, at least some of, the nodes. Another requirement is that the system contain three or more nodes so that non-trivial probability currents, or rather fluxes of particles, can exist in the steady-state solution to the master equation, see section 2.9. A three-state loop system satisfies both of these requirements, provided the particles move in one direction with greater probability than in the opposite direction. It was indeed demonstrated that oscillations do appear in this system regardless of how small the non-zero directional preference may be.

The three-state loop system provides a simple foundation upon which to build in our search for ingredients of collective periodic behaviour - and build we must for oscilla-

tions produced in this system of non-interacting particles are necessarily decaying and the system will quickly settle down into a steady-state where particles are uniformly distributed around the network. The macroscopic equations for the system are linear and the approach of the system to the uniform distribution is characterised by eigenvalues of the rate matrix, which necessarily have negative real parts. If the eigenvalues can somehow be shifted into the positive half of the complex plane, disturbances from the time-invariant distribution will grow and allow for the possibility of emergent collect periodic behaviour. The birth-death process introduced in this chapter has such an effect.

The results presented in this chapter are fully original and have been summarised in [137, 138].

Section 4.1 provides an overview of the three-state loop system in the context of migrating particles. Section 4.2 introduces the birth process by which particles are introduced into the system and section 4.3 describes the death process whereby particles are removed from the system. A summary of Monte-Carlo simulations that demonstrate the various behaviours of the system are provided in section 4.5. In section 4.4 the macroscopic equations of the system at the boundaries of the phase-space are derived. Section 4.6 uses the macroscopic equations to explain the qualitative behaviours of the system that were seen in simulations of the system. Section 4.7 and section 4.8 then provide a more quantitative analysis of the system.

4.1 Migration Process

This section begins the chapter by discussing some of the main features of the three-state loop system analysed in section 3.8. The next two sections then describe how the dynamics can be supplemented in order for the particles to begin to behave collectively.

Consider an initial population of $n(0)$ non-interacting particles that are constrained to a network of three nodes forming a closed loop. At any instant t the i^{th} node is populated by $n_i(t)$ particles, one of which *'migrates'* via a shared edge to an adjacent node at a rate rn_i with probability $(1+\rho)/2$ in one direction and $(1-\rho)/2$ in the other, where $-1 \leq \rho \leq 1$ provides a bias to the direction of migration; when $\rho = 0$ there is no directional preference.

When the number of particles in the system is large, the configuration can be approximated by the *macroscopic equations* that describe the evolution of the macroscopic variables $\boldsymbol{x}(t) = \boldsymbol{n}(t)/n(0)$ by assuming that the configuration of the system is sufficiently close to the mean $\langle \boldsymbol{n}(t) \rangle$. The macroscopic equations for the three-state loop

system are

$$\frac{d\boldsymbol{x}}{dt} \;=\; \boldsymbol{x}\,\boldsymbol{M}\,, \tag{4.1.1}$$

where $\boldsymbol{M}$ is the *migration rate matrix* of a single particle,

$$\boldsymbol{M}(r,\rho) \;\stackrel{\text{def}}{=}\; \frac{1}{2}r\begin{pmatrix} -2 & 1+\rho & 1-\rho \\ 1-\rho & -2 & 1+\rho \\ 1+\rho & 1-\rho & -2 \end{pmatrix}. \tag{4.1.2}$$

The macroscopic equations (4.1.1) are linear and so the evolution of the system is characterised by the three eigenvalues λ_i of the rate matrix $\boldsymbol{M}$,

$$\lambda_1 \;=\; 0\,, \quad \lambda_2 \,=\, \lambda_3^\dagger \,=\, -\frac{3}{2}\,r \,+\, \mathrm{i}\,\frac{\sqrt{3}}{2}\,r\rho\,. \tag{4.1.3}$$

The zero eigenvalue λ_1 corresponds to the uniform, *time-invariant distribution* $\boldsymbol{\pi} = (1/3, 1/3, 1/3)$ representing the particles being equally spread around the three nodes of the network. The remaining eigenvalues form a complex conjugate pair $\lambda_3 = \lambda_2^\dagger$, and are only real when the particles have no preference to the direction in which they jump around the network, $\rho = 0$. The solutions to the macroscopic equations (4.1.1) can be expressed as $\boldsymbol{x}(t) = \boldsymbol{x}(0)\;\boldsymbol{\Phi}(t)$, where $\boldsymbol{\Phi}(t) \equiv \exp(t\boldsymbol{M})$ is the *transition matrix* with components given by

$$\Phi_{ij}(t) \;=\; \frac{1}{3}\sum_{a=1}^{3} e^{\delta_a t}\,\cos\left(\omega_a\,t \,+\, \frac{2\pi}{3}(a-1)(i-j)\right). \tag{4.1.4}$$

The δ_a and ω_a are the real and imaginary parts of the eigenvalues λ_a, as in equation (4.1.3), respectively. The solutions of the macroscopic equations can therefore be expressed in terms of *wave-packets* that correspond to individual eigenvalues. The first is simply the time-invariant distribution $\boldsymbol{\pi}$. The two remaining wave-packets are time dependent and oscillate at a frequency given by the imaginary part of the eigenvalues. As the real parts of the corresponding eigenvalues are negative, the wave-packets decay with time, and solutions to the macroscopic equations approach the time-invariant distribution.

It was shown in section 3.8.1 that trajectories in the phase-space, corresponding to the solutions $\boldsymbol{x}(t)$, follow exponential spirals with an angular frequency $\omega_2 = -\omega_3$ and radial growth rate $\delta_2 = \delta_3$. The trajectories evolve towards the uniform distribution, because the real parts of the eigenvalues are negative.

4.2 Birth Process

The independent and incoherent behaviour of the particles in the migration process causes the dynamics to be dissipative in nature. Further to the migration dynamics

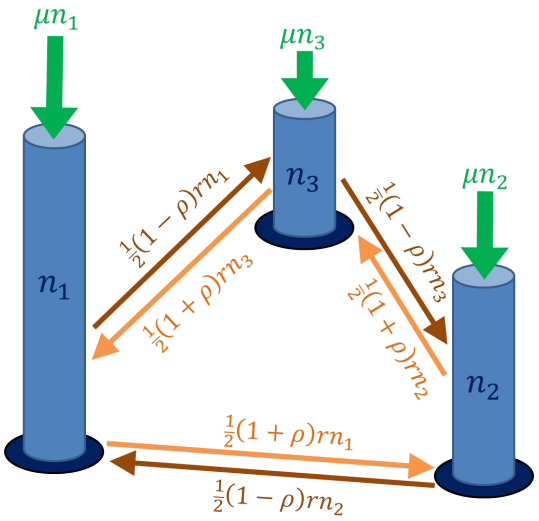


Figure 4.1: *Illustration of the dynamics of a three-state loop system with an added birth process. Bars (blue) represent populations at each of the three nodes of the network. Small arrows correspond to migration rates of particles between nodes. Large (green) arrows depict the rate of births of particles at each node.*

defined in the previous section 4.1, consider a birth-process [134, 135] whereby a single particle is added to the j^{th} node at a rate $\mu n_j(t)$ proportional to the population at that node, characteristic of each particle independently giving birth at a constant rate μ. A schematic of the dynamics is given in figure 4.1. By imposing that the births occur spontaneously the system remains memoryless and still satisfies the *Markov property* [106, 107]. This birth process has the effect of increasing the real parts of the eigenvalues (4.1.3), and thereby modulates the dynamics of the migration process and can cause disturbances from equilibrium to grow.

4.2.1 Master Equation

In addition to the transition rates corresponding to particle migrations the master equation, for the probabilities $P_{\boldsymbol{k}}(t)$ of the system having a particular configuration $\boldsymbol{k}$ at time t, has the transition rates

$$\Gamma\{\boldsymbol{k} \to \boldsymbol{k} + \boldsymbol{e}_j\} \quad = \quad \mu \, k_j \, , \tag{4.2.1}$$

where $\boldsymbol{e}_j$ is a row vector whose j^{th} component has the value unity, with all other components being zero. Each time a particle gives birth, the total population increases by one. The transition rates (4.2.1) can be used to calculate the effect of the birth process on the evolution of the mean configuration $\langle \boldsymbol{n}(t) \rangle$. By ignoring the contribution from the

migration process,

$$\begin{aligned}
\frac{d}{dt}\langle \boldsymbol{n}(t)\rangle &= \sum_{\boldsymbol{j}\in\Omega} P_{\boldsymbol{j}}(t) \sum_{\boldsymbol{k}\in\Omega} \boldsymbol{k}\, \Gamma\{\boldsymbol{j}\to\boldsymbol{k}\} \\
&= \sum_{\boldsymbol{j}\in\Omega} P_{\boldsymbol{j}}(t) \left[\sum_{a=1}^{3} (\boldsymbol{j}+\boldsymbol{e}_a)\,\mu\, j_a \;-\; \sum_{a=1}^{3} \boldsymbol{j}\,\mu\, j_a\right] \\
&= \sum_{\boldsymbol{j}\in\Omega} P_{\boldsymbol{j}}(t) \sum_{a=1}^{3} \boldsymbol{e}_a\,\mu\, j_a \\
&= \mu\,\langle \boldsymbol{n}(t)\rangle\,. \qquad (4.2.2)
\end{aligned}$$

The second equality follows from the definition of $-\Gamma\{\boldsymbol{k}\to\boldsymbol{k}\}$ sum of all transition rates out of the configuration $\boldsymbol{k}$.

4.2.2 Macroscopic Equations

The transition rates are linear because the particles give birth independently of all other particles. Therefore the macroscopic equations are also linear and are found by combining (4.2.2) with the contribution from the migration process (4.1.1),

$$\frac{d\boldsymbol{x}}{dt} \;=\; \boldsymbol{x}\;(\boldsymbol{M}\;+\;\mu\,\boldsymbol{I})\,. \qquad (4.2.3)$$

where $\boldsymbol{I}$ is the 3×3 identity matrix. The eigenvalues of the matrix within the parentheses has the eigenvalues

$$\lambda_1 \;=\; \mu\,,\quad \lambda_2 \;=\; \lambda_3^{\dagger} \;=\; \mu \;-\; \frac{3}{2}\,r \;+\; \mathrm{i}\,\frac{\sqrt{3}}{2}\,r\rho\,. \qquad (4.2.4)$$

The birth process increases the real part of the eigenvalues by an amount equal to the birth rate μ. The solutions to the macroscopic equations (4.2.3) can be expressed as $\boldsymbol{x}(t) = \boldsymbol{x}(0)\;\boldsymbol{\Phi}(t)$, where $\boldsymbol{\Phi}(t) \equiv \exp(t\boldsymbol{M} + t\mu\boldsymbol{I})$ is the matrix with components found from equation (4.1.4) to be given by

$$\Phi_{ij}(t) \;=\; \frac{1}{3}e^{\mu t} \;+\; \frac{2}{3}\,e^{\mu t-\frac{3}{2}rt}\,\cos\left(\frac{\sqrt{3}}{2}\,r\rho\,t \;+\; \frac{2\pi}{3}(i-j)\right). \qquad (4.2.5)$$

The frequency of the time-dependent wave-packets in equation (4.2.5) is unaffected by the inclusion of particle births into the dynamics, but the growth rate is now $\mu - \frac{3}{2}r$, which can be positive and so perturbations from the uniform distribution of particles may grow over time. However the system does not have a time-invariant distribution because the total population of particles in the system is an increasing function of time,

$$x_1(t) + x_2(t) + x_3(t) \;=\; e^{\mu t}, \qquad (4.2.6)$$

using the initial condition $x_1(0) + x_2(0) + x_3(0) = 1$. Defining new variables by $\boldsymbol{y}(t) \stackrel{\text{def}}{=} e^{-\mu t}\, \boldsymbol{x}(t)$ to represent the proportion of particles at each node, gives

$$\frac{d\boldsymbol{y}}{dt} \;=\; \boldsymbol{y}\, \boldsymbol{M}\ . \tag{4.2.7}$$

The evolution of the proportions is unaffected by the inclusion of the births process and so introduction of the birth process alone is not enough for collective periodic behaviours.

4.3 Death Process

In the previous section it was shown that a system of non-interacting particles that independently give birth at a fixed rate μ results in an exponentially increasing population size and therefore does not admit collective periodic behaviour, despite disturbances growing with time. This section introduces the third and final element of the dynamics - a *death process* [134, 135] that is introduced to balance the birth-process by spontaneously removing particles from the system.

The birth process increases the total population size $n(t)$ at a rate $\mu n(t)$. If the death process is to balance the birth process, the total rate that particles are removed from the system must also be equal to $\mu n(t)$ - the average death rate of a particle must be μ. Perhaps the simplest way to achieve this is to allow particles to 'die' independently at a rate μ, so that the rate in which particles are removed from the j^{th} node is $\mu n_j(t)$. However in this case the birth process and death process cancel each other out on average and the macroscopic equations remain unchanged from those of the migration process (4.1.1). If the system is to exhibit collective periodic phenomena, an alternative variety of the death process is required.

Instead of removing each particle from the system at an independent rate, the death process is defined so that particles are sampled with equal probability from each *populated* node. The death rate at a populated node is thus $\mu n(t)/Z(t)$ where $Z(t)$ is the number of populated nodes at time t. Unlike the birth and migration processes, which are defined locally at each node, the death rate at a node is dependent on the configuration of the whole system and is therefore defined globally over the entire network. This mechanism instils coherence upon the system because each particle is affected by the entire ensemble - the death process contains the property that is imbued by a field, albeit through being manifested stochastically.

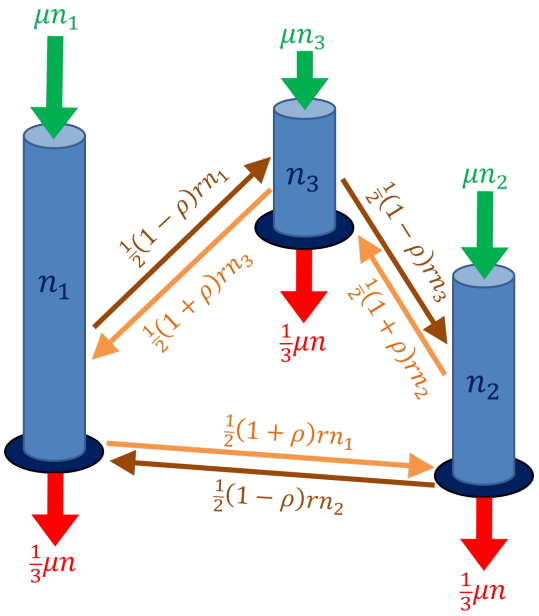


Figure 4.2: *Illustration of the dynamics with all nodes populated. Bars (blue) represent populations at each of the three nodes of the network. Small arrows correspond to migration rates of particles between nodes. Large arrows depict the rate of (green) births and (red) deaths of particles at each node.*

4.3.1 Master Equation

The effect that the death process has on the evolution of the mean configuration $\langle \boldsymbol{n}(t) \rangle$ can be determined from the master equation. Ignoring the contributions from the migration process and birth process,

$$\begin{aligned} \frac{d}{dt}\langle \boldsymbol{n}(t) \rangle &= \sum_{\boldsymbol{j}\in\Omega} P_{\boldsymbol{j}}(t) \sum_{\boldsymbol{k}\in\Omega} \boldsymbol{k}\, \Gamma\{\boldsymbol{j} \to \boldsymbol{k}\} \\ &= \sum_{\boldsymbol{j}\in\Omega} P_{\boldsymbol{j}}(t) \sum_{a=1}^{3} [(\boldsymbol{j} - \boldsymbol{e}_a)\, \Gamma\{\boldsymbol{j} \to \boldsymbol{j} - \boldsymbol{e}_a\} - \boldsymbol{j}\, \Gamma\{\boldsymbol{j} \to \boldsymbol{j} - \boldsymbol{e}_a\}] \\ &= -\sum_{\boldsymbol{j}\in\Omega} P_{\boldsymbol{j}}(t) \sum_{a=1}^{3} \boldsymbol{e}_a\, \Gamma\{\boldsymbol{j} \to \boldsymbol{j} - \boldsymbol{e}_a\}\ . \end{aligned} \tag{4.3.1}$$

The transition rates for the death process are not linear because they are dependent on the number of populated nodes. If a configuration $\boldsymbol{k}$ corresponds to all of the nodes being populated with particles, $k_j > 0$, the contribution to the master equation from the death process is given by the transition rates

$$\Gamma\{\boldsymbol{k} \to \boldsymbol{k} - \boldsymbol{e}_j\} = \frac{1}{3}\,\mu\,(k_1 + k_2 + k_3)\ , \tag{4.3.2}$$

for $j = 1$, 2, and 3. A diagram of the dynamics when all nodes are populated is given by figure 4.2. These rates must be adjusted if the configuration corresponds to some of the

nodes being unpopulated, as considered in section 4.4. Assuming that the probability of all nodes being populated is equal to one, the transition rates (4.3.2) can be used in equation (4.3.1),

$$\begin{aligned}\frac{d}{dt}\langle \boldsymbol{n}(t)\rangle &= -\frac{1}{3}\,\mu\,\sum_{\boldsymbol{j}\in\Omega}(j_1+j_2+j_3)\,P_{\boldsymbol{j}}(t)\,\sum_{a=1}^{3}\boldsymbol{e}_a \\ &= -\frac{1}{3}\,\mu\,\sum_{\boldsymbol{j}\in\Omega}\boldsymbol{j}\;P_{\boldsymbol{j}}(t)\;\mathbf{1}^{\dagger}\,\mathbf{1} \\ &= -\frac{1}{3}\,\mu\,\langle \boldsymbol{n}(t)\rangle\,\boldsymbol{U}\;, \end{aligned} \tag{4.3.3}$$

where $\boldsymbol{U} \stackrel{\text{def}}{=} \mathbf{1}^{\dagger}\,\mathbf{1}$ is a 3×3 matrix with all elements unity. Under the assumption that all of the nodes are populated, the equations for the mean configuration are linear.

4.3.2 Macroscopic Equations

Equation (4.3.3) for the mean configuration can be used with the equations (4.2.3) for the migration and birth processes to find the macroscopic equations,

$$\frac{d\boldsymbol{x}}{dt} \;=\; \boldsymbol{x}\left(\boldsymbol{M}\;+\;\mu\,\boldsymbol{I}\;-\;\frac{1}{3}\mu\,\boldsymbol{U}\right). \tag{4.3.4}$$

These equations are only valid for times t when the assumption that all of the nodes are populated is almost certainly true. Situations that do not adhere to this assumption are considered in section 4.4. For systems containing a large, essentially infinite, number of particles the macroscopic equations (4.3.4) are reasonable when $x_j(t) > 0$.

Solutions of the macroscopic equations (4.3.4) can be characterised by the eigenvalues of the matrix within the parentheses. The matrix $\boldsymbol{U}$ is *circulant* [132] and so the death process does not affect the eigenvectors of the system. The eigenvalues of the matrix within the parenthesis of equation (4.3.4) are given by

$$\lambda_1 \;=\; 0\,,\quad \lambda_2 \;=\; \lambda_3^{\dagger} \;=\; \mu\;-\;\frac{3}{2}\,r\;+\;\mathrm{i}\,\frac{\sqrt{3}}{2}\,r\rho\,. \tag{4.3.5}$$

The effect of the death process is to shift the first eigenvalue (zero eigenvalue of $\boldsymbol{M}$) to the left in the complex plane by an amount μ. Therefore the death process cancels the effect of the birth process on the first eigenvalue, but not the other two. The compounded effect of the birth and death processes on the macroscopic equations is to shift the pair of non-zero eigenvalues of the rate matrix $\boldsymbol{M}$ to the right in the complex plane by an amount equal to the birth and death rates μ. Solutions to the macroscopic equations (4.3.4) can be expressed in the form $\boldsymbol{x}(t) = \boldsymbol{x}(0)\,\boldsymbol{\Phi}(t)$ where the components of the matrix $\boldsymbol{\Phi}(t)$ are found by using the eigenvalues (4.3.5) in equation (4.1.4),

$$\Phi_{ij}(t) \;=\; \frac{1}{3}\;+\;\frac{2}{3}\,e^{\mu t-\frac{3}{2}rt}\,\cos\left(\frac{\sqrt{3}}{2}\,r\rho\,t\;+\;\frac{2\pi}{3}(i-j)\right). \tag{4.3.6}$$

The first term in equation (4.3.6) corresponds to the time-invariant distribution $\boldsymbol{\pi} = (1/3, 1/3, 1/3)$, which has been recovered because the balance of the birth and death processes ensures that the total population of particles in the system remains fixed on average. The second term in equation (4.3.6) corresponds to time-dependent component of the evolution $\boldsymbol{x}(t)$. The frequency of these oscillating wave-packets is unaffected by the birth and death processes, but the growth rate is now given by $\mu - 3r/2$.

For relatively small values of μ, such that $\mu < 3r/2$, the birth and death processes are not enough to overcome the diffusive nature of the migration process. Solutions of the macroscopic equations $\boldsymbol{x}(t)$ follow trajectories that spiral *towards* the centre of the phase-space where particles are uniformly distributed around the three nodes of the network. This behaviour is confirmed by simulations of the system presented in the next section 4.5.

The system undergoes a *bifurcation*, a qualitative change of behaviour, at the parameter values $\mu = 3r/2$ as the time-invariant distribution becomes unstable. When $\mu > 3r/2$, the combined effect of the particles giving birth and being removed from the system sufficiently counteract the migration process. Trajectories corresponding to $\boldsymbol{x}(t)$ spiral *away from* the centre of the phase-space as perturbations of the system from the time-invariant distribution grow with time. The growing disturbance is eventually large enough that one of the nodes becomes *unpopulated*. At such an instant the assumption leading to equation (4.3.4) is violated and another equation must be found in order to describe the evolution of the system at the boundaries of the phase-space, where one of the $x_j(t) = 0$.

4.4 Dynamics at the Boundaries

When the macroscopic variables $\boldsymbol{x}(t)$ are at the boundary of the phase-space, it may not be reasonable to assume that all nodes of the network are populated with particles. If the likelihood that one of the nodes being unpopulated is significant, equation (4.3.3) does not describe the macroscopic dynamics. Instead a different equation must be derived from equation (4.3.1). The reason for needing a separate macroscopic equation at a boundary is the dependence of the death process on the number of populated nodes in the system - deaths are equally likely from each *populated* node. If a configuration $\boldsymbol{k}$ is such that $k_2 = 0$ and $k_1, k_3 > 0$, then the transition rate $\Gamma\{\boldsymbol{k} \to \boldsymbol{k} - \boldsymbol{e}_2\} = 0$, because populations cannot become negative. The two other transition rates corresponding to the removal of a particle from the first and third nodes are respectively

$$\Gamma\{\boldsymbol{k} \to \boldsymbol{k} - \boldsymbol{e}_1\} \;=\; \Gamma\{\boldsymbol{k} \to \boldsymbol{k} - \boldsymbol{e}_3\} \;=\; \frac{1}{2}\,\mu\,(k_1 + k_3)\,. \tag{4.4.1}$$

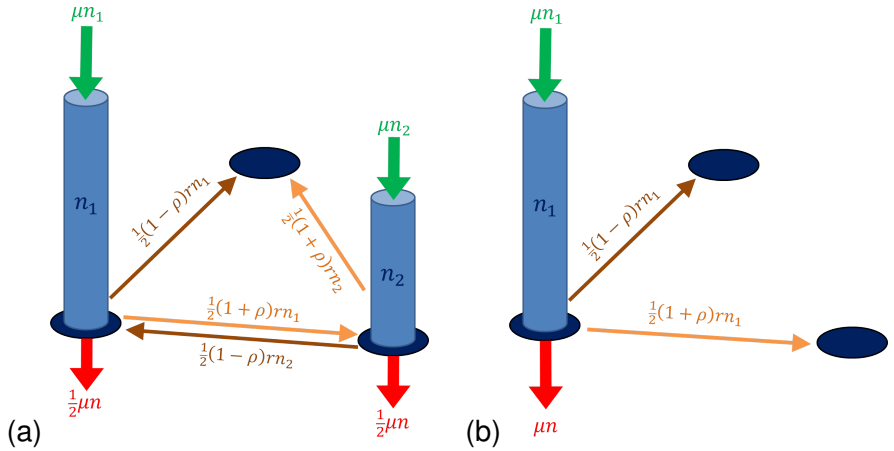


Figure 4.3: *Illustration of the dynamics with: (a) two nodes populated and (b) one node populated. Bars (blue) represent populations at each of the three nodes of the network. Small arrows correspond to migration rates of particles between nodes. Large arrows depict the rate of (green) births and (red) deaths of particles at each node.*

Figure 4.3 provides a schematic of the dynamics at the boundaries. The transition rates (4.4.1) can be used to derive the macroscopic equations at the $x_2 = 0$ boundary where the population at the second node is approximately zero, i.e. $n_2(t) \approx 0$. The equations for the other two boundaries will be similar.

4.4.1 Stochastic Behaviour at the Boundary

When $x_2(t) = 0$ the number of particles that are at the second node is approximately zero, $n_2(t) \approx 0$, when compared to the total number of particles in the system. In fact the true value of $n_2(t)$ follows a random walk on the non-negative integers. Increases in $n_2(t)$ occur at a rate

$$u(\boldsymbol{n}(t)) \quad \stackrel{\text{def}}{=} \quad \mu n_2(t) + \frac{1}{2}r(1+\rho)n_1(t) + \frac{1}{2}r(1-\rho)n_3(t) \;, \tag{4.4.2}$$

due to births and migrations from the other two nodes. Decreases in non-zero $n_2(t)$ occur at a rate

$$d(\boldsymbol{n}(t)) \quad \stackrel{\text{def}}{=} \quad \frac{1}{3}\mu n(t) + rn_2(t) \;, \tag{4.4.3}$$

due to migrations to the other two nodes and deaths. By approximating these rates using the macroscopic variables, $n_j(t) \approx n(0)x_j(t)$ these rates become

$$u \;\approx\; \frac{1}{2}rn(0)[(1+\rho)x_1(t) + (1-\rho)x_3(t)] \;, \quad d \;\approx\; \frac{1}{3}\mu n(0) \;. \tag{4.4.4}$$

Both of these rates are proportional to the (initial) number of particles in the system $n(0)$, and so the random walk behaviour of $n_2(t)$ occurs extremely quickly, relative to

the evolution of the system on the macroscopic scale - which happens over times of order $1 \ll n(0)$. If $u > d$ the population at the second node quickly grows and the approximation that all nodes are populated is reasonable. This is the case when

$$x_1(t) \;\; > \;\; \frac{1}{2}\left(1+\frac{\theta}{3}\right) \;\; \stackrel{\text{def}}{=} \;\; \kappa_b(\theta)\,, \tag{4.4.5}$$

where $\theta(r,\rho,\mu) \stackrel{\text{def}}{=} (2\mu - 3r)/r\rho$ is a *dimensionless* parameter involving all three dynamical parameters of the system. A plot of $\kappa_b(\theta)$ is shown in figure 4.4. For points on the $x_2 = 0$ boundary satisfying the inequality (4.4.5), the macroscopic dynamics are simply explained by the macroscopic equations (4.3.4) for the interior of the phase-space. However for points on the boundary such that $x_1(t) < \kappa_b(\theta)$, it happens that $u < d$ and there is a non-zero probability that the population of particles at the second node is zero. Define $w(t)$ to be the probability that all of the nodes are populated with particles,

$$w(t) \;\; \stackrel{\text{def}}{=} \;\; \mathsf{Pr}\{n_1(t) > 0,\; n_2(t) > 0,\; n_3(t) > 0\}\,. \tag{4.4.6}$$

Because the random walk behaviour of $n_2(t)$ occurs so quickly, the probability $w(t)$ can simply be approximated from the stationary distribution of this, approximately simple [114], random walk to be $w(t) = u/d$, or equivalently

$$w(t) \;\; = \;\; \frac{3r}{2\mu}\;(2\rho\, x_1(t) \;+\; 1 - \rho)\,, \tag{4.4.7}$$

for $x_1(t) < \kappa_b(\theta)$. The probability $w(t) = 1$ when $x_1(t) = \kappa_b(\theta)$, which is the point at which a trajectory in the interior of the phase-space is tangent to the boundary.

4.4.2 Macroscopic Equations at the Boundary

The contribution of the death process to the macroscopic equations on the $x_2 = 0$ boundary is made up of two parts - the contribution from $n_2(t) > 0$, and the contribution from $n_2(t) = 0$. The first part is already given by equation (4.3.3). For the second part, assume that $n_2(t) = 0$ ($n_1(t)$, $n_3(t) > 0$). Then equation (4.3.1) for the effect of the death process on the evolution of the mean configuration gives

$$\begin{aligned}
\frac{d}{dt}\langle \boldsymbol{n}(t)\rangle \;\; &= \;\; -\frac{1}{2}\,\mu \sum_{\boldsymbol{j}\in\Omega} (j_1 + j_3)\, P_{\boldsymbol{j}}(t)\;\; (\boldsymbol{e}_1 + \boldsymbol{e}_3) \\
&= \;\; -\frac{1}{2}\,\mu \sum_{\boldsymbol{j}\in\Omega} \boldsymbol{j}\; P_{\boldsymbol{j}}(t)\;\; (\boldsymbol{e}_1 + \boldsymbol{e}_3)^{\dagger}\,(\boldsymbol{e}_1 + \boldsymbol{e}_3) \\
&= \;\; -\frac{1}{2}\,\mu\, \langle \boldsymbol{n}(t)\rangle\, \boldsymbol{U}_2\,,
\end{aligned} \tag{4.4.8}$$

where $\boldsymbol{U}_2 \stackrel{\text{def}}{=} (\boldsymbol{e}_1 + \boldsymbol{e}_3)^{\dagger}\,(\boldsymbol{e}_1 + \boldsymbol{e}_3)$ is the matrix $\boldsymbol{U}$ with its second column and second row set equal to zero. Each part of the contribution is weighted by its respective probability,

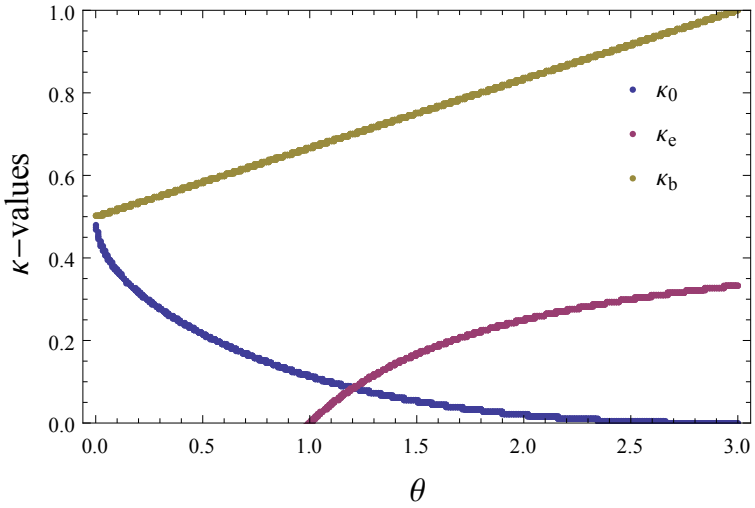


Figure 4.4: *The three values of κ_b, κ_e and κ_0 plotted against θ. $\kappa_b(\theta)$ corresponds to the point where the trajectory in the interior is tangent to the boundary. $\kappa_e(\theta)$ gives the position of the equilibrium point of the macroscopic equations on the boundary. $\kappa_0(\theta)$ corresponds to the point at which the limit cycle first reaches the boundary. The intersection $\kappa_e(\theta) = \kappa_0(\theta)$ is the value of $\theta = \theta_c \approx 1.2$ above which periodic behaviour cannot occur.*

and hence the macroscopic equations at the $x_2 = 0$ boundary can be written as,

$$\frac{d\boldsymbol{x}}{dt} \;=\; \boldsymbol{x}\left(\boldsymbol{M} \;+\; \mu\,\boldsymbol{I}_3 \;-\; \mu\left[\frac{1}{3}w\,\boldsymbol{U} + \frac{1}{2}(1-w)\,\boldsymbol{U}_2\right]\right). \tag{4.4.9}$$

Eliminating $w(t)$ from this equation and using $x_3(t) = 1 - x_1(t)$ results in the macroscopic equations that describe the motion along the $x_2 = 0$ boundary,

$$\frac{dx_1}{dt} \;=\; \frac{r\rho\,\theta}{2}\left[x_1 - \frac{1}{2}\left(1 - \frac{1}{\theta}\right)\right]. \tag{4.4.10}$$

Equations at the two other boundaries are found by simply permuting the indices in equation (4.4.10). The direction in which the trajectory moves along the boundary depends on the sign of the right-hand-side of equation (4.4.10), which vanishes when $x_1(t)$ has the value

$$\frac{1}{2}\left(1 - \frac{1}{\theta}\right) \;\stackrel{\text{def}}{=}\; \kappa_e(\theta)\,. \tag{4.4.11}$$

This corresponds to an *unstable* equilibrium point on the boundary when $\theta > 1$. A plot of $\kappa_e(\theta)$ alongside $\kappa_b(\theta)$ is given by figure 4.4. Together with the macroscopic equations (4.3.4), equation (4.4.10) can be used to describe the various behaviours of the system that are observed in the Monte-Carlo simulations presented the next section.

4.5 Monte-Carlo Simulations

Insight into the behaviour of the system is gained from Monte-Carlo simulated realizations [112] of the dynamics for various parameter values. Figure 4.5 shows simulation results for a network with $\rho = 1$, $r = 1$ and values of μ taken in increasing order. Simulations are performed using the Gillespie algorithm [111], which is *exact* for Markov processes. The qualitative behaviour of the system is similar for all $|\rho| > 0$.

Beginning with a system that does not include births and deaths, $\mu = 0$, the diffusive nature of the migration process causes particles to spread uniformly around the three nodes of the network, seen in figure 4.5(a). Introducing the birth and death processes by slightly increasing μ results in an increased correlation between particles and causes larger fluctuations about this time-invariant distribution. The dissipation of particles caused by the migration process dominates the overall behaviour of the system.

For values of $\mu > 3r/2$ correlations between the particles manifest at the macroscopic level. Particles start to behave collectively and move in a coherent, wave-like fashion, around the network with each node of the network periodically emptying and filling with particles. Figure 4.5(b) demonstrates that this collective periodic phenomenon is shown to emerge from an initial state where particles are uniformly spread around the network. The system exhibits collective periodic behaviour, despite the movements of the particles being completely independent. Figure 4.5(e) shows that collective behaviour is not evident in the time evolution of the total population in the entire system. The periodic behaviour requires that the particles have a preference to the direction in which they move around the network. Indeed simulations for the case where $\rho = 0$ do not exhibit oscillations.

Periodic behaviours do not emerge for all values of $\mu > 3r/2$. Further increase of the birth and death rates causes the system to enter an *intermittent state* where the orderly behaviour is disrupted by particles temporarily lodging at single nodes, see figure 4.5(c). The collective periodic behaviour requires a balance between the two rates r and μ.

Simulations of the system for larger values of μ (approximately $\mu > 2.1$) result in the vast majority of the particles *condensing* at a single node of the network, figure 4.5(d). The precise node on which this condensation phenomena occurs is dependent upon the initial configuration of the particles and is equally likely at each node when the system is initiated with particles uniformly distributed around the network. This lodging of particles at a node happens because the death process essentially 'punishes' any particles that do not conform to the majority - particles are removed from small populations at the same rate as from large populations.

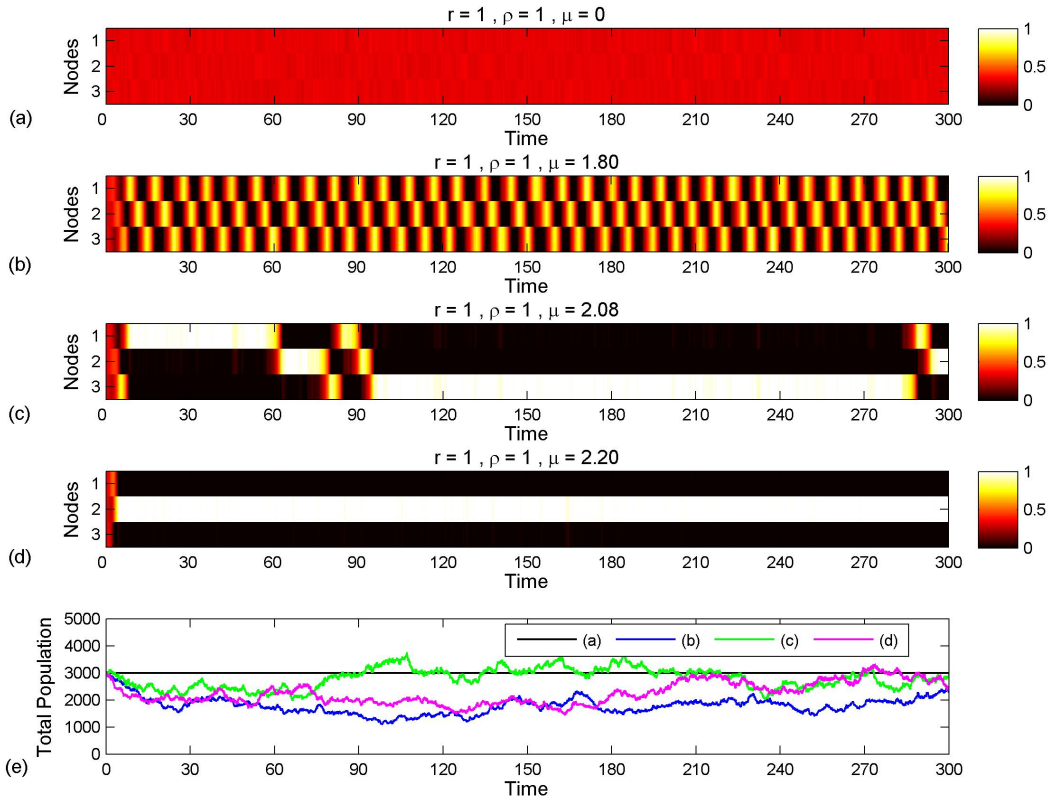


Figure 4.5: *Heat plot of simulated data for four different values of the birth rate μ with common migration rate $r = 1$, preference $\rho = 1$. Each simulation initiated with a population of 1000 particles at each node. Colour intensities in the rows correspond to the proportion of particle at each node number of particles at each of the three nodes with the scales being given on the right. (a) Dissipative behaviour, $\mu = 0$. (b) Periodic behaviour, $\mu = 1.8$ $(\theta = 0.6)$. (c) Intermittent behaviour, $\mu = 2.08$ $(\theta = 1.16)$. (d) Condensed behaviour, $\mu = 2.2$ $(\theta = 1.4)$. The control parameter $\theta = (2\mu - 3r)/r\rho$ is discussed in the analysis. (e) Total populations in each of the four simulations.*

The remainder of this chapter aims to explain the various behaviours of the system both qualitatively and quantitatively.

4.6 Qualitative Behaviour of the System

When the birth and death rate $\mu < 3r/2$, the migration process dominates the dynamics and the particles spread uniformly around the three nodes of the network. The macroscopic equations describe trajectories that spiral towards the time-invariant distribution at the centre of the phase space, as demonstrated in figure 4.6(a). When $\mu > 3r/2$ situation is more complex. This section uses the macroscopic equations (4.3.4) and (4.4.10) to explain the various behaviours of the system when $\mu > 3r/2$, and identify the parameter values that correspond to each of phenomena seen in Monte-Carlo simulations of the system, figure 4.5.

Four supplementary videos have been provided on an accompanying compact-disc - (hyperlink provided in electronic version). Videos show Monte-Carlo simulations, including the corresponding evolution of the trajectory in the phase-space, for each of the different types of behaviour. Supplementary video 1 demonstrates the dissipative behaviour of the system when $\mu = 0$.

4.6.1 Collective Periodic Behaviour

Monte-Carlo simulations of the system when the birth and death rate $\mu > 3r/2$ show that the particles behave collectively and form a wave that travels around the network, provided that μ is not too large. Collective period behaviours are identified with limit cycles in the phase-space of the macroscopic equations. To understand how this limit cycle can arise, consider the trajectory depicted in figure 4.6(b) that is initially at a point (i). As $\mu > 3r/2$ the trajectory spirals away from the centre of the phase-space and eventually meets the $x_2 = 0$ boundary at a point (ii) corresponding to the second node being almost empty. The direction in which the trajectory moves on the boundary is determined by equation (4.4.10). The trajectory moves in the direction of increasing $x_1(t)$ when $x_1(t) > \kappa_e(\theta)$. This occurs unconditionally for $0 < \theta < 1$, in which case the trajectory moves along the boundary until it reaches the point (iii) where $x_1(t) = \kappa_b$. The trajectory then leaves the $x_2 = 0$ boundary and moves in the interior of the phase-space until it reaches the neighbouring $x_3 = 0$ boundary, at the point (iv). Because the dynamics at every boundary is the same, the behaviour of the trajectory is similar to before and a limit cycle is established that represents a wave of particles travelling around the network as in figure 4.5(b). Collective periodic behaviours are therefore guaranteed

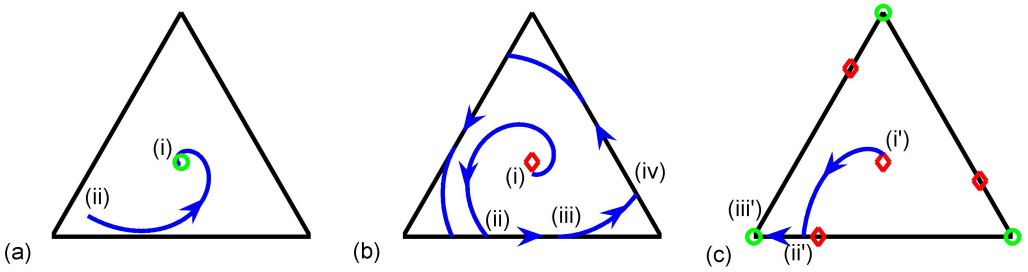


Figure 4.6: *Trajectory of the mean state in the phase-space. Circles (green) represent stable equilibrium points. Diamonds (red) represent unstable equilibrium points. (a) Dissipative behaviour - points (i) and (ii) are finishing and starting points respectively. (b) Periodic behaviour - (i) is the starting point, (ii) is where the second node empties, (iii) is where the population in the second node begins to repopulate and (iv) is where third node empties. (c) Condensed behaviour - (i') is the starting point, (ii') is where the second node empties and (iii') is where all particles are at the third node.*

to occur when $0 < \theta < 1$. Supplementary video 2 demonstrates this periodic behaviour.

4.6.2 Condensed Behaviour

When $\theta > 1$ there exist unstable equilibrium points on the boundaries of the phase-space. At the $x_2 = 0$ boundary there is an equilibrium point at $x_1 = \kappa_e(\theta)$, given in equation (4.4.11). The existence of these equilibrium points can interrupt a trajectory from forming a limit cycle and instead result in the particles condensing at a single node of the network, as is demonstrated by the realisation in figure 4.5(d). To see why, consider the case depicted in figure 4.6(c). The system is initiated at a point (i') and subsequently follows a trajectory that spirals away from the centre of the phase-space until it meets the $x_2 = 0$ boundary at the point (ii') such that $x_1(t) < \kappa_e$. From equation (4.4.10) the trajectory moves in the direction of decreasing $x_1(t)$. Therefore the trajectory does not escape the boundary and instead moves towards the point (iii') at the corner of the phase-space where $x_3(t) = 1$, corresponding to particles being condensed at the third node. Hence in addition to the unstable equilibrium points on the boundaries, there also exist three stable equilibrium points as the corners of the phase-space when $\theta > 1$. Supplementary video 4 demonstrates this condensed behaviour.

4.6.3 Intermittent Behaviour

For some values of $\theta > 1$, it is possible that a limit cycle exists alongside the stable equilibrium points at the corners of the phase-space. This causes the system to display intermittent behaviour because fluctuations about the trajectory given by the macroscopic equations cause the system to interchange sporadically between the two different types of behaviour. The fluctuations arise because the dynamics are inherently stochastic and discrete, and their magnitude is determined by the number of particles in the system - the greater the number of particles, the less frequent the interchanges between the states will be.

The limit cycle exists as long as the unstable equilibrium points on the boundaries lie outside of the region enclosed by the cycle in the phase-space. The condition for this is $\kappa_e(\theta) < \kappa_0(\theta)$, where $\kappa_0(\theta)$ corresponds to the points at which the limit cycle in the interior of the phase space meets the boundaries. The values of $\kappa_0(\theta)$ are plotted in figure 4.4 which shows that the critical value of θ above which the limit cycle does not exist is $\theta_c \approx 1.2$. Simulations of the system confirm that the intermittent behaviour does indeed occur when $1 < \theta < \theta_c$, with an example being given by figure 4.5(c). Supplementary video 3 demonstrates this intermittent behaviour.

The intermittent behaviour is a finite size effect that does not exist in the infinite particle limit. In a system with an infinite number of particles, particles will display periodic behaviour or they will enter a collapsed state, dependent on their initial configuration. This gives rise to a type of hysteresis behaviour as the parameter θ is varied in and out of the range $1 < \theta < \theta_c$. Consider initiating the system in the periodic state with $0 < \theta < 1$ and then slowly increasing θ into the range $1 < \theta < \theta_c$. In this case the particles will continue to oscillate. Indeed the periodic behaviour will persist until $\theta > \theta_c$, when the particles collapse onto a single node. If one were to then decrease θ the periodic behaviour would not return until $\theta < 1$. Thus the behaviour of the system when $1 < \theta < \theta_c$ depends upon past values of θ.

4.7 Frequency of the Limit Cycle

In the previous section the qualitative behaviours of the system were explained using the macroscopic equations (4.3.4) and (4.4.10). The two remaining sections in this chapter use these equations to describe some quantitative features of the system. The frequency of the collective oscillations of the particles is considered in addition to the critical value of θ above which collective periodic behaviours do not to exist. Calculation of the amplitude of these oscillations is presented in section 4.8.

The limit cycles that correspond to collective periodic behaviours spend time both on and off of the boundaries of the phase-space. Determining the frequency of the cycle requires calculation of the time T_i spent by the system moving between neighbouring boundaries and the time T_b spent by the system moving along a boundary. This is achieved by analysing the geometry of the limit cycle in the phase-space, as depicted in figure 4.7. However it is first useful to express the macroscopic dynamics in terms of *dimensionless* variables.

4.7.1 Dimensionless Variables

It has been shown that both the region at which the trajectory moves along the boundary, determined by $\kappa_b(\theta)$, and position $\kappa_e(\theta)$ of the equilibrium point of the macroscopic equations on the boundary are dependent on a single *dimensionless* parameter $\theta(r,\rho,\mu) \stackrel{\text{def}}{=} (2\mu - 3r)/r\rho$. By scaling the units of time by defining the new *dimensionless* parameter $\tau \stackrel{\text{def}}{=} r\rho\, t$ the macroscopic equations (4.4.10) for evolution along points on the boundary, such that $x_1(t) < \kappa_b$, can be rewritten as

$$\frac{dx_1}{d\tau} \;=\; \frac{\theta}{2}\,(x_1 - \kappa_e)\,. \tag{4.7.1}$$

Similarly, the macroscopic equations (4.3.4) for evolution in the interior, can be rewritten as

$$\frac{d\boldsymbol{x}}{d\tau} \;=\; \boldsymbol{x}\left[\frac{1}{2}\begin{pmatrix} 0 & 1 & -1 \\ -1 & 0 & 1 \\ 1 & -1 & 0 \end{pmatrix} - \frac{1}{6}\,\theta \begin{pmatrix} -2 & 1 & 1 \\ 1 & -2 & 1 \\ 1 & 1 & -2 \end{pmatrix}\right], \tag{4.7.2}$$

which has the dimensionless eigenvalues

$$\lambda_1 \;=\; 0\,, \quad \lambda_2 \;=\; \lambda_3^{\dagger} \;=\; \frac{1}{2}\,\theta \;+\; \mathrm{i}\,\frac{\sqrt{3}}{2}\,. \tag{4.7.3}$$

Therefore the dynamics describing the macroscopic evolution of the system can be expressed in terms of a single dimensionless variable θ, by using an appropriate time scaling. Such a time scaling implicitly assumes that the preference ρ to the direction in which particles jump around the network is non-zero.

Dimensionless variables are used throughout the remainder of this section and section 4.8. In particular this includes the time scaling $\tau = r\rho\, t$ and as such the determined times T_i, T_b and therefore the calculated frequency are also dimensionless.

4.7.2 Calculating T_i

Let $R(\tau)$ be the radial distance of the trajectory from the centre of the phase-space. In the interior of the phase space, the radial component increases exponentially at a rate

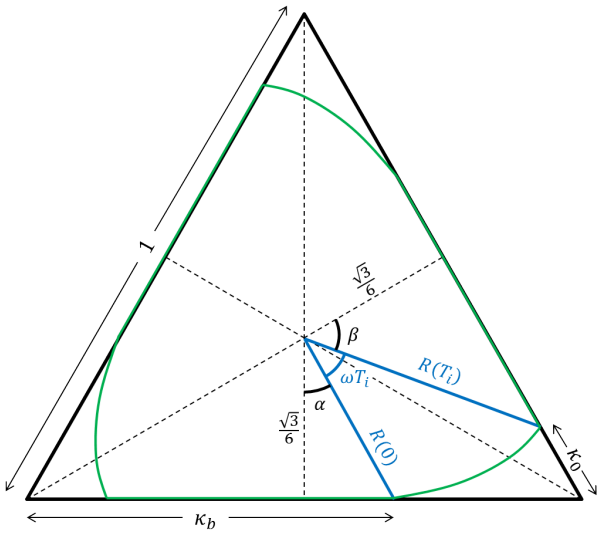


Figure 4.7: *Geometrical picture of the limit cycle (green) in the phase-space. The trajectory leaves the boundaries at a point κ_b, where it then follows an exponential spiral in the interior of the phase-space. The trajectory meets the boundaries at a point κ_0. It then moves along the boundary until the point κ_b, and so on.*

$\delta = \frac{1}{2}\theta$, so that

$$R(T_i) \;=\; R(0)\;\exp\left(\frac{1}{2}\,\theta\,T_i\right), \tag{4.7.4}$$

where $\tau = 0$ is defined to be the point on the limit cycle at which the trajectory leaves the boundary. Because the angular frequency of the trajectory in the interior of the phase-space is $\omega = \frac{\sqrt{3}}{2}$, the angle swept out by the trajectory as it crosses the boundaries is ωT_i.

Figure 4.7 provides a diagram of the phase-space. By defining the angles α and β as in this figure, it is clear that

$$\alpha \;+\; \omega T_i \;+\; \beta \;=\; \frac{2\pi}{3}\,. \tag{4.7.5}$$

These angles are related to the radial variable $R(\tau)$ through the equation

$$R(0)\;\cos\alpha \;=\; \frac{\sqrt{3}}{6} \;=\; R(T_i)\;\cos\beta\,, \tag{4.7.6}$$

where $\sqrt{3}/6$ is the closest, perpendicular, distance from the boundaries to centre of the phase space. From equation (4.7.5)

$$\cos\beta \;=\; \cos\alpha\;\cos\left(\omega T_i - \frac{2\pi}{3}\right) \;-\; \sin\alpha\;\sin\left(\omega T_i - \frac{2\pi}{3}\right). \tag{4.7.7}$$

The angle α is simply related to the control parameter θ,

$$\tan\alpha \;=\; \frac{\kappa_b - \frac{1}{2}}{\frac{\sqrt{3}}{6}} \;=\; \frac{\theta}{\sqrt{3}}\,. \tag{4.7.8}$$

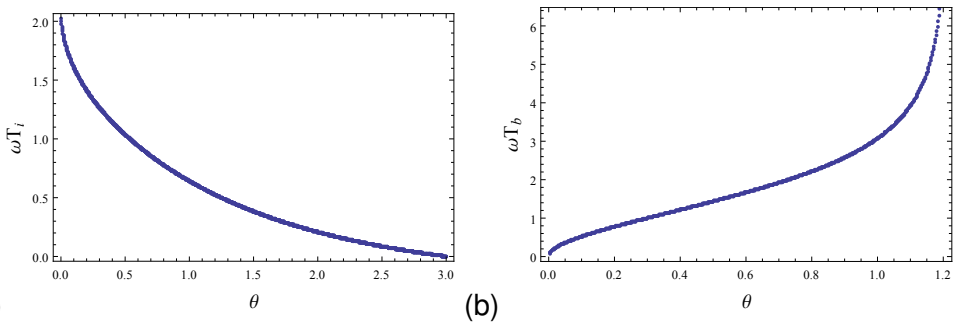


Figure 4.8: *Numerical solutions for (a) ωT_i and (b) ωT_b plotted against θ. Values of T_b tend to infinity as $\theta \to \theta_c$.*

By combining equations (4.7.6), (4.7.7) and (4.7.8) it follows that

$$\frac{R(0)}{R(T_i)} \;=\; \cos\left(\omega T_i - \frac{2\pi}{3}\right) \;-\; \frac{\theta}{\sqrt{3}}\,\sin\left(\omega T_i - \frac{2\pi}{3}\right). \tag{4.7.9}$$

Finally using equation (4.7.4) leads to an implicit equation for θ and T_i,

$$\exp\left(-\frac{1}{2}\,\theta\,T_i\right) \;=\; \cos\left(\omega T_i - \frac{2\pi}{3}\right) \;-\; \frac{\theta}{\sqrt{3}}\,\sin\left(\omega T_i - \frac{2\pi}{3}\right). \tag{4.7.10}$$

This equation can be solved numerically to determine T_i for each given θ, The result is shown in figure 4.8(a).

4.7.3 Calculating κ_0

Before calculating the time T_b spent by the trajectory of the limit cycle moving along a boundary, it is useful to find $\kappa_0(\theta)$ the point at which the trajectory first meets the boundary. This point is illustrated in figure 4.7, where it can be seen that a simple application of Pythagoras' theorem gives

$$R(T_i)^2 \;=\; \frac{1}{12} \;+\; \left(\frac{1}{2} - \kappa_0\right)^2. \tag{4.7.11}$$

Similarly, the point κ_b at which the trajectory leaves the boundary satisfies

$$R(0)^2 \;=\; \frac{1}{12} \;+\; \left(\kappa_b - \frac{1}{2}\right)^2. \tag{4.7.12}$$

Therefore by using equations (4.7.11) and (4.7.12) with equation (4.7.4) it follows that

$$\left[\frac{1}{12} \;+\; \left(\frac{1}{2} - \kappa_0\right)^2\right] \;=\; \exp\left(\theta\,T_i\right)\left[\frac{1}{12} \;+\; \left(\kappa_b - \frac{1}{2}\right)^2\right]. \tag{4.7.13}$$

As T_i can be found numerically for each θ, this equation can be rearranged to find κ_0 for each θ. The result is shown in figure 4.4. This figure shows that there is a value

of θ for which $\kappa_0 = \kappa_e$, i.e. the trajectory meets the boundary at the equilibrium point of the macroscopic equations on the boundary. This therefore marks the value of θ above which the limit cycle ceases to exist. To find this critical value θ_c, substitute $\kappa_0(\theta_c) = \kappa_e(\theta_c)$ into equation (4.7.11) and use equation (4.4.11) to get

$$R(T_i)^2 \;=\; \frac{1}{12} \;+\; \left(\frac{1}{2\theta_c}\right)^2 \;=\; \left(\frac{1}{2\theta_c}\right)^2 \left(1 + \frac{\theta_c^2}{3}\right). \tag{4.7.14}$$

Similarly rearrange equation (4.7.12) using equation (4.4.5) to get

$$R(0)^2 \;=\; \frac{1}{12} \;+\; \left(\frac{\theta_c}{6}\right)^2 \;=\; \frac{1}{12}\left(1 + \frac{\theta_c^2}{3}\right). \tag{4.7.15}$$

It follows from equation (4.7.4) that

$$\exp\left(-\frac{1}{2}\,\theta_c\,T_i\right) \;=\; \frac{\theta_c}{\sqrt{3}}\,. \tag{4.7.16}$$

This equation can be rewritten using equation (4.7.10),

$$\cos\left(\omega T_i - \frac{2\pi}{3}\right) \;=\; \frac{\theta}{\sqrt{3}}\,\left[1 \;+\; \sin\left(\omega T_i - \frac{2\pi}{3}\right)\right]. \tag{4.7.17}$$

Equality holds when $\omega T_i = \frac{\pi}{6}$, and so substituting this value into equation (4.7.16) gives

$$\exp\left(-\frac{\pi}{6}\,\frac{\theta_c}{\sqrt{3}}\right) \;=\; \frac{\theta_c}{\sqrt{3}}\,, \tag{4.7.18}$$

or equivalently

$$\frac{\log\left(\theta_c/\sqrt{3}\right)}{\theta_c/\sqrt{3}} \;=\; -\frac{\pi}{6}\,, \tag{4.7.19}$$

from which θ_c can be determined numerically to be approximately $\theta_c \approx 1.2037$. This corresponds to the parameter values in which the Monte-Carlo simulations reveal a transition from intermittent behaviour to condensed behaviour, where particles collect at a single node.

4.7.4 Calculating T_b

What remains is to calculate the time T_b that the trajectory spends moving along a boundary. As the macroscopic equations (4.7.1) describing the motion of the trajectory along a boundary are linear, they can easily be used with the initial condition $x_1(0) = \kappa_0$ and the final condition $x_1(T_b) = \kappa_b$ to find

$$\exp\left(-\frac{1}{2}\,\theta_c\,T_b\right) \;=\; \frac{\kappa_0 - \kappa_e}{\kappa_b - \kappa_e}\,. \tag{4.7.20}$$

This equation can therefore be used to determine T_b for each value of θ, as shown in figure 4.8(b). The value of T_b becomes unbounded at θ_c because $\kappa_0(\theta) \to \kappa_e(\theta)^+$ as

$\theta \to \theta_c^-$. By taking a Taylor expansion of $\kappa_0 - \kappa_e$ around θ_c, it is found that $T_b(\theta)$ goes to infinity like

$$T_b(\theta) \quad \sim \quad - \frac{2 \ \log(\theta_c - \theta)}{\theta_c} \ , \tag{4.7.21}$$

as $\theta \to \theta_c^-$. For values of θ greater than θ_c, the limit cycle does not exist, and T_b is essentially infinite.

4.7.5 Frequency

The total time for the trajectory to make one traversal around the limit cycle is given by $3T_i + 3T_b$ and so the frequency of the oscillations in the wave-state is given by

$$f(\theta) \quad \stackrel{\text{def}}{=} \quad \frac{1}{2\pi} \ \frac{1}{3T_i(\theta) + 3T_b(\theta)} \ . \tag{4.7.22}$$

In figure 4.9 the full (blue) line shows the frequency plotted $f(\theta)$ as a function of θ, which has a good agreement with the (red) crosses that show the mean frequency determined from 10 Monte Carlo simulated realisations of the system with the network populated with an initial population of 30,000 particles. Each simulation was run for long enough to produce 100 cycles - resulting in a total sample of 1000 cycles. Sample frequencies were simply determined by the intervals between local maxima of the population at the first node $n_1(t)$ and thus standard deviations, shown by bars on the data, may be reduced by using a less variant estimator of the period.

The frequency decreases with increasing θ, falling rapidly to zero in the vicinity of $\theta = \theta_c$. Indeed it follows from equation (4.7.21) that the sharp cut-off of the frequency as $\theta \to \theta_c^-$ decays like

$$f(\theta) \quad \sim \quad - \frac{\theta_c}{12\pi \ \log(\theta_c - \theta)} \ . \tag{4.7.23}$$

The frequency $f(\theta)$ is dimensionless and so for the fully dimensional system the frequency must be multiplied by $r\rho$.

4.8 Amplitude of the Limit Cycle

The amplitude $A(\theta)$ of the limit cycle is defined as the maximum value of the $x_i(t)$ over a whole period of the cycle. For sufficiently small values of θ, the maximum value of $x_1(t)$ is at a point P_2 where the trajectory is tangential to the lines of constant x_1. These lines make an angle $\pi/3$ with the two boundaries, as seen in figure 4.10 which depicts one third of the phase-space, containing the corner where $x_1 = 1$. For larger values of

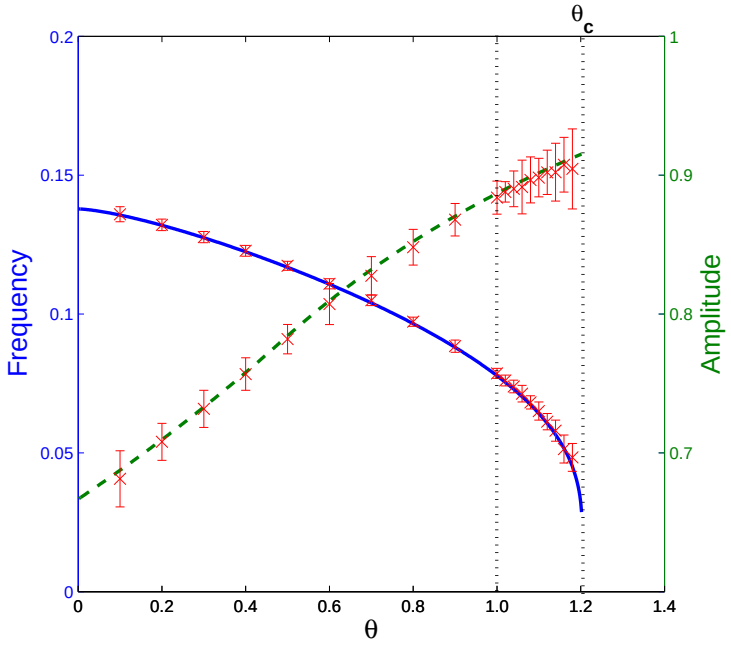


Figure 4.9: *Frequency (solid blue) and amplitude (dashed green) of the limit cycle. Crosses (red) show the estimated means, with the bars giving the estimated standard deviations. The region between the dashed vertical lines indicates the intermittent regime.*

θ, the point P_2 may not exist within the boundaries of the phase-space, in which case $x_1(\tau)$ attains its maximum value of $1 - \kappa_0(\theta)$, at the point where the trajectory meets the boundary.

Assume that θ is indeed small enough that the point P_2 exists within the boundaries of the phase-space. Then the maximum value of $x_1(\tau)$ occurs when the trajectory has swept out an angle $\pi/3$ from the point P_1 where it left the boundary, as shown in figure 4.10. It follows that the two triangles OP_1Q_1 and OP_2Q_2 are similar. The length of OQ_1 is $\sqrt{3}/6$, and the length of OQ_2 is $\sqrt{3}/3 \; - \; \sqrt{3}(1 - A)/2$. Defining time $\tau = 0$ to be when the trajectory leaves the boundary, the length of OP_1 is simply $R(0)$. The length OP_2 is $R(\pi/3\omega)$, because the angular frequency of the trajectory in the interior of the phase-space is $\omega = \sqrt{3}/2$. Hence by the similarity of the two triangles OP_1Q_1 and OP_2Q_2

$$\frac{R\left(\pi/3\omega\right)}{R(0)} \;\; = \;\; \frac{\frac{\sqrt{3}}{3} - \frac{\sqrt{3}}{2}(1 - A(\theta))}{\frac{\sqrt{3}}{6}} \;\; = \;\; 3A(\theta) \;\; - \;\; 1 \; . \tag{4.8.1}$$

Using equation (4.7.4) for the exponential growth of the radial variable $R(\tau)$, equation (4.8.1) becomes, after a simple rearrangement

$$A(\theta) \;\; = \;\; \frac{1}{3}\left[1 \; + \; \exp\left(\frac{\pi}{3} \; \frac{\theta}{\sqrt{3}}\right)\right] . \tag{4.8.2}$$

This equation holds provided θ is small enough that the point P_2 lies within the boundaries of the phase-space. As the control parameter θ increases to a value θ_a, the point P_2 becomes coincident with the point where the trajectory meets the boundary. This happens when $T_i(\theta_a) = \pi/3\omega$. Inserting this into equation (4.7.10) gives

$$\exp\left(-\frac{\pi}{3} \; \frac{\theta_a}{\sqrt{3}}\right) \;\; = \;\; \frac{1}{2}\left(1 + \theta_a\right) . \tag{4.8.3}$$

The numerical solution to this equation is $\theta_a \approx 0.4885$. For θ larger than this value, the point P_2 would be found outside of the boundaries of the phase space. It then follows that the amplitude A is found at the point where the trajectory meets the boundary, i.e. $A(\theta) = 1 - \kappa_0(\theta)$.

Amplitudes for various values of θ are shown in figure 4.9 by the dashed (green) line with the (red) crosses and bars showing the values and their standard deviations obtained from the Monte-Carlo simulation described in section 4.7.5. The relatively large variance of the sampled amplitudes may be an artifact of the maxima being identified with single points in the time series of $n_1(t)$. Similar to the sample frequencies, the amplitudes become more variant as the behaviour of the system becomes more sporadic when $\theta > 1$. The amplitude increases with θ and changes discontinuously at $\theta = \theta_c$ where collective periodic behaviour ceases to exist and the particles begin to condense at a single node.

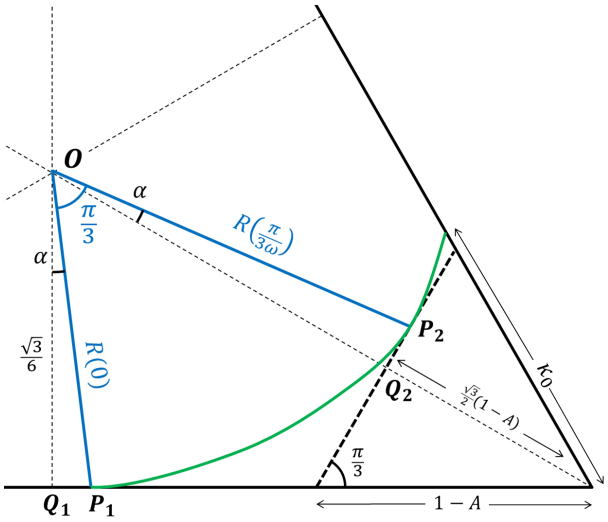


Figure 4.10: *Diagram of one third of the phase-space, used in calculating the amplitude* A.

4.9 Discussion

In this chapter we have studied a simple system whereby particles display collective periodic behaviour in the form of a self-sustaining disturbance that moves coherently through a discrete medium represented by a network of three nodes connected by edges. A summary of the results presented has recently been published [137, 138]. The dynamics is made up of three parts, each of which are essential in allowing oscillations to emerge from intrinsic fluctuations and persist. The migration process describes the coupling between the particles and the network structure and, on its own, causes particles to diffuse over the network to a time-invariant distribution. The birth process provides a crucial imbalance that results in instability of the time-invariant distribution and causes disturbances to grow. The death process balances with the birth process to prevent the system from growing infinitely large. It also introduces and important global coupling amongst the particles that allows action to occur at a distance between the nodes of the network.

The combination of the birth, death and migration processes can result in the emergence of collective periodic phenomena provided the particles have a directional preference to their migrations. This raises a question as to how important directional preference is for the emergence of periodic behaviours in general interacting particle systems - are edges of the network required to be undirected? A second question that arises due to the results in this chapter regards the importance of non-local interactions between the particles. In the present model this is facilitated by the death process, which when combined with the birth processes emulates a type of attractive force that causes par-

ticles to collect together by penalising smaller populations with a relatively high death rate, while supplementing larger populations with a higher birth rate. The answer to both of these questions is provided in the next chapter.

The analysis presented in this chapter demonstrates the extent to which the macroscopic equations can be used to explain various kinds of phenomena that occur in interacting particle systems. Once explicit equations are found quantitative properties of the limit cycle, corresponding to collective periodic behaviour, can be calculated as in sections 4.7 and 4.8. If the microscopic behaviour of the system varies discontinuously, at the boundaries or elsewhere, the derivation of the macroscopic equations may be rather involved. An example of this was at the boundaries of the phase-space as described in section 4.4. The method used for deriving the macroscopic equations in this section is generalised in the next chapter.

Nonlinearity in the dynamics of the birth-death-migration process is solely due to the constraints imposed on the death process. Such nonlinearity is important for collective behaviours as it is characteristic of interactions between particles. An alternative way to introduce non-linearity is to include quadratic effects to the rate at which a particle migrates from the i^{th} node to the j^{th} node is proportional to $n_i n_j$, essentially representing additive forces between particles. Such systems have been demonstrated to display wave-like behaviour [7], providing the interactions are not symmetric. More recently these models have been used to study condensation phenomena [2] similar to that demonstrated in figure 4.5(d). The present model captures both condensation and periodic phenomena without explicitly defining a force between particles.

Chapter 5

Conditions of Collective Periodic Behaviours

In this chapter we discuss necessary conditions for collective periodic behaviour in the general framework of interacting particle systems. Three questions regarding essential ingredients for periodic behaviour were posed at the beginning of the thesis:

1. “What is the minimum number of nodes needed for periodic behaviour?”
2. “Can periodic behaviour emerge when single particles jump at an equal rate in both directions along an edge joining nodes?”
3. “Does collective periodic behaviour rely on interactions between particles that are at different nodes?”

This chapter provides conclusive answers to these questions.

Interacting particle systems, where the total number of particles in the system is fixed, were first introduced in chapter 2. Collective periodic behaviour of the system was identified with limit cycle solutions of the macroscopic equations. Section 5.1 describes a method for deriving the macroscopic equations from the microscopic dynamics.

Section 5.2 describes how the birth-death-migration process from chapter 4 can be reframed as an interacting particle system that has identical macroscopic equations. This is then used to answer the question (1) stated above.

Section 5.3 addresses the importance of a directional preference to the way in which particles jump between states. A machinery for examining the possibility of limit cycle solutions to the macroscopic equations is developed and used to provide an answer to the question (2).

Local interactions between particles, whereby a particle affects other particles at the same node, but not particles different nodes, are described in section 5.4. A particular type of these local interactions is then analysed in section 5.5 where the usefulness of action at a distance is demonstrated. Finally, the answer to question (3) regarding the necessity of action at a distance is presented in section 5.6.

5.1 Deriving the Macroscopic Equations

In a general interacting particle system particles interact by affecting the rate at which other particles jump between nodes of the network. The rate at which a particle jumps from the i^{th} node to the j^{th} node is specified by the rate matrix $M_{ij}(\boldsymbol{n}(t))$ which is dependent on the configuration of the particles. The type of interaction between the particles determines the particular form of the rate matrix. The configuration of the system $\boldsymbol{n}(t)$ follows a Markov process on the set of all possible configurations Ω, stated explicitly in equation (2.1.1). The probabilities $P_{\boldsymbol{k}}(t)$ of the system having particular configurations at each time t evolve according to the master equation

$$\frac{d}{dt}P_{\boldsymbol{k}}(t) \;=\; \sum_{\boldsymbol{j}\in\Omega}\Gamma\left\{\boldsymbol{j}\to\boldsymbol{k}\right\}P_{\boldsymbol{j}}(t) \;-\; \Gamma\left\{\boldsymbol{k}\to\boldsymbol{j}\right\}P_{\boldsymbol{k}}(t)\;, \tag{5.1.1}$$

where the transition rate from the i^{th} node to the j^{th} node is given by

$$\Gamma\left\{\boldsymbol{k}\to\boldsymbol{k}-\boldsymbol{e}_i+\boldsymbol{e}_j\right\} \;=\; k_i\,M_{ij}(\boldsymbol{k})\;. \tag{5.1.2}$$

The vectors $\boldsymbol{e}_i$ are defined with the i^{th} component unity and all other components zero. Because all non-zero transition rates are of the form given in equation (5.1.2), it follows that the total number of particles in the system, n, is constant. In contrast the birth-death-migration process discussed in chapter 4, the total number of particles in the system varied stochastically with time and so this process is not included in this framework of an interacting particle system. This is addressed again in section 5.2.

5.1.1 Macroscopic Equations

Solving the master equation (5.1.1) provides a complete probabilistic specification of the evolution of the system. However in general it is not possible to express the solution in an informative and useful form when the (fixed) total number of particles in the system is large. A description of the system that is more easily interpreted is given by the macroscopic equations that describe the evolution of the macroscopic variables, $\boldsymbol{x}(t) = \boldsymbol{n}(t)/n$, by making the approximation $\boldsymbol{n}(t) = \langle\boldsymbol{n}(t)\rangle = \sum_{\boldsymbol{k}\in\Omega}\boldsymbol{k}P_{\boldsymbol{k}}(t)$. In section 3.2 an

equation describing the evolution of the mean configuration was found in the context of non-interacting particles,

$$\frac{d}{dt}\langle \boldsymbol{n}(t)\rangle \;=\; \langle\, \boldsymbol{n}(t)\, \boldsymbol{M}(\boldsymbol{n}(t))\,\rangle\,. \tag{5.1.3}$$

In the absence of particle interactions $\boldsymbol{M}$ is independent of $\boldsymbol{n}(t)$ which provides a closed equation for $\langle \boldsymbol{n}(t)\rangle$. However for interacting particle systems, equation (5.1.3) is not closed. An approximation is needed [108]. Assume that $\boldsymbol{M}(\boldsymbol{n}(t))$ can be expanded in terms of the total number of particles n, which is assumed to be fixed,

$$\boldsymbol{M}(\boldsymbol{n}(t)) \;=\; a(n)\sum_{i=0}^{\infty} n^{-i}\boldsymbol{B}_i(\boldsymbol{x}(t)) \tag{5.1.4}$$

where $a(n)$ is some positive function of the number of particles in the system, and the matrices $\boldsymbol{B}_i$ are functions over the phase-space. By re-scaling time, $a(n)t \to t$, equation (5.1.3) becomes

$$\frac{d}{dt}\langle \boldsymbol{x}(t)\rangle \;=\; \langle\, \boldsymbol{x}(t)\, \boldsymbol{B}_0(\boldsymbol{x}(t))\,\rangle \;+\; \mathcal{O}(n^{-1})\,. \tag{5.1.5}$$

The macroscopic equations are found by making the assumption that the probability distribution describing the configuration of the system is peaked around its mean, $\boldsymbol{n}(t) = \langle \boldsymbol{n}(t)\rangle + \mathcal{O}\left(n^{1/2}\right)$. As long as the matrix $\boldsymbol{B}_0$ is sufficiently continuous, i.e. $\boldsymbol{B}_0\left(\boldsymbol{x} + \mathcal{O}\left(n^{1/2}\right)\right) \approx \boldsymbol{B}_0\left(\boldsymbol{x}\right)$, equation (5.1.5) can be approximated as

$$\frac{d}{dt}\langle \boldsymbol{x}(t)\rangle \;\approx\; \langle \boldsymbol{x}(t)\rangle\, \boldsymbol{B}_0\left(\langle \boldsymbol{x}(t)\rangle\right). \tag{5.1.6}$$

The macroscopic equations are then given by

$$\frac{d\boldsymbol{x}}{dt} \;=\; \boldsymbol{x}(t)\, \boldsymbol{B}\left(\boldsymbol{x}(t)\right), \tag{5.1.7}$$

where the subscript on the matrix $\boldsymbol{B}_0$ has been dropped for notational convenience and $\boldsymbol{x}(t)$ is interpreted as the mean density distribution of the particles at time t.

5.1.2 Dealing with Discontinuities

At points in the phase-space where $\boldsymbol{B}(\boldsymbol{x})$ is not continuous, it cannot be assumed that $\boldsymbol{B}(\boldsymbol{x}) \approx \boldsymbol{B}(\langle \boldsymbol{x}\rangle)$. Suppose that $\mathcal{P}$ is such a point that lies on the boundary between two regions, $\mathcal{R}_1$ and $\mathcal{R}_2$, of the phase-space where $\boldsymbol{B}$ is continuous. In each region $\mathcal{R}_i$ the macroscopic equations are given by

$$\frac{d\boldsymbol{x}}{dt} \;=\; \boldsymbol{x}(t)\, \boldsymbol{B}_{\mathcal{R}_i}(\boldsymbol{x}(t)), \tag{5.1.8}$$

with the matrices $\boldsymbol{B}_{\mathcal{R}_i}$ being found by the method described in section 5.1.1. Let $\boldsymbol{v}_i$ be the unit normal vectors to the boundary at $\mathcal{P}$, directed into the regions $\mathcal{R}_i$ respectively,

so that on the boundary between $\mathcal{R}_1$ and $\mathcal{R}_2$; $\boldsymbol{v}_1 = -\boldsymbol{v}_2$. The components of the equations (5.1.8) perpendicular to the boundary in each region are $\boldsymbol{v}_1 \cdot \boldsymbol{x}\boldsymbol{B}_{\mathcal{R}_1}$ and $\boldsymbol{v}_2 \cdot \boldsymbol{x}\boldsymbol{B}_{\mathcal{R}_2}$. The sign of these scalar products determines whether the trajectories in each region are away from (positive) or towards (negative) the boundary. If the trajectories in either region move away from the boundary, the boundary is called *simple*. In this case, the system only remains at the boundary for an instant of time, and the macroscopic equation of the boundary is somewhat redundant - the rates on the boundary can be chosen as either of those for the regions $\mathcal{R}_i$. However if the trajectories in *both* regions move towards the boundary, the boundary is called *adhesive*, as the system becomes constrained to the boundary. Macroscopic equations must then be found that determine the evolution along the adhesive boundary.

To determine the macroscopic equations at an adhesive boundary, consider the dynamics at the level of single particles. At this microscopic scale the evolution of the system is a random walk that fluctuates between the two regions $\mathcal{R}_1$ and $\mathcal{R}_2$. Let w_1 and w_2 be the proportion of time the system spends in each region respectively. This implies that w_i is the probability of finding the system in the region $\mathcal{R}_i$. At the boundary between the two regions one can make the approximation

$$\boldsymbol{B}(\boldsymbol{x}(t)) \quad \approx \quad w_1 \, \boldsymbol{B}_{\mathcal{R}_1}(\langle \boldsymbol{x}(t) \rangle) + w_2 \, \boldsymbol{B}_{\mathcal{R}_2}(\langle \boldsymbol{x}(t) \rangle), \tag{5.1.9}$$

thus the macroscopic equations at this point are simply,

$$\frac{d\boldsymbol{x}}{dt} \quad = \quad \boldsymbol{x}(t) \; \left[w_1 \, \boldsymbol{B}_{\mathcal{R}_1}(\boldsymbol{x}(t)) + w_2 \, \boldsymbol{B}_{\mathcal{R}_2}(\boldsymbol{x}(t)) \right]. \tag{5.1.10}$$

This describes the motion on the adhesive boundary. It is a weighted sum of the macroscopic equations in the two regions either side of the discontinuity. The equation is not very useful while probabilities w_i remain unknown. One method of calculating the probabilities would be from analysing at the microscopic level, as was done in the previous section 4.4.1, however a much more efficient method is to use the condition that the macroscopic flow is parallel to the boundary, i.e. $\boldsymbol{v}_1 \cdot d\boldsymbol{x}/dt = 0$, or equivalently

$$w_1 \, \boldsymbol{v}_1 \cdot \boldsymbol{x} \, \boldsymbol{B}_{\mathcal{R}_1} \quad = \quad w_2 \, \boldsymbol{v}_2 \cdot \boldsymbol{x} \, \boldsymbol{B}_{\mathcal{R}_2}. \tag{5.1.11}$$

By using $w_2 = 1 - w_1$, the probabilities follow,

$$\begin{aligned} w_1 \quad &= \quad \frac{\boldsymbol{v}_2 \cdot \boldsymbol{x} \, \boldsymbol{B}_{\mathcal{R}_2}}{\boldsymbol{v}_1 \cdot \boldsymbol{x} \, \boldsymbol{B}_{\mathcal{R}_1} + \boldsymbol{v}_2 \cdot \boldsymbol{x} \, \boldsymbol{B}_{\mathcal{R}_2}} \, , \\ w_2 \quad &= \quad \frac{\boldsymbol{v}_1 \cdot \boldsymbol{x} \, \boldsymbol{B}_{\mathcal{R}_1}}{\boldsymbol{v}_1 \cdot \boldsymbol{x} \, \boldsymbol{B}_{\mathcal{R}_1} + \boldsymbol{v}_2 \cdot \boldsymbol{x} \, \boldsymbol{B}_{\mathcal{R}_2}} \, . \end{aligned} \tag{5.1.12}$$

These equations say that the probability w_1 is proportional to the flow into region $\mathcal{R}_1$ from region $\mathcal{R}_2$. Note the similarity between this and the time-invariant distribution

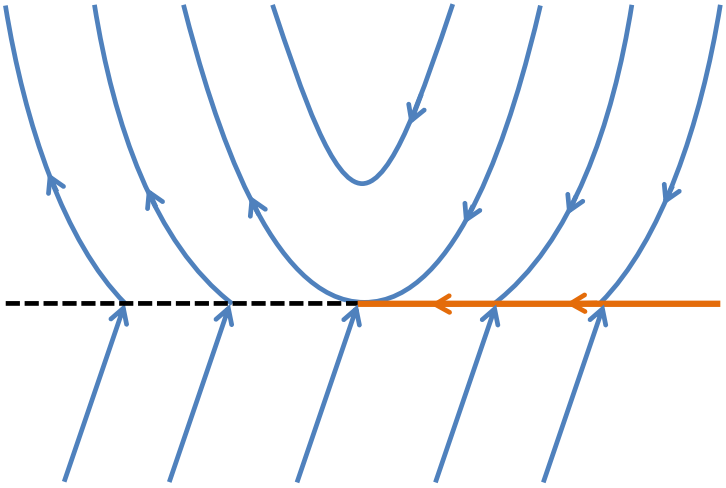


Figure 5.1: *Illustration of a discontinuity in the macroscopic equations. Solid lines (blue) show the direction of the trajectories in the two regions where the equations are continuous. Arrows show the direction of the trajectories. The dashed (black) line shows the points where the boundary is simple. The solid (orange) line shows the points at which the boundary is adhesive. The trajectory moves along the adhesive boundary until it reaches a point at which the boundary is simple, where it then moves away from the boundary.*

for the two-state Markov chain in section 3.6. This suggests a way to generalise the method of dealing with discontinuities to boundaries between more than two regions.

Upon substituting equations (5.1.12) into the equation (5.1.10), one then finds the macroscopic equation along the adhesive boundary. While the system evolves along the boundary, it is possible that it reaches a point where the boundary is no longer adhesive, and is instead simple. There the trajectory is no longer confined to the boundary and may continue to move into one of the regions $\mathcal{R}_i$, as illustrated in figure 5.1. This was the case with the trajectory corresponding to the wave-state in birth-death-migration-process described in section 4.6 - the limit cycle moved along the boundary until it reaches a point where the flow in the interior of the phase-space was no longer towards the boundary. The trajectory then left the boundary and continued on in the interior of the phase space.

5.1.3 Boundaries of the Phase-Space

Equations (5.1.10) are valid when the discontinuity is at a boundary of the phase space, say the $x_i = 0$ boundary. In this case the two regions correspond to the interior $\mathcal{I}$ where

$n_i > 0$, and the boundary $\mathcal{B}$ with one of the $n_i = 0$. The macroscopic equations have the form

$$\frac{d\boldsymbol{x}}{dt} = \boldsymbol{x}\ [w_{\mathcal{I}}\ \boldsymbol{B}_{\mathcal{I}}(\boldsymbol{x}) + w_{\mathcal{B}}\ \boldsymbol{B}_{\mathcal{B}}(\boldsymbol{x})]\,, \tag{5.1.13}$$

where $w_{\mathcal{I}}$ and $w_{\mathcal{B}}$ are the respective probabilities of the system being in either region. The probability $w_{\mathcal{B}}$ can be expressed as

$$w_{\mathcal{B}} = \frac{-\boldsymbol{e}_i \cdot \boldsymbol{x}\ \boldsymbol{B}_{\mathcal{I}}}{\boldsymbol{e}_i \cdot \boldsymbol{x}\,(\boldsymbol{B}_{\mathcal{B}} - \boldsymbol{B}_{\mathcal{I}})}\,, \tag{5.1.14}$$

so the boundary is adhesive if and only if $\boldsymbol{e}_i \cdot \boldsymbol{x}\ \boldsymbol{B}_{\mathcal{I}} < 0$, i.e. the trajectories in the interior of the phase space are directed towards the boundary. These formulae are used in both the next section and section 5.6.

5.2 BDM-process in the context of interacting particle systems

The first question posed at the begin of the thesis was:

1. "What is the minimum number of nodes needed for periodic behaviour?"

In section 2.9 it was proven that periodic behaviour could not emerge in a system with only two nodes. The birth-death-migration process (BDM-process) from chapter 4 provides an example of how collective periodic behaviours can emerge in a system with three nodes. However the BDM-process does not fit into the general framework of interacting particles systems studied in this chapter because the total number of particles in the system, n, varies stochastically with time. Nevertheless it is possible to find an equivalent system to the BDM-process, with the same macroscopic equations, where the total number of particles is constant. The equivalent system is found by recognising that the fluctuations in the total population arise solely due to the birth-death process, in which the number of particles entering the system and leaving the system are not equal, but instead balance on average. This suggests that one may be able to couple the births and deaths so they occur at the same instant. In other words, when a particle is born another dies at exactly the same time, thus holding the total population constant. Given that all particles are indistinguishable, one can then view the combined birth-death simply as the movement of one single particle between states.

The transition rates of a particle are given by $\boldsymbol{M}(\boldsymbol{n})$. One contribution to $M_{ij}(\boldsymbol{n})$ comes from the original migration process and is $r(1 \pm \rho)/2$, depending on the corresponding

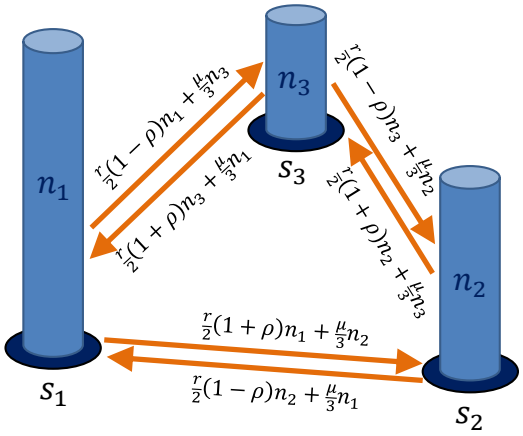


Figure 5.2: *Illustration of the dynamics of the birth-death-migration process with coupled births and deaths. Bars (blue) represent populations at each of the three nodes of the network. Arrows correspond to total jump rates of particles between nodes. This figure can be compared with figure 4.2 for the original BDM-process.*

direction of migration. Of course this is independent of $\boldsymbol{n}(t)$ because this corresponds to the movement of non-interacting particles. The interaction between particles arises from the coupled birth-death process. To find the contribution to $M_{ij}(\boldsymbol{n})$ corresponding to this, note that the total rate at which particles are removed from the (populated) i^{th} node is $\mu n/Z$, where $Z(\boldsymbol{n})$ is the number of populated nodes. Hence the rate at which a single particle at the i^{th} node dies is $\mu n/Zn_i$. Once a particle dies, a concurrent birth occurs at the j^{th} node with probability n_j/n. Therefore the joint combination of the birth and death is for a particle to leave the i^{th} node and enter the j^{th} node at a rate $(\mu n/Zn_i)(n_j/n) = \mu n_j/Zn_i$. Upon including the contribution from the migrations the components of the rate matrix are given by $M_{ij}(\boldsymbol{n}) = r(1\pm\rho)/2+\mu n_j/Zn_i$. Dependence between the particles is expressed in three terms n_i, n_j and $Z(\boldsymbol{n})$. This makes explicit the action at a distance that occurs from the death process - the transition rate of a particle at the i^{th} node is dependent upon the particles at other nodes.

5.2.1 In the Interior of the Phase-Space

When all three of the nodes are populated with particles, the rate matrix is given by $M_{ij}(\boldsymbol{n}) = r(1 \pm \rho)/2 + \mu n_j/3n_i$, for $i \neq j$. Therefore the macroscopic equations in the

interior region $\mathcal{I}$ of the phase space, where $x_i = n_i/n > 0$, can be written as

$$\frac{d\boldsymbol{x}}{dt} = \boldsymbol{x}\, \boldsymbol{B}_{\mathcal{I}}(\boldsymbol{x}) \tag{5.2.1}$$

with the matrix $\boldsymbol{B}_{\mathcal{I}}(\boldsymbol{x})$ being given by $M_{ij}(\boldsymbol{n}) = B_{ij}(\boldsymbol{x}) = r(1 \pm \rho)/2 + \mu x_j/3x_i$, for $i \neq j$, i.e.

$$\begin{aligned} \boldsymbol{B}_{\mathcal{I}}(\boldsymbol{x}) &= \frac{r}{2}\begin{pmatrix} -2 & 1+\rho & 1-\rho \\ 1-\rho & -2 & 1+\rho \\ 1+\rho & 1-\rho & -2 \end{pmatrix} \\ &+ \frac{\mu}{3}\begin{pmatrix} -(x_2+x_3)/x_1 & x_2/x_1 & x_3/x_1 \\ x_1/x_2 & -(x_1+x_3)/x_2 & x_3/x_2 \\ x_1/x_3 & x_2/x_3 & -(x_1+x_2)/x_3 \end{pmatrix}. \end{aligned} \tag{5.2.2}$$

Figure 5.2 gives an illustration of the process when the system is in the interior region $\mathcal{I}$ where all $n_i > 0$. The contribution of the joint birth-death process to $\boldsymbol{x}\ \boldsymbol{B}_{\mathcal{I}}$ in the macroscopic equations (5.2.1) is equal to the vector

$$\frac{\mu}{3}\begin{pmatrix} 2x_1 - x_2 - x_3 \\ -x_1 + 2x_2 - x_3 \\ -x_1 - x_2 + 2x_3 \end{pmatrix}^{\dagger} = \boldsymbol{x}\, \frac{\mu}{3}\begin{pmatrix} 2 & -1 & -1 \\ -1 & 2 & -1 \\ -1 & -1 & 2 \end{pmatrix}. \tag{5.2.3}$$

It follows that the macroscopic equations in the interior region are the same as those for the BDM-process (4.3.4), despite the births and deaths being combined into a single process, i.e.

$$\frac{d\boldsymbol{x}}{dt} = \boldsymbol{x}(t)\left[\frac{r}{2}\begin{pmatrix} -2 & 1+\rho & 1-\rho \\ 1-\rho & -2 & 1+\rho \\ 1+\rho & 1-\rho & -2 \end{pmatrix} - \frac{\mu}{3}\begin{pmatrix} -2 & 1 & 1 \\ 1 & -2 & 1 \\ 1 & 1 & -2 \end{pmatrix}\right]. \tag{5.2.4}$$

Unlike the matrix $\boldsymbol{B}_{\mathcal{I}}$ in equation (5.2.1), the combined matrix in equation (5.2.4) is not a Markov rate matrix for all values of μ. It can be seen that these macroscopic equations (5.2.4) are the same as those described for the BDM-process, equation (4.3.4).

5.2.2 At the Boundaries of the Phase-Space

When the population at the second node is zero, $n_2 = 0$, the only rates that are affected by the birth-death process are $M_{13} = r(1-\rho)/2 + \mu n_3/2n_1$ and $M_{31} = r(1+\rho)/2 + \mu n_1/2n_3$. All other rates are only affected by migrations. By using equation (5.1.13), the macroscopic equations describing the system at the boundaries of the phase-space are

$$\frac{d\boldsymbol{x}}{dt} = \boldsymbol{x}\left[w_{\mathcal{I}}\, \boldsymbol{B}_{\mathcal{I}}(\boldsymbol{x}) + w_{\mathcal{B}}\, \boldsymbol{B}_{\mathcal{B}}(\boldsymbol{x})\right]. \tag{5.2.5}$$

where $w_{\mathcal{I}}$ and $w_{\mathcal{B}} = 1 - w_{\mathcal{I}}$ are respectively the probabilities that the system is in the interior region $\mathcal{I}$ and at the boundary $\mathcal{B}$. The matrix $\boldsymbol{B}_{\mathcal{B}}$ is given by,

$$\boldsymbol{B}_{\mathcal{B}}(\boldsymbol{x}) \;=\; \frac{r}{2}\begin{pmatrix} -2 & 1+\rho & 1-\rho \\ 1-\rho & -2 & 1+\rho \\ 1+\rho & 1-\rho & -2 \end{pmatrix} \;+\; \frac{\mu}{2}\begin{pmatrix} -x_3/x_1 & 0 & x_3/x_1 \\ 0 & 0 & 0 \\ x_1/x_3 & 0 & -x_1/x_3 \end{pmatrix}. \tag{5.2.6}$$

The contribution of the birth-death process to the vector $\boldsymbol{x}\ \boldsymbol{B}_{\mathcal{B}}$ is

$$\frac{\mu}{2}\begin{pmatrix} x_1 - x_3 \\ 0 \\ -x_1 + x_3 \end{pmatrix}^{\dagger} \;=\; \boldsymbol{x}\ \frac{\mu}{2}\begin{pmatrix} 1 & 0 & -1 \\ 0 & 0 & 0 \\ -1 & 0 & 1 \end{pmatrix}. \tag{5.2.7}$$

Hence it follows that,

$$\boldsymbol{x}\ \boldsymbol{B}_{\mathcal{B}}(\boldsymbol{x}) \;=\; \boldsymbol{x}\left[\frac{r}{2}\begin{pmatrix} -2 & 1+\rho & 1-\rho \\ 1-\rho & -2 & 1+\rho \\ 1+\rho & 1-\rho & -2 \end{pmatrix} - \frac{\mu}{2}\begin{pmatrix} -1 & 0 & 1 \\ 0 & 0 & 0 \\ 1 & 0 & -1 \end{pmatrix}\right], \tag{5.2.8}$$

and from equation (5.2.4), it follows that

$$\boldsymbol{x}\ \boldsymbol{B}_{\mathcal{B}}(\boldsymbol{x}) \;=\; \boldsymbol{x}\ \boldsymbol{B}_{\mathcal{I}}(\boldsymbol{x}) \;+\; \frac{\mu}{6}\boldsymbol{x}\begin{pmatrix} -1 & 2 & -1 \\ 2 & -4 & 1 \\ -1 & 2 & -1 \end{pmatrix}. \tag{5.2.9}$$

This can be used to rewrite the macroscopic equations (5.2.5) as

$$\frac{d\boldsymbol{x}}{dt} \;=\; \boldsymbol{x}\left[\boldsymbol{B}_{\mathcal{I}} + w_{\mathcal{B}}\ \frac{\mu}{6}\begin{pmatrix} -1 & 2 & -1 \\ 2 & -4 & 1 \\ -1 & 2 & -1 \end{pmatrix}\right]. \tag{5.2.10}$$

The probability $w_{\mathcal{B}}$ of $n_2 = 0$ can be eliminated from this equation by taking the scalar product of equation (5.2.10) with the vector $(1, 1/2, 0)$, i.e. by calculating $dx_1/dt + (1/2)dx_2/dt$, for it then follows from the condition $dx_2/dt = 0$, on an adhesive boundary, that

$$\frac{dx_1}{dt} \;=\; \frac{d\boldsymbol{x}}{dt}\begin{pmatrix} 1 \\ 1/2 \\ 0 \end{pmatrix} \;=\; \boldsymbol{x}\ \boldsymbol{B}_{\mathcal{I}}\begin{pmatrix} 1 \\ 1/2 \\ 0 \end{pmatrix}. \tag{5.2.11}$$

Expanding this equation out gives the macroscopic equation for the boundary, at points where the boundary is adhesive. An equation for dx_3/dt can be found from $dx_1/dt + dx_3/dt = 0$ on the boundary. It follows that equation (5.2.11) is equivalent to the macroscopic equations (4.4.10) for the BDM-process. This system therefore has the same

collective behaviour as the BDM-process and provides an example of an interacting particle system with three nodes that can admit collective periodic behaviour, provided that the particles have a preferred direction of migrating. The minimum number of nodes needed for periodic behaviour is three.

5.3 Undirected Systems

In chapter 4 it was demonstrated, among other things, that the emergence of periodic behaviours in the birth-death-migration process relies on the migrations having a directional preference. The second of the questions posed at the start of the thesis was:

2. "Can periodic behaviour emerge when single particles jump at an equal rate in both directions along an edge joining nodes?"

In section 3.5.1 it was shown that a system of non-interacting particles that jump at an equal rate in both directions between nodes of the network always settles into a time-invariant distribution with particles being uniformly spread between the nodes of the network. This section shows that this always happens in undirected systems, regardless of the interactions between particles. Hence it is subsequently proven that collective periodic behaviours cannot emerge in undirected systems and therefore, directional preference is a key ingredient for periodic behaviours to occur.

Undirected systems were first introduced in section 3.5.1 in the context of non-interacting particles where it was shown that such systems did not display oscillatory behaviour. An *undirected system* is defined to be an interacting particle system in which, at any instant, the rate that a particle jumps between every pair of nodes is equal to the rate that a particle jumps in the opposite direction. A particle at the i^{th} node jumps to the j^{th} node at a rate equal to that of a particle at the j^{th} node jumping to the i^{th} node, i.e. $M_{ij}(\boldsymbol{n}(t)) = M_{ji}(\boldsymbol{n}(t))$. Thus the corresponding network structure is undirected, with edge weights being dependent on the configuration of the system.

The macroscopic equations of an undirected system have the general form

$$\frac{d\boldsymbol{x}}{dt} \;=\; \boldsymbol{x}\,\boldsymbol{B}(\boldsymbol{x}), \tag{5.3.1}$$

where $\boldsymbol{B}(\boldsymbol{x})$ is a symmetric Markov rate matrix. Equation (5.3.1) holds not only in regions of continuity but also at the boundaries of discontinuity because the sum of two symmetric Markov rate matrices is also a symmetric Markov rate matrix. Collective periodic behaviours are dependent on the macroscopic equations (5.3.1) having a limit

cycle. It can be proven that a limit cycle cannot exist by considering the function

$$\phi(\boldsymbol{x}(t)) \quad \stackrel{\text{def}}{=} \quad \frac{1}{2}\sum_{i=1}^{N} x_i(t)^2 \; . \tag{5.3.2}$$

The rate at which $\phi(\boldsymbol{x})$ changes with time is then

$$\frac{d\phi}{dt} \quad = \quad \frac{d\boldsymbol{x}}{dt} \cdot \boldsymbol{\nabla}\phi(\boldsymbol{x}) \; = \; \sum_{i,j=1}^{N} B_{ij}(\boldsymbol{x}) \; x_i \; x_j \; . \tag{5.3.3}$$

At each time t, the symmetric matrix $\boldsymbol{B}(\boldsymbol{x}(t))$ is a Markov rate matrix and so its eigenvalues are non-positive. It follows that the quadratic form on the right-hand side of equation (5.3.3) is non-positive, and is only equal to zero when $\boldsymbol{x}(t)$ is a time-invariant solution of the macroscopic equations (5.3.1). This proves that an undirected system necessarily evolves towards a time-invariant distribution, where particles are uniformly spread between the nodes of the network, and is therefore incapable of possessing collective periodic behaviour. If periodic behaviours are to emerge, particles must have a directional preference to the way in which they jump between nodes, so that $M_{ij} \neq M_{ji}$ in general.

5.3.1 Diffusive Dynamics

A fundamental reason why an undirected system does not admit collective periodic behaviour is because the dynamics are diffusive. If the i^{th} and j^{th} nodes are connected by an edge, the average flux of particles from the i^{th} node to the j^{th} node is $n_i M_{ij}(\boldsymbol{n}) - n_j M_{ji}(\boldsymbol{n}) \; = \; (n_i - n_j) M_{ij}(\boldsymbol{n})$. Thus the flux is always directed towards the smaller population. The dynamics works to equilibrate all of the populations regardless of the dependence of the rates $\boldsymbol{M}$ on the configuration of the system $\boldsymbol{n}(t)$.

The expected direction of jumping in the configuration space is in the direction $\boldsymbol{n}\,\boldsymbol{M}(\boldsymbol{n})$, where the i^{th} component corresponds to the average flux of particles into the i^{th} node. This direction is never directed away from the centre $n\mathbf{1}/N$ of the configuration space because

$$\boldsymbol{n}\,\boldsymbol{M}(\boldsymbol{n})\,(\boldsymbol{n} - n\mathbf{1}/N)^{\dagger} \quad = \quad \boldsymbol{n}\,\boldsymbol{M}(\boldsymbol{n})\,\boldsymbol{n}^{\dagger} \; \leq \; 0 \; . \tag{5.3.4}$$

The equality in equation (5.3.4) follows from $\mathbf{1}^{\dagger}$ being a right-eigenvector of the rate matrix $\boldsymbol{M}$, with a corresponding zero eigenvalue. The inequality, which applies to each component, follows from the fact that the rate matrix is non-positive definite. The expected evolution of the system is towards the uniform configuration unless the configuration is fixed on average, i.e. $\boldsymbol{n}\;\boldsymbol{M}(\boldsymbol{n}) = \mathbf{0}$. Provided the system is ergodic, see section 3.3.2, this shows that an undirected system tends to evolve towards a configuration $n\mathbf{1}/N$ where particles are uniformly distributed around the network.

5.4 Local Interactions

The interacting particle system presented in section 5.2 provides a simple example of a system that admits collective periodic behaviours. A key feature of this system is that the particles interact with other particles located at different nodes and therefore *action at a distance* occurs in the spatial structure of the network. Action at a distance provides a particle with information about particles at other nodes. The third question posed at the beginning of the thesis was:

3. "Does collective periodic behaviour rely on interactions between particles that are at different nodes?"

The remainder of this chapter seeks to provide an answer to this question.

If an interacting particle system does not allow for action at a distance, the rate of particles jumping from the i^{th} node can only depend upon the number $n_i(t)$ of particles located at that node, and no other $n_j(t)$. Alternatively if particles are viewed as interacting indirectly, by influencing the network itself, particles can only affect the local structure of the network, i.e. edges coming from the node where the particle is located. Transition rates corresponding to such *local interactions* are of the form

$$\Gamma\{\boldsymbol{k} \to \boldsymbol{k} - \boldsymbol{e}_i + \boldsymbol{e}_j\} \quad = \quad k_i \, M_{ij}(k_i) \; . \tag{5.4.1}$$

These transition rates differ from those of the most general case, given by equation (5.1.2), where the rate M_{ij} of a particle jumping from the i^{th} node to the j^{th} node may also depend on any component of $\boldsymbol{k}$ and not only k_i.

The rate M_{ij} of a particle jumping from the i^{th} node to the j^{th} node is composed of two parts, such that $M_{ij} = r_i Q_{ij}$. The first part r_i is the total rate at which the particle leaves the i^{th} node, $r_i = -M_{ii}$. The second part Q_{ij} is the probability that the particle jumps to the j^{th} node, upon leaving the i^{th} node. In the most general systems with local interactions, both r_i and Q_{ij} can be dependent on the number $n_i(t)$ of particles at the i^{th} node, meaning that a particle can influence both the rate and direction of other particles, located at the same node. An example of such a system is given in section 5.6, however the next section is concerned with analysing conditions for periodic behaviours in less general systems, whereby the probabilities Q_{ij} are independent of $n_i(t)$.

5.5 Local Speed-Altering Interactions

Introduce the notion of *local speed-altering interactions* with the property that a particle can only interact with another particle at the same node through influencing the rate

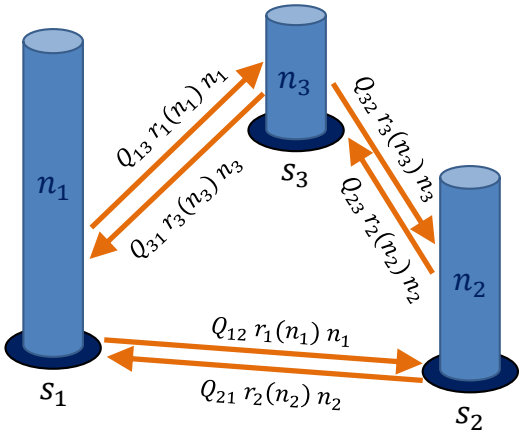


Figure 5.3: *Illustration of the dynamics of a three-state system with a local speed-altering interaction. Bars (blue) represent populations at each of the three nodes of the network. Arrows correspond to total jump rates of particles between nodes.*

at which the other particle leaves the node, whilst having no effect on what node the particle actually jumps to. Particles only influence *when* other particles jump, but not *where* they jump to. The rate matrix corresponding to these interactions has the form $M_{ij}(n_i(t)) = Q_{ij}\ r_i(n_i(t))$, where r_i is the total rate at which the particle leaves the i^{th} node and $\boldsymbol{Q}$ is a constant matrix with Q_{ij}, $i \neq j$, giving the probability of a particle jumping to the j^{th} node, upon leaving the i^{th} node. The diagonal components of the matrix $\boldsymbol{Q}$ are simply $Q_{ii} = -1$, so that the rows of the matrix sum to zero, meaning the matrix $\boldsymbol{Q}$ is itself a Markov rate matrix. The dynamics resulting from local speed-altering interactions is illustrated in figure 5.3.

Assuming that the system is *ergodic*, see section 3.3.2, the matrix $\boldsymbol{Q}$ has an associated unique left-eigenvector $\boldsymbol{\pi}$ satisfying $\boldsymbol{\pi Q} = \mathbf{0}$. The eigenvector $\boldsymbol{\pi}$ can be interpreted as the time-invariant distribution of a system of non-interacting particles with a corresponding rate matrix $\boldsymbol{Q}$. If $\boldsymbol{\pi}$ is not unique, the system with local speed-altering interactions is not ergodic. In this case, either the system splits into several non-interacting systems, and each can be considered separately, or the populations at some of the nodes are transient and eventually become zero, therefore playing no part in any periodic solution in the macroscopic equations. It follows that it is reasonable to assume that the system is indeed ergodic.

5.5.1 Non-existence of Periodic Behaviours

Systems with local speed-altering interactions cannot admit periodic behaviours for any network of any size. To prove this, start with the macroscopic equations which have the general form

$$\frac{dx_j}{dt} \;=\; \sum_{i=1}^{N} Q_{ij}\; x_i\; f_i(x_i)\;, \tag{5.5.1}$$

for all $1 \leq j \leq N$. The functions $f_i(x_i)$ are the macroscopic limit of the rates $r_i(n_i)$ respectively - possibly requiring a scaling of time. In order to show that the macroscopic equations (5.5.1) cannot possess a limit cycle, define the function

$$\phi(\boldsymbol{x}(t)) \;\stackrel{\text{def}}{=}\; \sum_{i=1}^{N} \frac{1}{\pi_i} \int_0^{x_i(t)} s\; f_i(s)\; ds, \tag{5.5.2}$$

where integrability is assumed. The time derivative of the function $\phi(t)$ is given by,

$$\begin{aligned}
\frac{d\phi}{dt} &= \frac{d\boldsymbol{x}}{dt} \cdot \boldsymbol{\nabla}\phi(\boldsymbol{x}) \\
&= \sum_{i,j=1}^{N} Q_{ij}\; x_i\; f_i(x_i) \left[\frac{1}{\pi_j}\; x_j\; f_j(x_j)\right] \\
&= \sum_{i,j=1}^{N} \pi_i\; Q_{ij} \left[\frac{1}{\pi_i}\; x_i\; f_i(x_i)\right] \left[\frac{1}{\pi_j}\; x_j\; f_j(x_j)\right] \\
&= \sum_{i,j=1}^{N} \left(\frac{\pi_i\; Q_{ij} + \pi_j\; Q_{ji}}{2}\right) \left[\frac{1}{\pi_i}\; x_i\; f_i(x_i)\right] \left[\frac{1}{\pi_j}\; x_j\; f_j(x_j)\right].
\end{aligned} \tag{5.5.3}$$

The matrix within the parentheses is a symmetric Markov rate matrix - its rows sum to zero and its off-diagonal terms are non-negative. Because any symmetric Markov rate matrix has (real) non-positive eigenvalues, see section 3.5, it follows that $d\phi/dt \leq 0$. Furthermore, ergodicity of the system implies that $d\phi/dt = 0$ only when $x_i\; f_i(x_i) \propto \pi_i$. Hence $d\phi/dt = 0$ if and only if $d\boldsymbol{x}/dt = 0$, as seen from equation (5.5.1) and the fact that π is an eigenvector of $\boldsymbol{Q}$ with corresponding zero eigenvalue. The function $\phi(t)$ is only non-decreasing at fixed points of the macroscopic equations (5.5.1). This proves that a periodic orbit cannot exist in the phase-space and therefore the particles in this system cannot display collective periodic behaviour.

5.5.2 Steady-State Solution and Associated Probability Currents

Another reason why collective periodic behaviours do not emerge from local speed-altering interactions is found by considering the steady-state solution of the master

equation (5.1.1). It happens that the steady-state solution can be stated explicitly [91],

$$P^s_{\boldsymbol{k}} \;\propto\; \prod_{i=1}^{N} \frac{\pi_i^{k_i}}{[k_i\; r_i(k_i)]!}\;, \tag{5.5.4}$$

where the generalised factorial of a function $g(k)$ defined on the non-negative integers is a functional defined by

$$[g(k)]! \;\stackrel{\text{def}}{=}\; \prod_{j=1}^{k} g(j)\;, \tag{5.5.5}$$

and $[g(0)]! = 1$. If the $r_i \equiv 1$ the steady-state solution (5.5.4) simply corresponds to that of a non-interacting particle system, see equation (3.4.9). The probability currents associated with the steady-state solution (5.5.4) are defined as

$$J\{\boldsymbol{j} \to \boldsymbol{k}\} \;\stackrel{\text{def}}{=}\; P^s_{\boldsymbol{j}}\; \Gamma\{\boldsymbol{j} \to \boldsymbol{k}\} \;-\; P^s_{\boldsymbol{k}}\; \Gamma\{\boldsymbol{k} \to \boldsymbol{j}\}. \tag{5.5.6}$$

The probability currents quantify the irreversibility in the dynamics governing the evolution of the system. From equation (5.4.1), the only non-zero transition rates are of the form

$$\Gamma\{\boldsymbol{k} \to \boldsymbol{k} - \boldsymbol{e}_i + \boldsymbol{e}_j\} \;=\; k_i\; M_{ij}(k_i) \;=\; k_i\; r_i(k_i)\; Q_{ij}\;, \tag{5.5.7}$$

with $i \neq j$, and so the non-zero probability currents are of the form

$$J\{\boldsymbol{k} \to \boldsymbol{k} - \boldsymbol{e}_i + \boldsymbol{e}_j\} \;=\; P^s_{\boldsymbol{k}}\; k_i\; r_i(k_i)\; Q_{ij} - P^s_{\boldsymbol{k}-\boldsymbol{e}_i+\boldsymbol{e}_j}\; (k_j+1)\; r_j(k_j+1)\; Q_{ji}\;. \tag{5.5.8}$$

It follows immediately from the form of the steady-state solution (5.5.4) that

$$(k_j+1)\; r_j(k_j+1)\; \frac{1}{\pi_j}\; P^s_{\boldsymbol{k}-\boldsymbol{e}_i+\boldsymbol{e}_j} \;=\; k_i\; r_i(k_i)\; \frac{1}{\pi_i}\; P^s_{\boldsymbol{k}}\;, \tag{5.5.9}$$

and so the probability currents (5.5.8) associated with the steady-state solution (5.5.4) can be written as

$$J\{\boldsymbol{k} \to \boldsymbol{k} - \boldsymbol{e}_i + \boldsymbol{e}_j\} \;=\; \frac{1}{\pi_i}\; P^s_{\boldsymbol{k}}\; k_i\; r_i(k_i)\; (\pi_i\; Q_{ij} - \pi_j\; Q_{ji})\,. \tag{5.5.10}$$

The terms within the parentheses correspond to the probability currents of a system of non-interacting particles with rate matrix $\boldsymbol{Q}$, see equation (3.4.10). If this system satisfies detailed balance the probability currents are zero, see equation (3.5.1). As this implies that the probability currents (5.5.10) are also zero, it follows that the system with local speed-altering interactions satisfies detailed balance. From the discussion in section 2.8, this rules out periodic behaviours. By contrast if the probability currents

are not equal to zero, the system does not satisfy detailed balance and periodic behaviours are not immediately prohibited. However by taking the sum over all $j \neq i$, in equation (5.5.10), one finds that the result is identically zero,

$$\sum_{j \neq i} J\{\boldsymbol{k} \to \boldsymbol{k} - \boldsymbol{e}_i + \boldsymbol{e}_j\} \;=\; \frac{1}{\pi_i}\, P^s_{\boldsymbol{k}}\, k_i\, r_i(k_i) \sum_{j=1}^{N} (\pi_i\, Q_{ij} - \pi_j\, Q_{ji}) \;=\; 0\,. \tag{5.5.11}$$

The last equality follows from $\sum_j Q_{ij} = 0$ and $\boldsymbol{\pi Q} = \boldsymbol{0}$. Because equation (5.5.11) implies the weaker condition $\sum_{ij} J\{\boldsymbol{k} \to \boldsymbol{k} - \boldsymbol{e}_i + \boldsymbol{e}_j\} = 0$, it subsequently proves that the steady-state solution is indeed given by equation (5.5.4).

In order to see what equation (5.5.11) is saying about the probability currents, consider a system of three particles constrained to a network of three nodes, i.e. $N = 3$ and $n = 3$. The configuration space is shown in figure 5.4, along with the probability currents. It is seen that the probability currents form closed loops that partition the edges of the configuration space. Increasing the number of particles in the system would result in a greater number of loops.

For systems with a large number of particles the flux of probabilities are contained to individual loops that only extend across microscopic length-scales in the phase-space of the macroscopic variables $\boldsymbol{x} = \boldsymbol{n}/n$. Thus the irreversibility that is represented by non-zero probability currents (5.5.10) does not manifest on the macroscopic level. Therefore in the steady-state the system appears macroscopically reversible. This rules out collective periodic phenomena, which rely on the system being irreversible on the macroscopic scale. The situation is similar for networks with a larger number of nodes N, where instead the probability currents form single 'cells' (hyper-tetrahedra) of the configuration space. It follows that periodic behaviours do not emerge from local speed-altering interactions, for systems of any size.

In the next section we consider a system with a class of local interactions that are not of the speed-altering type.

5.6 Periodic Behaviour from Local Interactions

This section demonstrates that periodic behaviours can emerge in interacting particle systems without invoking action at a distance. This provides a negative answer to the third and final question posed at the beginning of the thesis:

3. "Does collective periodic behaviour rely on interactions between particles that are at different nodes?"

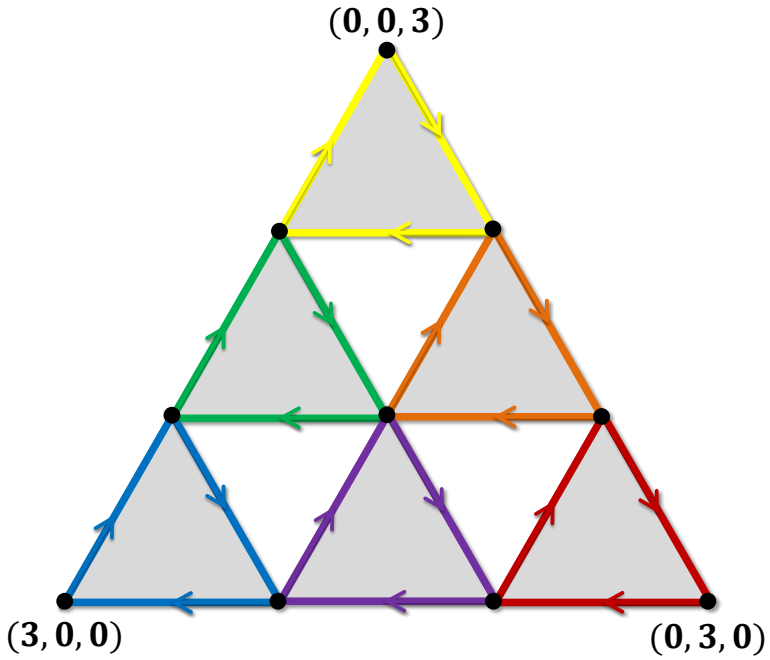


Figure 5.4: *Illustration of the probability currents for a system with a local speed-altering interaction. The system has three particles constrained to a three node network. The probability currents are represented by arrows between different configurations, shown by black circles. These currents form closed loops (around the shaded triangles) that partition the edges of the configuration space, with colours representing different magnitudes. The orientation of the currents in this example is clockwise.*

To begin to understand how periodic behaviours can emerge from local interactions, one can search for inspiration from the birth-death-migration system of chapter 4, or equivalently that described in section 5.2. The birth-death-migration system is built upon a system of non-interacting particles jumping or rather 'migrating' around a network comprising three nodes in a closed loop. By itself this migration process is diffusive and causes particles to become uniformly distributed around the nodes of the network. The migration process is then supplemented by birth and death process that introduce correlations between the particles. It was shown that collective periodic behaviours emerge provided there is a balance between the rate of the migration process and the rate of the birth-death process.

The effect of the births and deaths causes particles to group together and condense at a single node and so is akin to an attractive force between the particles. In section 5.2 this was made explicit by coupling the births and deaths. The resulting components of the rate matrix $M_{ij}(\boldsymbol{n}) = r(1 \pm \rho)/2 + \mu n_j/Z n_i$, corresponding to particles leaving the i^{th} node and entering the j^{th} node, have a term that is inversely proportional to the population of particles in the i^{th} node. However in the birth-death-migration process the attractive nature of the birth-death process also includes a non-local ingredient, through the dependence of M_{ij} on n_j and $Z(\boldsymbol{n})$. This section defines a system in which the attractive force between particles manifests solely through local interactions. Moreover it follows that the macroscopic behaviour of this system is strongly linked with that of the BDM-process.

5.6.1 Dynamics

As was the case for the BDM-process, start by considering the three-state loop system from section 3.8, whereby particles jump independently with rates given by $M_{12} = M_{23} = M_{31} = r(1+\rho)/2$ and $M_{21} = M_{32} = M_{13} = r(1-\rho)/2$. In addition consider a local interaction between particles at the same node, causing a particle at the i^{th} nodes to jump to another node, with equal probability in both directions, at a total rate $\nu f(n_i(t)/n)$, where ν is non-negative constant and $f(x)$ is a non-negative function defined by,

$$f(x) \;=\; \begin{cases} \frac{1+\beta}{x} - 1, & x > 0\,; \\ 0, & x = 0\,. \end{cases} \tag{5.6.1}$$

The parameter $\beta \geq 0$. The rate matrix for the system is given by the components $M_{ij}(\boldsymbol{n}) = r(1 \pm \rho)/2 + \nu f(n_i/n)/2$, which possess a term that is inversely proportional to n_i. To see that this system does not have local speed-altering interactions, express the rate matrix in the terms $M_{ij} = r_i Q_{ij}$, where $r_i = r + \nu f$ is the total rate in which a

particle leaves the i^{th} node and $Q_{ij} = 1/2 \pm r\rho/2(r+\nu f)$ is the probability of the particle jumping to the j^{th} node. If $\rho = 0$, the probabilities Q_{ij} are constant, and the interactions between particles are of the local speed-altering type. In fact, the system satisfies detailed balance. From the discussion in the previous section, this rules out periodic behaviours. However this is not the case if $\rho \neq 0$. In order to analyse the behaviour of the system, one must determine the macroscopic equations for this system in the interior and at the boundaries of the phase-space.

5.6.2 Interior of the Phase-Space

The macroscopic equations in the interior region $\mathcal{I}$ of the phase space, where $x_i > 0$, can be written as

$$\frac{d\boldsymbol{x}}{dt} \;=\; \boldsymbol{x}\, \boldsymbol{B}_{\mathcal{I}}(\boldsymbol{x}) \tag{5.6.2}$$

with the matrix $\boldsymbol{B}_{\mathcal{I}}(\boldsymbol{x})$ being given by

$$\begin{aligned} \boldsymbol{B}_{\mathcal{I}}(\boldsymbol{x}) \;&=\; \frac{r}{2}\begin{pmatrix} -2 & 1+\rho & 1-\rho \\ 1-\rho & -2 & 1+\rho \\ 1+\rho & 1-\rho & -2 \end{pmatrix} \\ &+\; \frac{\nu}{2}\begin{pmatrix} \frac{1+\beta}{x_1}-1 & 0 & 0 \\ 0 & \frac{1+\beta}{x_2}-1 & 0 \\ 0 & 0 & \frac{1+\beta}{x_3}-1 \end{pmatrix}\begin{pmatrix} -2 & 1 & 1 \\ 1 & -2 & 1 \\ 1 & 1 & -2 \end{pmatrix}. \end{aligned} \tag{5.6.3}$$

Despite the matrix $\boldsymbol{B}_{\mathcal{I}}(\boldsymbol{x})$ being non-linear, the macroscopic equations (5.6.2) are nevertheless linear. To see this, consider the following contribution to $\boldsymbol{x}\, \boldsymbol{B}_{\mathcal{I}}(\boldsymbol{x})$,

$$\boldsymbol{x}\,\frac{\nu}{2}\begin{pmatrix} \frac{1+\beta}{x_1}-1 & 0 & 0 \\ 0 & \frac{1+\beta}{x_2}-1 & 0 \\ 0 & 0 & \frac{1+\beta}{x_3}-1 \end{pmatrix} \;=\; \frac{\nu}{2}\left((1+\beta)\mathbf{1} - \boldsymbol{x}\right). \tag{5.6.4}$$

Hence the contribution of the local interactions to the macroscopic equations (5.6.2) is

$$\frac{\nu}{2}\left((1+\beta)\mathbf{1} - \boldsymbol{x}\right)\begin{pmatrix} -2 & 1 & 1 \\ 1 & -2 & 1 \\ 1 & 1 & -2 \end{pmatrix} \;=\; -\frac{\nu}{2}\,\boldsymbol{x}\begin{pmatrix} -2 & 1 & 1 \\ 1 & -2 & 1 \\ 1 & 1 & -2 \end{pmatrix}. \tag{5.6.5}$$

The macroscopic equations (5.6.2) in the interior of the phase space can therefore be written as

$$\frac{d\boldsymbol{x}}{dt} \;=\; \boldsymbol{x}\left[\frac{r}{2}\begin{pmatrix} -2 & 1+\rho & 1-\rho \\ 1-\rho & -2 & 1+\rho \\ 1+\rho & 1-\rho & -2 \end{pmatrix} - \frac{\nu}{2}\begin{pmatrix} -2 & 1 & 1 \\ 1 & -2 & 1 \\ 1 & 1 & -2 \end{pmatrix}\right]. \tag{5.6.6}$$

The macroscopic evolution of the system is independent of the parameter β. To understand why consider the total rate at which particles jump from the first node to the second node due to the local interactions, $n_1 f(n_1/n)/2 = (1+\beta)n/2 - n_1/2$. Similarly the total rate of particles jumping from the second node to the first node is $n_2 f(n_2/n)/2 = (1+\beta)n/2 - n_2/2$. The first terms in both of these expressions are equal and so the net flow of particles between these two nodes is independent of β. The situation is the same for each pair of nodes and hence β does not affect the macroscopic equations. Including the parameter β corresponds to a Poisson process operating between each pair of nodes. Particles jump at a total (constant) rate βn.

5.6.3 Boundary of the Phase-Space

The function $f(x)$ approaches infinity like $1/x$ as $x \to 0$, such that $xf(x) \to 1+\beta$ is finite. However $xf(x)|_{x=0} = 0$, and so there is a discontinuity in the macroscopic equations at the boundary of the phase-space. Hence the arguments and considerations of section 5.1.3 are required. Define $\mathcal{B}$ to be the boundary region where $n_2 = 0$, i.e. configurations with the second node unpopulated. The macroscopic equations that describe the motion along the boundary are given by

$$\frac{d\boldsymbol{x}}{dt} \;=\; \boldsymbol{x}\,[\,w_{\mathcal{I}}\,\boldsymbol{B}_{\mathcal{I}} \,+\, w_{\mathcal{B}}\,\boldsymbol{B}_{\mathcal{B}}\,]\,, \tag{5.6.7}$$

where $w_{\mathcal{I}}$ and $w_{\mathcal{B}} = 1 - w_{\mathcal{I}}$ are respectively the probabilities that the system is in the regions $\mathcal{I}$ and $\mathcal{B}$. The matrix $\boldsymbol{B}_{\mathcal{B}}(\boldsymbol{x})$ is given by

$$\begin{aligned}\boldsymbol{B}_{\mathcal{B}}(\boldsymbol{x}) \;&=\; \frac{r}{2}\begin{pmatrix} -2 & 1+\rho & 1-\rho \\ 1-\rho & -2 & 1+\rho \\ 1+\rho & 1-\rho & -2 \end{pmatrix} \\ &+\; \frac{\nu}{2}\begin{pmatrix} \frac{1+\beta}{x_1}-1 & 0 & 0 \\ 0 & 0 & 0 \\ 0 & 0 & \frac{1+\beta}{x_3}-1 \end{pmatrix}\begin{pmatrix} -2 & 1 & 1 \\ 1 & -2 & 1 \\ 1 & 1 & -2 \end{pmatrix}. \end{aligned} \tag{5.6.8}$$

Consider the following contribution to $\boldsymbol{x}\,\boldsymbol{B}_{\mathcal{B}}(\boldsymbol{x})$, bearing in mind that $x_2 = 0$,

$$\boldsymbol{x}\,\frac{\nu}{2}\begin{pmatrix} \frac{1+\beta}{x_1}-1 & 0 & 0 \\ 0 & 0 & 0 \\ 0 & 0 & \frac{1+\beta}{x_3}-1 \end{pmatrix} \;=\; \frac{\nu}{2}\,((1+\beta)(1,0,1) - \boldsymbol{x})\,. \tag{5.6.9}$$

By inserting this in equation (5.6.8) and using equation (5.6.6), it follows that

$$\boldsymbol{x}\,\boldsymbol{B}_{\mathcal{B}} \;=\; \boldsymbol{x}\,\boldsymbol{B}_{\mathcal{I}} \,+\, \frac{\nu}{2}(1+\beta)\,(-1,\,2,-1)\,. \tag{5.6.10}$$

The macroscopic equations (5.6.7) can then be rewritten as

$$\frac{d\boldsymbol{x}}{dt} \;=\; \boldsymbol{x}\,\boldsymbol{B}_{\mathcal{I}} \,+\, \frac{\nu}{2}\,(1+\beta)\,w_{\mathcal{B}}\;(-1,\,2,-1)\,. \tag{5.6.11}$$

The probability $w_{\mathcal{B}}$ can be eliminated from this equation by taking the scalar product with $(1, 1/2, 0)$, i.e. calculating $dx_1/dt + (1/2)dx_2/dt$ as seen in equation (5.2.11). However, as trajectories evolve along the boundary (while it is adhesive), $dx_2/dt = 0$ and so

$$\frac{dx_1}{dt} \;=\; \frac{dx_1}{dt} \,+\, \frac{1}{2}\frac{dx_2}{dt} \;=\; \boldsymbol{x}\, \boldsymbol{B}_{\mathcal{I}} \begin{pmatrix} 1 \\ 1/2 \\ 0 \end{pmatrix}. \tag{5.6.12}$$

This equation holds at all points where the boundary is adhesive - where trajectories in the interior point towards the boundary. An equation for dx_3/dt can be found from $dx_1/dt + dx_3/dt = 0$ on the boundary. The equations at the two remaining boundaries are found by a similar method. The macroscopic equations (5.6.6) and (5.6.12) can be used to describe the behaviour of the system.

5.6.4 Relation to the Birth-Death-Migration Process

In order to prove that the particles in this system behave periodically, it must be shown that a limit cycle can exist in the macroscopic equations. However, instead of analysing the macroscopic equations, it is revealing to make the substitution $\nu/2 = \mu/3$ in the equation (5.6.6) and simply compare with the macroscopic equations (5.2.4) for the birth-death-migration system. It is apparent that the macroscopic behaviours of both systems are equivalent in the interior of the phase-space. At the boundaries, equation (5.6.12) can be compared with equation (5.2.11) to see that the macroscopic equations on the boundaries are also equivalent. Both systems are macroscopically indistinguishable and therefore display the same collective phenomena despite having different microscopic behaviours.

The same control parameter $\theta = (2\mu - 3r)/r\rho \equiv (3\nu - 3r)/r\rho$ can be used to describe the various behaviours of the system as was used for the BDM-process of chapter 4. When the value of ν is relatively small compared to r, so that $\theta < 0$, the particles will become uniformly distributed around the three nodes of the network. When $0 < \theta < 1$ collective periodic behaviours will emerge as the particle form a wave that travels around the network. The frequency and amplitude of the oscillations is given by the quantitative analysis in sections 4.7 and 4.8. Increasing ν further so that $1 < \theta < \theta_c \approx 1.2$ causes the oscillations begin to break down as the system displays intermittent behaviour. Finally, when $\theta > \theta_c$ the particles condense onto a single node of the network. This qualitative analysis is confirmed by Monte-Carlo simulations, figure 5.5, of the system for four different values of ν, with $r = 1$ and $\mu = 1$. The simulation results can be compared with those of the BDM-process presented in figure 4.5 to confirm

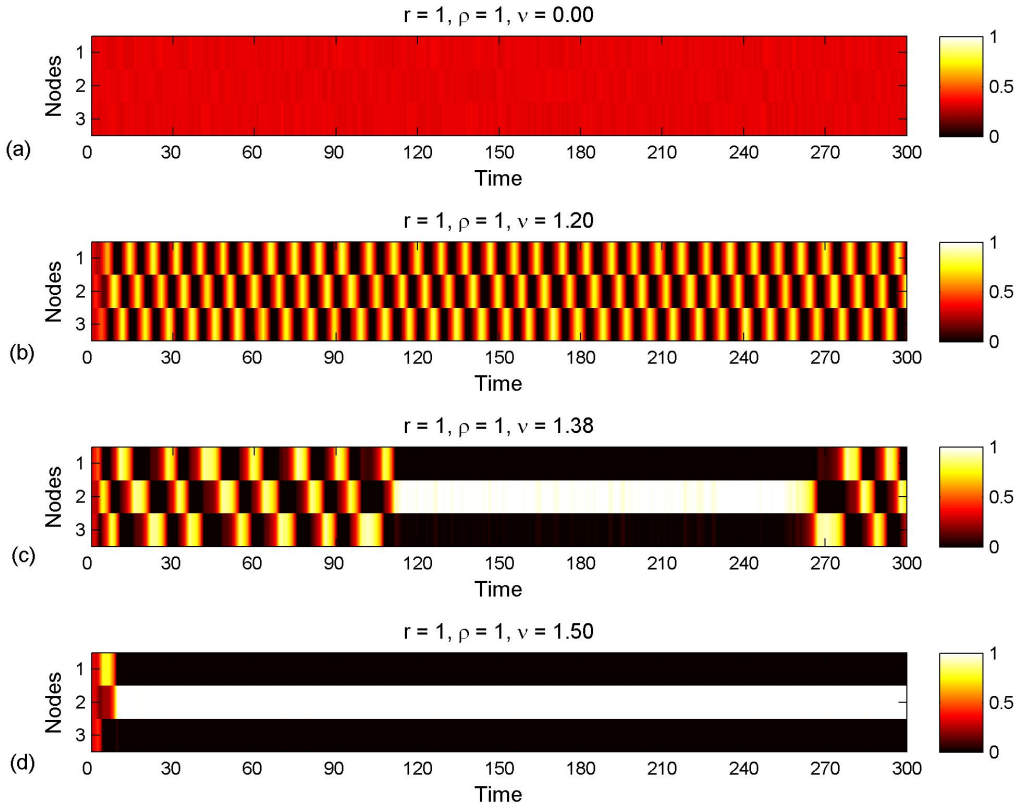


Figure 5.5: *Heat plot of simulated data for four different values of the interaction rate ν with common migration rate $r = 1$, preference $\rho = 1$. Each simulation initiated with a population of 1000 particles at each node. Colour intensities in the rows correspond to the proportion of particle at each node number of particles at each of the three nodes with the scales being given on the right. (a) Dissipative behaviour, $\nu = 0$. (b) Periodic behaviour, $\nu = 1.2$. (c) Intermittent behaviour, $\nu = 1.38$. (d) Condensed behaviour, $\nu = 1.5$.*

that the two systems do indeed show the same macroscopic behaviour, regardless of their differing microscopic dynamics. In particular it has been demonstrated that an interacting particle system can indeed admit collective periodic behaviour without invoking action at a distance.

5.7 Discussion

In this chapter we have discussed necessary conditions for collective periodic behaviours in interacting particle systems. In particular we have discussed the minimum number of nodes that are needed and the importance of directionality and non-local interactions.

In section 5.1 we began the chapter by developing a method for deriving the macroscopic equations from the microscopic dynamics. This involved dealing with situations where continuity of the rate matrix could not be assumed. The macroscopic equations were then analysed, in subsequent sections, for particular interactions to assess the possibility of limit cycles that are associated with periodic phenomena.

In section 2.9 it was proven that periodic behaviours could not exist in a system in which particles are constrained to only two nodes. In section 5.2 we found an equivalent interacting particle system to the birth-death-migration process which gave an example of a three node interacting particle system in which emergent periodic behaviours are possible. This consequently proved that the minimum number of nodes necessary for periodic behaviour is three.

In section 5.3 it was proven that a necessary condition for collective periodic behaviours is that the underlying network structure must have directed edges, so that particles jump in opposite directions between nodes at different rates. For systems with a network structure that has only undirected edges, the dynamics are fundamentally diffusive and result in particles becoming uniformly distributed around the nodes of the network.

The birth-death-migration process from chapter 4 and its equivalent interacting particle system, described in section 5.2, both gave particles the ability to influence each other at separate nodes. This suggested that this kind of action at a distance plays an important role in allowing periodic behaviours to emerge. This is indeed the case for systems with local speed-altering interactions, considered in section 5.5, whereby particles only affect the rate at which other particles jump away from a node and not the node which they subsequently jump to. For such systems the irreversibility required for collective periodic phenomena does not manifest on the macroscopic scale and so periodic behaviour cannot emerge and persist.

Action at a distance is not, however, a necessary ingredient for periodic behaviour. This was demonstrated in section 5.6, which describes a system with local interactions that possesses exactly the same macroscopic behaviour as the birth-death-migration process from chapter 4. In order to observe collective periodic behaviours without invoking action at a distance, the local interactions were defined in such a way that they corresponded to an attractive force between particles that is able to overcome the diffusive nature of the independent motion of the particles. It is the absence of such an attractive force in undirected systems, section 5.3, that results in particles becoming equally distributed around the nodes of the network. This suggests that such an attractive aspect to the interactions is a vital mechanism by which particles synchronise to form collective periodic phenomena from dynamics that are fundamentally incoherent and memoryless.

Chapter 6

Conclusions and Further Work

In this chapter we provide a brief summary of the work undertaken in this thesis and discuss the key results. We then provide ideas for work that could extend the results presented in the previous chapters.

6.1 Overview of the Thesis

The aim of this thesis was to identify the essential ingredients that are required for the emergence of collective periodic behaviours in a system whose components change incoherently between a finite number of states. Throughout the thesis the components are represented as indistinguishable particles that jump spontaneously between the states, represented as the nodes of a network. Considered systems are assumed to be memoryless, implying that the time evolution of the configuration of the system can be described by a Markov process. In section 1.3.1 it was argued that Markov processes provide an excellent context in which to study emergent collective phenomena because they do not introduce artificial correlations into the system. Any correlations that arise emerge from intrinsic, incoherent fluctuations of the system.

6.1.1 Need for Irreversibility

In chapter 2 we introduced interacting particle systems, whereby particles interact by affecting the rate at which other particles jump to other nodes forming the network. For systems with a large number of particles the collective behaviour of the entire ensemble is approximated by a set of deterministic nonlinear differential equations, known as the macroscopic equations. A method for deriving the macroscopic equations from the microscopic dynamics was presented in section 5.1. The long-term collective behaviour

of the system is determined by the steady-state behaviour of the macroscopic equations. In particular, collective periodic behaviours are associated with stable limit cycle solutions of the macroscopic equations. A necessary condition for such limit cycles is that the system must violate the principle of detailed balance. Indeed it was shown in section 2.8 that a system that satisfies detailed balance is consequently time-reversible, implying that the dynamics appear the same when time runs backwards. Because the system is memoryless, this rules out periodic behaviour.

6.1.2 Need for Interactions

Systems of non-interacting particles were analysed in chapter 3. When particles do not interact in any way, their movement is independent of the configuration of the particles in the system. As the particles move spontaneously, the dynamics is diffusive and the steady-state of the system is for particles to spread around the nodes of the network according to a time-invariant distribution that is dependent on the rates at which particles jump, see section 3.4. It is therefore apparent that interactions between particles are crucial for the emergence of collective periodic behaviours. However, while systems of non-interacting particles lack the mechanism by which disturbances from the time-invariant distribution may be sustained, the system can display damped oscillations as it approaches equilibrium, provided the system is irreversible. The simplest system which can display oscillations was demonstrated to be a three-node loop, section 3.8, where particles have a preferred direction of jumping to other nodes. In section 3.9 it was shown that these oscillations could last longer in systems with a larger number of nodes. The simple three-node network is adopted as a fundamental element for periodic behaviour upon which to build.

6.1.3 Birth-Death-Migration-process

In chapter 4 we saw how the damped oscillations that can arise in systems of non-interacting particles migrating around a three node loop can be made to persist with the help of simple birth and death processes. The birth and death processes implicitly introduce correlations between the particles and play a key role in counteracting the diffusive collective behaviour of the non-interacting particles. However, these two processes alone do not allow for periodic behaviours but instead result in particles becoming condensed at a single node of the network. In order for collective periodic behaviours to emerge and persist, there must be a trade-off between the diffusion caused by the particle migrations and the ‘attraction’ caused by the births and deaths. This was demonstrated by Monte-Carlo simulations, see figure 4.5.

An important aspect to the dynamics was that the particles have a preference to the way in which they migrate around the network. This lead to the hypothesis that such a directional preference may play a key role in general interacting particle systems. Another important feature of the dynamics was that the death process was defined globally over the network, providing particles with information about particles that are located at other nodes. If the death process was local, like the birth process, then no oscillations can occur. It was therefore postulated that an 'action at a distance' may be an important ingredient for collective periodic behaviours.

6.1.4 Three Important Questions

At the beginning of the thesis, three questions were posed regarding conditions for collective periodic behaviours to emerge from randomness. In chapter 5 we discussed and attained conclusive answers to each of these questions in the context of general interacting particle systems:

1. "What is the minimum number of nodes needed for periodic behaviour?"

Three. It was shown in section 2.9 that if particles were constrained to only two possible states, there cannot exist collective periodic behaviours. The reason for this is that the system necessarily satisfies detailed balance and is therefore time-reversible. In other words it must appear statistically indistinguishable if the direction of time is reversed. Combined with the memoryless property, this forbids periodic behaviours from emerging. A three node network that admitted periodic behaviours was demonstrated in section 5.2.

2. "Can periodic behaviour emerge when single particles jump at an equal rate in both directions along an edge joining nodes?"

No, regardless of the form of the interactions between particles. It was proven in section 5.3 that if the network has only undirected edges, the macroscopic equations do not contain the limit cycle behaviour that is associated with collective periodic behaviour. Without a directional preference to the way in which particles jump between nodes, the microscopic dynamics is fundamentally diffusive and evolves to a steady-state with particles being uniformly spread around the nodes of the network. Therefore a necessary ingredient for collective periodic phenomena is a directional preference to the way in which particles jump.

3. "Does collective periodic behaviour rely on interactions between particles that are at different nodes?"

No. An example of a system that admits periodic phenomena despite particles only interacting locally at the same nodes as each other was provided in section 5.6. In fact this system had exactly the same collective behaviour as the birth-death-migration process of chapter 4. However in section 5.5 is was proven that a requirement of periodic behaviours emerging from local interactions is that particles affect where other particles jump to, and not only the rate at which they jump. If this is not the case, the irreversibility that is necessary for periodic behaviour does not manifest on the macroscopic level.

6.1.5 Summary of the Essential Ingredients

This thesis has identified several important ingredients that are necessary for collective periodic behaviours. A main condition is that the microscopic dynamics must be irreversible, i.e. must violate detailed balance. A system with two nodes cannot be irreversible and so it is necessary that the system have at least three nodes. However it is not sufficient for the microscopic dynamics to be irreversible, but rather that this irreversibility manifest itself on the macroscopic scale.

There must be a trade-off between diffusion and attraction. If the dynamics is solely diffusive, such as for an undirected system, particles become spread around the network in a time-invariant distribution. If the dynamics is solely attractive, particles become condensed at a single node.

6.2 Further Work

One possible way to extend the work presented in this thesis is to consider particle systems with a different type of interaction. For the systems considered in this thesis, the particles interact by affecting the rate at which other particles move. As an alternative, it is possible to consider an interaction whereby particles move together, so that more than one particle moves at the same time. If it is possible to find macroscopic equations, the results from chapter 5 would remain applicable. However finding such macroscopic equations may not be possible. Furthermore, some of the arguments used for the microscopic behaviour of the systems in this thesis cannot be used to rule out periodic behaviours. For instance, a two-state system need no longer satisfy detailed balance and so it may be possible for periodic behaviours to emerge.

Another possible extension to this thesis would be to consider systems with different varieties of particles, e.g. red and blue particles. It is not too difficult to fit such systems into the framework developed in this thesis; an N-state system with K varieties of particle could be expressed as K sub-networks of size N, making a total network size

of NK nodes. Each state is represented by K different nodes corresponding to each variety of particle - a red particle at a state is seen as being at a different node than a blue particle at the same state. Assuming that the variety of a particle is constant, an undirected system with more than one variety of particle is still represented by an undirected network. This means that collective periodic behaviours do not emerge in an undirected system, even with different varieties of particle. However a two state-system with $K > 1$ varieties of particle may admit periodic behaviours as the effective network size is $2K$, and detailed balance does not necessarily hold.

In addition to these suggested extensions to the thesis, one might also consider the effects of including memory into the system, thus removing the Markov assumption. In any case, this thesis has provided a methodology for assessing the emergence of collective periodic behaviours in discrete systems with random dynamics that may provide a foundation for further research.

Bibliography

[1] Jesse Stricker, Scott Cookson, Matthew R Bennett, William H Mather, Lev S Tsimring, and Jeff Hasty. A fast, robust and tunable synthetic gene oscillator. *Nature*, 456(7221):516–519, 2008.

[2] Johannes Knebel, Markus F Weber, Torben Krüger, and Erwin Frey. Evolutionary games of condensates in coupled birth-death processes. *Nature communications*, 6, 2015.

[3] Ozalp Babaoglu, Toni Binci, Márk Jelasity, and Alberto Montresor. Firefly-inspired heartbeat synchronization in overlay networks. In *First International Conference on Self-Adaptive and Self-Organizing Systems (SASO 2007)*, pages 77–86. IEEE, 2007.

[4] Alexandre Rosas, Daniel Escaff, Katja Lindenberg, et al. Globally coupled stochastic two-state oscillators: synchronization of infinite and finite arrays. *Journal of Physics A: Mathematical and Theoretical*, 49(9):095001, 2016.

[5] Chunguang Li, Luonan Chen, and Kazuyuki Aihara. Synchronization of coupled nonidentical genetic oscillators. *Physical Biology*, 3(1):37, 2006.

[6] Albert Goldbeter. Computational approaches to cellular rhythms. *Nature*, 420(6912):238–245, 2002.

[7] Enrico Di Cera, Paul E Phillipson, and Jeffries Wyman. Chemical oscillations in closed macromolecular systems. *Proceedings of the National Academy of Sciences*, 85(16):5923–5926, 1988.

[8] Enrico Di Cera, Paul E Phillipson, and Jeffries Wyman. Limit-cycle oscillations and chaos in reaction networks subject to conservation of mass. *Proceedings of the National Academy of Sciences*, 86(1):142–146, 1989.

[9] Matthew Bennett, Michael F Schatz, Heidi Rockwood, and Kurt Wiesenfeld. Huygens's clocks. *Proceedings: Mathematics, Physical and Engineering Sciences*, pages 563–579, 2002.

[10] John Buck and Elisabeth Buck. Toward a functional interpretation of synchronous flashing by fireflies. *American naturalist*, pages 471–492, 1978.

[11] Bard Ermentrout. An adaptive model for synchrony in the firefly pteroptyx malaccae. *Journal of Mathematical Biology*, 29(6):571–585, 1991.

[12] Céline Feillet, Peter Krusche, Filippo Tamanini, Roel C Janssens, Mike J Downey, Patrick Martin, Michèle Teboul, Shoko Saito, Francis A Lévi, Till Bretschneider, et al. Phase locking and multiple oscillating attractors for the coupled mammalian clock and cell cycle. *Proceedings of the National Academy of Sciences*, 111(27):9828–9833, 2014.

[13] Gen Kurosawa, Atsushi Mochizuki, and Yoh Iwasa. Comparative study of circadian clock models, in search of processes promoting oscillation. *Journal of theoretical biology*, 216(2):193–208, 2002.

[14] Bernd Blasius, Amit Huppert, and Lewi Stone. Complex dynamics and phase synchronization in spatially extended ecological systems. *Nature*, 399(6734):354–359, 1999.

[15] BENNO Hess and ARNOLD Boiteux. Oscillatory phenomena in biochemistry. *Annual review of biochemistry*, 40(1):237–258, 1971.

[16] Joseph D Challenger and Alan J McKane. Synchronization of stochastic oscillators in biochemical systems. *Physical Review E*, 88(1):012107, 2013.

[17] Alan L Hodgkin and Andrew F Huxley. A quantitative description of membrane current and its application to conduction and excitation in nerve. *The Journal of physiology*, 117(4):500, 1952.

[18] György Buzsáki and Andreas Draguhn. Neuronal oscillations in cortical networks. *science*, 304(5679):1926–1929, 2004.

[19] Marlene Bartos, Imre Vida, and Peter Jonas. Synaptic mechanisms of synchronized gamma oscillations in inhibitory interneuron networks. *Nature reviews neuroscience*, 8(1):45–56, 2007.

[20] Steven H Strogatz, Daniel M Abrams, Allan McRobie, Bruno Eckhardt, and Edward Ott. Theoretical mechanics: Crowd synchrony on the millennium bridge. *Nature*, 438(7064):43–44, 2005.

[21] Steven Strogatz. *Sync*. Hyperion Books.[TKS], 2003.

[22] Arkady Pikovsky, Michael Rosenblum, and Jürgen Kurths. *Synchronization: a universal concept in nonlinear sciences*, volume 12. Cambridge university press, 2003.

[23] Derek Paley, Naomi Ehrich Leonard, Rodolphe Sepulchre, Daniel Grünbaum, Julia K Parrish, et al. Oscillator models and collective motion. *Control Systems, IEEE*, 27(4):89–105, 2007.

[24] Steven H Strogatz. From kuramoto to crawford: exploring the onset of synchronization in populations of coupled oscillators. *Physica D: Nonlinear Phenomena*, 143(1):1–20, 2000.

[25] Yoshiki Kuramoto. Self-entrainment of a population of coupled non-linear oscillators. In *International symposium on mathematical problems in theoretical physics*, pages 420–422. Springer, 1975.

[26] Juan A Acebrón, Luis L Bonilla, Conrad J Pérez Vicente, Félix Ritort, and Renato Spigler. The kuramoto model: A simple paradigm for synchronization phenomena. *Reviews of modern physics*, 77(1):137, 2005.

[27] Renato E Mirollo and Steven H Strogatz. Synchronization of pulse-coupled biological oscillators. *SIAM Journal on Applied Mathematics*, 50(6):1645–1662, 1990.

[28] Geoffrey Werner-Allen, Geetika Tewari, Ankit Patel, Matt Welsh, and Radhika Nagpal. Firefly-inspired sensor network synchronicity with realistic radio effects. In *Proceedings of the 3rd international conference on Embedded networked sensor systems*, pages 142–153. ACM, 2005.

[29] Steven H Strogatz, Ian Stewart, et al. Coupled oscillators and biological synchronization. *Scientific American*, 269(6):102–109, 1993.

[30] Florian Dörfler, Michael Chertkov, and Francesco Bullo. Synchronization in complex oscillator networks and smart grids. *Proceedings of the National Academy of Sciences*, 110(6):2005–2010, 2013.

[31] Arthur R Bergen and David J Hill. A structure preserving model for power system stability analysis. *Power Apparatus and Systems, IEEE Transactions on*, (1):25–35, 1981.

[32] Alex Arenas, Albert Díaz-Guilera, Jurgen Kurths, Yamir Moreno, and Changsong Zhou. Synchronization in complex networks. *Physics Reports*, 469(3):93–153, 2008.

[33] Alex Arenas, Albert Díaz-Guilera, and Conrad J Pérez-Vicente. Synchronization reveals topological scales in complex networks. *Physical review letters*, 96(11):114102, 2006.

[34] Dennis Lucarelli, I-Jeng Wang, et al. Decentralized synchronization protocols with nearest neighbor communication. In *Proceedings of the 2nd international conference on Embedded networked sensor systems*, pages 62–68. ACM, 2004.

[35] Adilson E Motter, CS Zhou, and Jürgen Kurths. Enhancing complex-network synchronization. *EPL (Europhysics Letters)*, 69(3):334, 2005.

[36] Takashi Nishikawa, Adilson E Motter, Ying-Cheng Lai, and Frank C Hoppensteadt. Heterogeneity in oscillator networks: Are smaller worlds easier to synchronize? *Physical review letters*, 91(1):014101, 2003.

[37] Jesús Gómez-Gardenes, Yamir Moreno, and Alex Arenas. Paths to synchronization on complex networks. *Physical review letters*, 98(3):034101, 2007.

[38] Roberto Benzi, Alfonso Sutera, and Angelo Vulpiani. The mechanism of stochastic resonance. *Journal of Physics A: mathematical and general*, 14(11):L453, 1981.

[39] Roberto Benzi, Giorgio Parisi, Alfonso Sutera, and Angelo Vulpiani. Stochastic resonance in climatic change. *Tellus*, 34(1):10–16, 1982.

[40] Catherine Nicolis and Grégoire Nicolis. Stochastic aspects of climatic transitions–additive fluctuations. *Tellus*, 33(3):225–234, 1981.

[41] C Nicolis. Stochastic aspects of climatic transitions—response to a periodic forcing. *Tellus*, 34(1):1–9, 1982.

[42] R Benzi. Stochastic resonance: from climate to biology. *Nonlinear Processes in Geophysics*, 17(5):431–441, 2010.

[43] Arkady S Pikovsky and Jürgen Kurths. Coherence resonance in a noise-driven excitable system. *Physical Review Letters*, 78(5):775, 1997.

[44] Herbert Treutlein and Klaus Schulten. Noise-induced neural impulses. *European Biophysics Journal*, 13(6):355–365, 1986.

[45] Mark D McDonnell and Derek Abbott. What is stochastic resonance? definitions, misconceptions, debates, and its relevance to biology. *PLoS Comput Biol*, 5(5):e1000348, 2009.

[46] Vadim Semenovich Anishchenko, Arkady B Neiman, F Moss, and L Shimansky-Geier. Stochastic resonance: noise-enhanced order. *Physics-Uspekhi*, 42(1):7–36, 1999.

[47] Luca Gammaitoni, Peter Hänggi, Peter Jung, and Fabio Marchesoni. Stochastic resonance. *Reviews of modern physics*, 70(1):223, 1998.

[48] Werner Horsthemke and René Lefever. Noise-induced transitions in physics, chemistry, and biology. *Noise-Induced Transitions: Theory and Applications in Physics, Chemistry, and Biology*, pages 164–200, 1984.

[49] Andreas Mielke. Noise induced transport. *Annalen der Physik*, 507(5):476–500, 1995.

[50] Charles R Doering, Werner Horsthemke, and Jason Riordan. Nonequilibrium fluctuation-induced transport. *Physical review letters*, 72(19):2984, 1994.

[51] R Dean Astumian. Thermodynamics and kinetics of a brownian motor. *science*, 276(5314):917–922, 1997.

[52] Frank Jülicher, Armand Ajdari, and Jacques Prost. Modeling molecular motors. *Reviews of Modern Physics*, 69(4):1269, 1997.

[53] Johan Paulsson, Otto G Berg, and Måns Ehrenberg. Stochastic focusing: fluctuation-enhanced sensitivity of intracellular regulation. *Proceedings of the National Academy of Sciences*, 97(13):7148–7153, 2000.

[54] José MG Vilar and JM Rubi. Noise suppression by noise. *Physical review letters*, 86(6):950, 2001.

[55] Dawei Hong, William M Saidel, Shushuang Man, and Joseph V Martin. Extracellular noise-induced stochastic synchronization in heterogeneous quorum sensing network. *Journal of theoretical biology*, 245(4):726–736, 2007.

[56] Chunguang Li, Luonan Chen, and Kazuyuki Aihara. Stochastic synchronization of genetic oscillator networks. *BMC Systems Biology*, 1(1):1, 2007.

[57] Vadim S Anishchenko and Alexander B Neiman. Stochastic synchronization. In *Stochastic Dynamics*, pages 154–166. Springer, 1997.

[58] John F Lindner, Brian K Meadows, William L Ditto, Mario E Inchiosa, and Adi R Bulsara. Array enhanced stochastic resonance and spatiotemporal synchronization. *Physical Review Letters*, 75(1):3, 1995.

[59] John F Lindner, Brian K Meadows, William L Ditto, Mario E Inchiosa, and Adi R Bulsara. Scaling laws for spatiotemporal synchronization and array enhanced stochastic resonance. *Physical Review E*, 53(3):2081, 1996.

[60] Daniel Vorberg, Waltraut Wustmann, Roland Ketzmerick, and André Eckardt. Generalized bose-einstein condensation into multiple states in driven-dissipative systems. *Physical review letters*, 111(24):240405, 2013.

[61] Claudio Castellano, Santo Fortunato, and Vittorio Loreto. Statistical physics of social dynamics. *Reviews of modern physics*, 81(2):591, 2009.

[62] Jos Van Bommel. Rumors. *The Journal of Finance*, 58(4):1499–1520, 2003.

[63] Vishal Sood and Sidney Redner. Voter model on heterogeneous graphs. *Physical review letters*, 94(17):178701, 2005.

[64] Clas Blomberg. Fluctuations for good and bad: The role of noise in living systems. *Physics of Life Reviews*, 3(3):133–161, 2006.

[65] Kenneth Denbigh. The principles of chemical equilibrium. *Cambridge University Press, Cambridge*, page 287, 1966.

[66] Valery Petrov, Qi Ouyang, and Harry L Swinney. Resonant pattern formation in a chemical system. *Nature*, 388(6643):655–657, 1997.

[67] Ernesto M Nicola, Markus Bär, and Harald Engel. Wave instability induced by nonlocal spatial coupling in a model of the light-sensitive belousov-zhabotinsky reaction. *Physical Review E*, 73(6):066225, 2006.

[68] MR Evans and B Waclaw. Condensation in stochastic mass transport models: beyond the zero-range process. *Journal of Physics A: Mathematical and Theoretical*, 47(9):095001, 2014.

[69] Lorens A Imhof, Drew Fudenberg, and Martin A Nowak. Evolutionary cycles of cooperation and defection. *Proceedings of the National Academy of Sciences of the United States of America*, 102(31):10797–10800, 2005.

[70] Ethan Akin and Viktor Losert. Evolutionary dynamics of zero-sum games. *Journal of mathematical biology*, 20(3):231–258, 1984.

[71] Johannes Knebel, Torben Krüger, Markus F Weber, and Erwin Frey. Coexistence and survival in conservative lotka-volterra networks. *Physical review letters*, 110(16):168106, 2013.

[72] G Rozhnova, A Nunes, and AJ McKane. Stochastic oscillations in models of epidemics on a network of cities. *Physical Review E*, 84(5):051919, 2011.

[73] Lucas Böttcher, Olivia Woolley-Meza, Nuno AM Araujo, Hans J Herrmann, and Dirk Helbing. Disease-induced resource constraints can trigger explosive pandemics. *Available at SSRN 2496128*, 2014.

[74] Ganna Rozhnova and Ana Nunes. Fluctuations and oscillations in a simple epidemic model. *Physical Review E*, 79(4):041922, 2009.

[75] Roy M Anderson, Robert M May, and B Anderson. *Infectious diseases of humans: dynamics and control*, volume 28. Wiley Online Library, 1992.

[76] Davit A Potoyan and Peter G Wolynes. On the dephasing of genetic oscillators. *Proceedings of the National Academy of Sciences*, 111(6):2391–2396, 2014.

[77] Arthur T Winfree. *The geometry of biological time*, volume 12. Springer Science & Business Media, 2001.

[78] Reinhard Mahnke, Jevgenijs Kaupužs, and I Lubashevsky. Probabilistic description of traffic flow. *Physics Reports*, 408(1):1–130, 2005.

[79] Sven Maerivoet and Bart De Moor. Cellular automata models of road traffic. *Physics Reports*, 419(1):1–64, 2005.

[80] Debashish Chowdhury, Ludger Santen, and Andreas Schadschneider. Statistical physics of vehicular traffic and some related systems. *Physics Reports*, 329(4):199–329, 2000.

[81] Mark EJ Newman. The structure and function of complex networks. *SIAM review*, 45(2):167–256, 2003.

[82] Mark Newman, Albert-Laszlo Barabasi, and Duncan J Watts. *The structure and dynamics of networks*. Princeton University Press, 2006.

[83] David I Shuman, Sunil K Narang, Pascal Frossard, Antonio Ortega, and Pierre Vandergheynst. The emerging field of signal processing on graphs: Extending high-dimensional data analysis to networks and other irregular domains. *Signal Processing Magazine, IEEE*, 30(3):83–98, 2013.

[84] Atieh Mirshahvalad, Alcides Viamontes Esquivel, Ludvig Lizana, and Martin Rosvall. Dynamics of interacting information waves in networks. *Physical Review E*, 89(1):012809, 2014.

[85] László Lovász. Random walks on graphs: A survey. *Combinatorics, Paul erdos is eighty*, 2(1):1–46, 1993.

[86] Jørgen Bang-Jensen and Gregory Z Gutin. *Digraphs: theory, algorithms and applications*. Springer Science & Business Media, 2008.

[87] Mary B Hesse. Action at a distance in classical physics. *Isis*, 46(4):337–353, 1955.

[88] Joseph Berkovitz. Action at a distance in quantum mechanics. 2007.

[89] Tommaso Biancalani, Tobias Galla, and Alan J McKane. Stochastic waves in a brusselator model with nonlocal interaction. *Physical Review E*, 84(2):026201, 2011.

[90] J Kaupužs, R Mahnke, and RJ Harris. Zero-range model of traffic flow. *Physical Review E*, 72(5):056125, 2005.

[91] Martin R Evans and Tom Hanney. Nonequilibrium statistical mechanics of the zero-range process and related models. *Journal of Physics A: Mathematical and General*, 38(19):R195, 2005.

[92] Jos Uffink. Compendium of the foundations of classical statistical physics. 2006.

[93] Xue-Juan Zhang, Hong Qian, and Min Qian. Stochastic theory of nonequilibrium steady states and its applications. part i. *Physics Reports*, 510(1):1–86, 2012.

[94] L Boltzmann. Lectures on gas theory, translated by sg brush university of california press, 1964.

[95] Richard Chace Tolman. *The principles of statistical mechanics*. Courier Corporation, 1938.

[96] Rud Wegscheider. Ueber die veresterung der 3-nitrophtalsäure. *Berichte der deutschen chemischen Gesellschaft*, 34(1):680–681, 1901.

[97] Lars Onsager. Reciprocal relations in irreversible processes. i. *Physical review*, 37(4):405, 1931.

[98] Lars Onsager. Reciprocal relations in irreversible processes. ii. *Physical Review*, 38(12):2265, 1931.

[99] NG Van Kampen. *Fundamental problems in statistical mechanics of irreversible processes*. North-Holland Publishing Company, 1962.

[100] Oliver Penrose. *Foundations of statistical mechanics: a deductive treatment*. Courier Corporation, 2005.

[101] JM Blatt. An alternative approach to the ergodic problem. *Progress of theoretical physics*, 22(6):745–756, 1959.

[102] Goran Lindblad and C Lindblad. *Non-equilibrium entropy and irreversibility*, volume 5. Springer Science & Business Media, 2001.

[103] Katinka Ridderbos. The coarse-graining approach to statistical mechanics: how blissful is our ignorance? *Studies In History and Philosophy of Science Part B: Studies In History and Philosophy of Modern Physics*, 33(1):65–77, 2002.

[104] Raymond F Streater. *Statistical dynamics: a stochastic approach to nonequilibrium thermodynamics*. Imperial College Press, 2009.

[105] Michael C Mackey. Microscopic dynamics and the second law of thermodynamics. *Time's Arrows, quantum Measurements and Superluminal Behavior*, 2001.

[106] Willliam Feller. *An introduction to probability theory and its applications*, volume 2. John Wiley & Sons, 2008.

[107] Richard Durrett. *Essentials of stochastic processes*. Springer Science & Business Media, 2012.

[108] NG Van Kampen. Stochastic processes in physics and chemistry, (north-holland personal library). 2007.

[109] Crispin W Gardiner et al. *Handbook of stochastic methods*, volume 3. Springer Berlin, 1985.

[110] Daniel T Gillespie. A general method for numerically simulating the stochastic time evolution of coupled chemical reactions. *Journal of computational physics*, 22(4):403–434, 1976.

[111] Daniel T Gillespie. Exact stochastic simulation of coupled chemical reactions. *The journal of physical chemistry*, 81(25):2340–2361, 1977.

[112] John Hammersley. *Monte carlo methods*. Springer Science & Business Media, 2013.

[113] Bernard Schutz. *A first course in general relativity*. Cambridge university press, 2009.

[114] William Feller. *An Introduction to Probability Theory and Its Applications. Volume I.* John Wiley & Sons London-New York-Sydney-Toronto, 1968.

[115] Nicolaas Godfried Van Kampen. *Stochastic processes in physics and chemistry*, volume 1. Elsevier, 1992.

[116] Alan J McKane, James D Nagy, Timothy J Newman, and Marianne O Stefanini. Amplified biochemical oscillations in cellular systems. *Journal of Statistical Physics*, 128(1-2):165–191, 2007.

[117] Alan J McKane and Timothy J Newman. Predator-prey cycles from resonant amplification of demographic stochasticity. *Physical review letters*, 94(21):218102, 2005.

[118] Thierry Dauxois, Francesca Di Patti, Duccio Fanelli, and Alan J McKane. Enhanced stochastic oscillations in autocatalytic reactions. *Physical Review E*, 79(3):036112, 2009.

[119] Alex J Bladon, Tobias Galla, and Alan J McKane. Evolutionary dynamics, intrinsic noise, and cycles of cooperation. *Physical Review E*, 81(6):066122, 2010.

[120] Richard P Boland, Tobias Galla, and Alan J McKane. How limit cycles and quasi-cycles are related in systems with intrinsic noise. *Journal of Statistical Mechanics: Theory and Experiment*, 2008(09):P09001, 2008.

[121] Andrew J Black and Alan J McKane. Stochastic amplification in an epidemic model with seasonal forcing. *Journal of Theoretical Biology*, 267(1):85–94, 2010.

[122] David Alonso, Alan J McKane, and Mercedes Pascual. Stochastic amplification in epidemics. *Journal of the Royal Society Interface*, 4(14):575–582, 2007.

[123] Badal Joshi. A detailed balanced reaction network is sufficient but not necessary for its markov chain to be detailed balanced. *arXiv preprint arXiv:1312.4196*, 2013.

[124] Oliver Penrose. Foundations of statistical mechanics. *Reports on Progress in Physics*, 42(12):1937, 1979.

[125] J Clerk Maxwell. On the dynamical theory of gases. *Philosophical transactions of the Royal Society of London*, 157:49–88, 1867.

[126] AN Gorban. Detailed balance in micro-and macrokinetics and micro-distinguishability of macro-processes. *Results in Physics*, 4:142–147, 2014.

[127] Frank P Kelly. *Reversibility and stochastic networks*. Cambridge University Press, 2011.

[128] Richard S Varga. *Matrix iterative analysis*, volume 27. Springer Science & Business Media, 2009.

[129] Richard S Varga. *Geršgorin and his circles*, volume 36. Springer Science & Business Media, 2010.

[130] Joseph La Salle and Solomon Lefschetz. *Stability by Liapunov's Direct Method with Applications by Joseph L Salle and Solomon Lefschetz*, volume 4. Elsevier, 2012.

[131] Roger A Horn and Charles R Johnson. *Matrix analysis*. Cambridge university press, 2012.

[132] Philip J Davis. *Circulant matrices*. American Mathematical Soc., 2012.

[133] Fredric J Harris. On the use of windows for harmonic analysis with the discrete fourier transform. *Proceedings of the IEEE*, 66(1):51–83, 1978.

[134] Keith Iain Hopcraft, Eric Jakeman, and Kevin D Ridley. *The Dynamics of Discrete Populations and Series of Events*. Taylor & Francis, 2014.

[135] Eric Renshaw. *Stochastic population processes: analysis, approximations, simulations*. Oxford University Press Oxford, UK, 2011.

[136] Arne Traulsen, Jens Christian Claussen, and Christoph Hauert. Coevolutionary dynamics: from finite to infinite populations. *Physical review letters*, 95(23):238701, 2005.

[137] JN Pickton, KI Hopcraft, and E Jakeman. Emergence of periodic behaviours from randomness. In *Journal of Physics: Conference Series*, volume 633, page 012121. IOP Publishing, 2015.

[138] John Pickton, Keith Iain Hopcraft, and Eric Jakeman. The emergence of waves in random discrete systems. *Scientific Reports*, 6(1):21, 2016.